



Hasan Mahmud Chowdhury, M. Pharm

Optimization of Interior Air Quality in Automotive Passenger Compartments

Master Thesis

In the fulfillment of the requirements for the degree of

Master of Science

Master Study Program Chemical and Pharmaceutical Engineering

Submitted to

Graz University of Technology

Supervisor

Associate Professor Dr. Mario Hirz

Institute of Automotive Engineering

Corporate Advisor

DI Dietmar Hofer

MAGNA STEYR FAHRZEUGTECHNIK AG & CO KG

Graz, May 2019

Dedicated to

My parents, my family and my little boy

DISCLOSURE AGREEMENT

The work includes confidential information subject to confidentiality. Unless otherwise specified, reproducing or publishing parts or the whole thesis without the prior written consent of the author and MAGNA STEYR FAHRZEUGTECHNIK AG & CO KG is prohibited and may cause legal action. This reservation of consent ends after three years from the date of completion.

Acknowledgement

This thesis has been carried out in collaboration with Magna Steyr Engineering Center, Austria and the Institute of Automotive Engineering at Graz University of Technology, Austria. The thesis project was performed in the environmental compliance group involved in a project within Magna Steyr.

This work has been supervised by Associate Professor, Dr. Mario Hirz from the Institute of Automotive Engineering at Graz University of Technology. I cordially express my gratitude for his kind guidance and assistance in developing the thesis as well as in conducting such an assessment.

I would like to express my heartiest appreciation to my industry supervisor DI Dietmar Hofer, Senior Environmental Officer, Magna Steyr. He did not only support and guide my work, but also inspired and showed me the right way. Another participating personnel from Magna Steyr, Eva Haberschreck, Group leader, Environmental Compliance, supported incessantly. Their experiences and competences have been a very helpful element in the research process of my thesis. I thank my study colleague Leonard Paul Egner, who revised and tried his best to correct this paper. I acclaim the online grammatical check from Abu Hanif Mohammad Abdul Ahad, one of my friends from Bangladesh.

Finally, I am grateful to family members, friends and my colleagues. I would never have come this far without their endless support.

Declaration of integrity

Declaration of integrity

I hereby declare that the master thesis has been written only by the undersigned and without any assistance from the third parties.

I have authored this thesis independently, and I have not used other than the declared sources/resources that I have explicitly marked.

Date/ Location

Signature

Modern car industries are continuously working on making their products more comfortable and luxurious, as well as better suited for their customers. Nevertheless, a luxurious interior compartment alone cannot ensure a healthy environment inside the car. Literature research conducted during this study has strengthened the claim that the exposure of harmful particles creates significant health hazard, which can lead to dangerous health concerns. The experiments conducted during this project were designed to evaluate both particle number and mass distribution in the outside ambient air and inside the passenger compartment. The measurements of particle number concentration were taken for diameters of 0.3 μm , 0.5 μm , 1.0 μm , 3.0 μm , 5.0 μm , and 10.0 μm , by using an optical particle counter. Additionally, a photometer was used to measure particle mass concentration. The conventional micro filter of the car was changed for a High-Efficiency Particulate Air (HEPA) filter for all measurements, repeatedly switched between those two filters without modifying the heating ventilation air conditioning (HVAC) box. A ventilation meter was installed in the car to monitor the differences regarding the environmental conditions including air pressure, airflow, temperature and humidity. The experiment was carried out during autumn 2018 at locations three locations (rural, freeway and inside a tunnel) in Graz, Austria. Result showed that HEPA filter significantly reduced more than 90 % of 0.3 μm -sized particles while measuring at optimum temperature and airflow. However, in micro filter condition, the particle mass concentration in the passenger compartment complied with the "Good" category according to AQI (Air Quality Index, EPA). Nevertheless, 90% of the 0.3 μm diameter particles contained less than 5 % of the total mass. In contrast, particles with a diameter of 10.0 μm contribute less than 1 % to the total number. In conclusion, the outcome of the work reflects the incoherence of the existing air quality regulation and legislation and thus provides hints for the developing future, effective air cleaning systems for automotive applications.

Die Automobileindustrie ist kontinuierlich darum bemüht ihre Produkte komfortabler und luxuriöser zu gestalten. Eine luxuriöse Innenausstattung allein ist jedoch nicht mit einem gesundheitsfreundlicheren Umfeld für die Insassen gleichbedeutend, beziehungsweise kann dies nicht garantieren. Die Einwirkung feiner Partikel auf den menschlichen Körper stellt eine ernste Gefährdung der Gesundheit dar, welche sich in weiterer Folge zu schweren Krankheiten entwickeln kann. Das in dieser Arbeit durchgeführte Experiment wurde darauf ausgelegt, die Teilchenanzahl und Massenverteilung der Partikel innerhalb eines Fahrzeugs sowie der Umgebungsluft mittels Partikelzähler zu messen. Die zur Messung herangezogenen Durchmesser waren 0.3 μm , 0.5 μm , 1.0 μm , 3.0 μm , 5.0 μm und 10 μm . Zusätzlich wurde ein Photometer benutzt, um die Partikel-Massenkonzentration zu messen. Die Messung wurde jeweils mit dem konventionellen Mikrofilter des Testautos sowie mit einem High-Efficiency Particulate Air-Filter (HEPA) durchgeführt. Die Einstellungen der Klimaanlage (HVAC) wurden unverändert belassen. Ein Lüftungsmessgerät wurde installiert um Luftdruck, Luftstrom, Temperatur und Feuchtigkeit zu messen. Die Messungen wurden im Herbst 2018 an drei unterschiedlichen Orten (Landstraße, Autobahn und innerhalb eines Tunnels) in Graz, Österreich, durchgeführt. Nach statistischer Auswertung der Daten konnte festgestellt werden, dass der Einbau eines HEPA-Filters die Anzahl der Partikel mit einem Durchmesser von 0.3 μm um mehr als 90% reduzierte. Die Partikel-Massenkonzentration innerhalb der Fahrzeugkabine erfüllte die Voraussetzungen der "Good"-Kategorie nach Air Quality Index der Amerikanischen Umweltbehörde EPA (AQI). Hierbei muss berücksichtigt werden, dass 90% der 0.3 μm -Partikel weniger als 5% der Gesamtmasse beitragen. Im Gegensatz dazu stellen 10 μm -Partikel weniger als 1% der Gesamtpartikelanzahl dar. Diese Arbeit und ihre Erkenntnisse zeigen die Inkonsistenz der existierenden Gesetzgebung zur Regulierung der Luftqualität auf und versuchen gleichzeitig einen Blick auf zukünftige Entwicklungen für effizientere Luftreinigungssysteme in der Automobilindustrie zu werfen.

TABLE OF CONTENTS

DISCLOSURE AGREEMENT	III
ACKNOWLEDGEMENT.....	IV
DECLARATION OF INTEGRITY	V
ABSTRACT.....	VI
LIST OF TABLES.....	XI
LIST OF FIGURES.....	XI
1. INTRODUCTION	1
1.1 Background of the work	1
1.2 Motivation	2
2. GLOBAL GUIDELINES AND REGULATIONS FOR AIR QUALITY	3
2.1 Air quality index	3
2.2 Comparison of different air quality indices	3
2.3 Global guideline and regulations for air quality	7
2.3.1 WHO regulations	7
2.3.2 EPA regulations	7
2.3.3 European council	7
3. HEALTH EFFECT	9
3.1 Deposition and excretion of particulate matter	9
3.2 Induced diseases by particulate matter	10
4. SOURCES OF PARTICULATE MATTER	14
4.1 Sources of particulate matter in the ambient air	14
4.2 Particulate matter emitted from vehicles	15
4.2.1 Particulate matter from exhaust sources	17
4.2.2 Particulate matter emitted from non-exhaust sources.....	18
5. CHARACTERISTIC OF AEROSOL PARTICLES.....	20
5.1 Chemical composition of particulate matter	20

5.2 Size, shape & diameter of particulate matter	20
5.3 Transportation of aerosol particle	24
5.3.1 Reynold's number	24
5.3.2 Settling velocity	25
5.3.3 Peclet number	26
5.3.4 Slip correction factor	26
5.3.5 Brownian motion and diffusion coefficient	27
5.4 Particle size distribution	28
5.5 Particulate mass concentration vs particulate number concentration	30
6. FILTRATION MECHANISMS.....	31
6.1 Types of filters	31
6.1.1 Fibrous filters.....	31
6.1.2 Membrane filters.....	32
6.2 Deposition mechanism and efficiency of fibrous filters	33
6.2.1 Interception	33
6.2.2 Inertial impaction	34
6.2.3 Diffusion.....	36
6.2.4 Gravitational settling	38
6.2.5 Electric filters	38
6.2.6 Efficiency of an isolated fiber filter.....	38
6.2.7 Total collection efficiency of a filter	39
6.3 Factors affecting filters efficiency	40
6.3.1 Influence of particle size.....	40
6.3.2 Influence of particle type.....	41
6.3.3 Influence of particle shape	41
6.3.4 Influence of fiber size	41
6.3.5 Influence of filtration velocity	41
6.3.6 Influence of solid fraction.....	41
6.3.7 Influence of air temperature	42
6.3.8 Influence of air humidity	42
6.3.9 Influence of airflow pressure.....	42
6.3.10 Influence of dust holding capacity.....	42
6.4 Conclusion of theoretical studies	43
7. COMPARATIVE EXPERIMENTAL AND ANALYSIS OF MEASURING DATA	44
7.1 Overview of experimental plan	44
7.1.1 Test procedure.....	44
7.1.2 Data analysis	45
7.2 Experimental setup and planning of measurement	46
7.3 Test environment	50
7.4 Test vehicle	52
7.5 Filter specifications	52

7.6	HVAC setting and testing conditions	54
7.7	Sampling of air	58
7.8	Instruments and test equipment	58
7.8.1	Optical particle counters	59
7.8.2	Photometer	60
7.8.3	Ventilation meter	62
8	RESULTS AND DISCUSSION	63
8.1	Total particle count	63
8.2	Influences of locations on particle size distribution	64
8.3	Geometric standard deviation in different location	66
8.4	Particle size distribution for all HVAC settings	67
8.5	Mass concentration in different locations	68
8.6	Filter efficiency	69
8.7	Number vs mass concentration	70
8.8	Velocity vs pressure	71
9	CONCLUSION	72
10	BIBLIOGRAPHY	74

LIST OF TABLES

Table 2. 1: Air Quality Index (AQI) and categories according to EPA (Environmental Protection Agency, USA)	5
Table 2. 2: Common Air Quality Index (CAQI) and categories according to EU (European Union)	6
Table 2. 3: Standards and guidelines for particulate matter less than 10 μm (PM10).....	8
Table 2. 4: Standards and guidelines for particulate matter less than 2.5 μm (PM2.5).....	8
Table 4. 1: Mass concentration of Particulate Matter throughout few mega cities.	14
Table 4. 2: Sources attribution of PM from traffic sectors in different cities	16
Table 5. 1: Relation between particle mass and particle number concentration	30
Table 7. 1: Experimental plan and set up for test-drive and sample collection.	47
Table 7. 2: Filters specifications	54
Table 7. 3: The multifunction control button of HVAC devices and their operations are described below.	55
Table 7. 4: Cabin environment settings for the experiment.....	58

LIST OF FIGURES

Figure 3. 1: Particles sizes and their deposition throughout the human respiratory and other tissues	9
Figure 3. 2: The engulfing process of ultrafine particles.....	10
Figure 3. 3: Hypothetical fate of particulate matter into the cardio vascular system.....	12
Figure 4. 1: The conceptual formation of PM from internal combustion engines including three layers of particle size. Coarse mode, accumulation mode, nucleation mode.	17
Figure 5. 1: Chemical composition of PM likely from conventional engines.	20
Figure 5. 2: Particles and their size ranges.....	22
Figure 5. 3: Comparison of particle diameters with a human hair.	23
Figure 5. 4: (a) An irregular shaped particle superimposed equivalent diameter, (b) stokes equivalent diameter, (c) aerodynamic equivalent diameter (spherical shape with unique density).....	23
Figure 5.5: Explanation of Reynolds number	25
Figure 6. 1: Microstructure of a glass fiber filter taken by Electronic microscope	31
Figure 6. 2: Electron micrograph of a membrane filter	32
Figure 6. 3: Interception mechanism of the fibrous filter.....	34
Figure 6. 4: Inertial impaction of the fibrous filter	35
Figure 6. 5: Diffusion mechanism of the fibrous filter	37
Figure 6. 6: Particle coagulation on filter medium	42

Figure 6. 7: Dust adherence of particles into the filter fiber.	43
Figure 7. 1: Test vehicle installed with required equipment	46
Figure 7. 2: Experimental model of the parking area.	49
Figure 7. 3: Experimental model of test drive in freeway.....	49
Figure 7. 4: Experimental model of test drive in tunnel.	50
Figure 7. 5 The freeway road for test-drives in Graz, Austria.....	51
Figure 7. 6: The Plabutsch Tunnel in Graz, Austria	51
Figure 7. 7: Reference vehicle	52
Figure 7. 8: Pollen filter installed under the windshield	53
Figure 7. 9: Micro cabin filter installed inside the HVAC box	53
Figure 7. 10: Alternative HEPA cabin filter.....	54
Figure 7. 11: HVAC control panel of BMW X5.....	55
Figure 7. 12: Selection of air circulation mode	56
Figure 7. 13: Air Flow (fresh air from outside and recirculation into the cabin) inside the HVAC box according to the different settings.	57
Figure 7. 14: Isokinetic sampling method.	58
Figure 7. 15: AeroTrak portable particle counter)	59
Figure 7. 16: Measurement principle of optical particle counter.	60
Figure 7. 17: Dusttrak Drx Aerosol Monitor.....	60
Figure 7. 18: Measurement principle of a photometer	61
Figure 7. 19: Ventilation meter with thermos-anemometer-probe	62
Figure 8. 1: Total number of particles in different locations (outside environment and window open) and climate control by using both filters.	63
Figure 8. 2. Location influences on particle size distribution.	64
Figure 8. 3. Filter activity against different locations.	65
Figure 8. 4. Geometric standard deviation of particle size distribution.	66
Figure 8.5. Performance of different climate controls in different locations.....	67
Figure 8. 6. Influence of different locations on mass concentration in the ambient air.	68
Figure 8. 7. Comparison of filter efficiency.....	69
Figure 8. 8. Particle mass against particle number distribution depends on variable particle size.	70
Figure 8. 9. Air pressure inside the cabin for both filters and changing blower speed.....	71

1. INTRODUCTION

1.1 Background of the work

Air quality has a significant impact on human health and is a comfort factor for passengers. Cars become increasingly part of modern life where people use vehicles for transportation. Moreover, the demand for vehicles increases gradually. Since the traffic and transportation is a major source of air pollution, the passengers inside the car as well as non-passenger can be at risk of health hazard. These pollutants can enter the vehicle cabin through the HVAC (heating ventilation air conditioning). Exposure to the outside air by windows and doors is another way of polluted air entering the cabin (1). Studies have found out that the concentration of fine particulate matter of heavy metal or carcinogenic PAH (polycyclic aromatic hydrocarbon) could be higher inside the passenger compartment than concentration of outside ambient air (2). In this way, it is a foremost area of development in automotive industries to attain information on number, concentration and the nature of particulate matter inside the passenger compartment.

The particles are mostly generated from natural or anthropogenic sources. Not only the heavy industries, agricultural sites, construction or unpaved road are the main sources of particulate matter; a significant fraction also comes from vehicles and these are even more dangerous than other sources. A study reported 15 to 25 % of diesel soot in 85 to 125 $\mu\text{m}/\text{m}^3$ of street dust concentration (3). This outcome is supported by another research group in California, USA who found Carbon (C) is dominated in 12 to 22% of the paved road dust (4). This carbon is a fraction of PM emitted from the traffic sources.

Vehicle emitted UFP (ultrafine particles) are mostly present in the urban area. The concentration of UFP in the street is much higher than the ambient air, which is calculated in a studies range from 10000 to 500000 particles / cm^3 (5). A usual average commuting time 1.3h/ day in the cabin can be responsible for almost 50% of total daily UFP exposure. The modern air carbon filter can protect 40 to 60% under OA (outside air) mode although the efficiency of filter mostly depends on the vehicle type, PM characteristic and so on.

Epidemiologically studies have reported a strong correlation between air pollution and mortality and morbidity rate (6). Among all respirable air pollutants, particulate matter is one of the most hazardous pollutants especially the fine particulate matter, which can reach not only our respiratory zone but also penetrate our systemic circulation and cause a severe health problem. It was assumed that not only bronchial asthma and diseases relevant lung is responsible for air pollution but also recent studies found out the association of cardiovascular diseases, visibility, headache, dizziness. In addition, there is a significant impact on human diseases those are exposed to the vehicular emissions especially fine particle (7). Very recent studies find out that, some of the fine particulate matter have the ability of crossing the blood-brain barrier, and also initiating mutagenic reaction into the cell (6). Studies done on UFP diameter < 100 nm found out that they could be translocated to the cardiovascular system from lungs; penetrate into the epithelium cell, circulatory system, and deposit into the heart, liver, kidney, and brain cell (8). The smaller size increases the surface area and also can localize into the mitochondria and destroy them. Some chemical species undergo ROS (reactive oxygen species) reaction (vehicle emitted UFP is the major source of this type) that can make genetic mutation.

Several independent groups of investigators have shown that toxicity and numerous health problems depend on the fraction of particles more precisely their size and composition (9). The chemical composition and its structure is depending on many factors such as sources, climate, season and type of pollution. The major components are adsorbed organic volatile and semi-volatile materials (e.g. PAH), transitional metal (e.g. Copper, Nickel, Iron) ions (e.g. Sulfate, Nitrate) reactive gases (Ozone, Peroxide, Aldehyde) and carbonaceous materials (mostly from combustion engines), biological origin endotoxins, bacteria, viruses) and minerals. These effects are stronger for fine and ultrafine particles because they can penetrate deeper into the airways of the respiratory tract and can reach the alveoli in which 50% are retained in the lung parenchyma (6).

In general, the evaluation of most of these studies shows that the smaller the size of PM, the higher the toxicity through mechanisms of oxidative stress and inflammation. Some studies showed that the extractable organic compounds (a variety of chemicals with mutagenic and cytotoxic properties) contribute to various mechanisms of cytotoxicity (6). In addition, the water-soluble fraction (mainly transition metals with redox potential) plays an important role in the initiation of oxidative DNA damage and membrane lipid peroxidation. Associations between chemical compositions and particle toxicity tend to be stronger for the fine and ultrafine PM size fractions. Vehicular exhaust particles are found to be most responsible for small-sized airborne PM air pollution in urban areas (6).

1.2 Motivation

The motivation of this work is to assist the development of a clean environment as well as a healthy comfort zone for the passengers inside the vehicles. To maintain a convenient climate inside the cabin it is necessary to improve the HVAC (heating ventilation air conditioning system) system and more precisely to increase the efficiency of the filtration mechanism and deposition of the pollutants. Therefore, attention is given to air pollutants. This study has considered the particulate matter especially 2.5 μm and fine particulate matter PM 1 μm and less due to their growing complexity in human health – related issues. Therefore, it was required to study and collect information on the fundamental of particulate matter, its source, composition, formation, distribution, concentration and number in a specific area, for this study in the passenger cabin. The outcomes could be helpful for the future development of filtration mechanism in the passenger car.

There is a lack of data on PM concentration, number, and composition (3). However, from the literature research, it is concluded that the composition, concentration and size distribution is depending upon the geographical location, traffic density and the composition of street construction as well as the condition of the vehicles. Beside those, environmental factors, i.e. temperature, humidity, has a direct impact on PM formation and its characteristics. In this study, the experiments were done within two days from morning to evening. This is why it is quite difficult to analyze the environmental effects on the PM properties and characteristics. To evaluate effect of different PM, this study was carried out in three different locations. Rural parking has a normal wind blow but less contribution from traffic source. The freeway also has the natural breeze but combination of air pollutants are mixed from different sources although the vehicle emission is dominant. However, in the tunnel, most of the pollutants come from the different sources of the vehicles. This combination of experimental works delivers better idea on particulate matter (PM) mass concentration and number concentration as well as their characteristics.

2. GLOBAL GUIDELINES AND REGULATIONS FOR AIR QUALITY

2.1 Air quality index

The AQI (Air Quality Index) is a numerical value that represents the purity of air and its associated health effects. It focuses on the exposure time (daily or hourly) to the unhealthy air and significance of concerned diseases. According to AQI, pollutant has its health influences depending upon their defined values. (10)

The database does not always deliver the same standard of AQI to scientific society or government official, regulatory authorities and the public. This is because of the AQI is determined by individual nationalities or authorities. No standard method is established universally throughout the world. Different methods and different calculations are used depending on the situation that represents the AQI or API (Air Pollution Index) value. (11) But most commonly all standards of AQI focus on five major pollutants and set up an individual value depending on their severity on human health.

The AQI itself is represented by numbers along with a color scheme and categories levels such as good, moderate and poor. (12)

The indices of AQI are established corresponding to different air quality standards, but the pollutants are identical. For defining a standard of each pollutant in the regional atmosphere, the AQI was developed. According to very common major AQI indices, five specific pollutants are considered as sensitive to human exposure (13)(14).

_ PM 2.5, PM 10 (PM = particulate matter)

_ O₃, (Ozone)

_ SO₂ (Sulfur dioxide)

_ NO₂, (Nitrogen dioxide)

_ CO (Carbon monoxide)

2.2 Comparison of different air quality indices

Air Quality Index Followed by US EPA

In 1976, the US EPA (Environmental Protection Agency) established a nationally uniform AQI (Air Quality Index) called PSI (Pollutant Standard Index), which had an index value of 0 – 500 with 100 equal to the NAAQS (National Ambient Air Quality Standards). The index was calculated following as NAAQS because it was developed on a scientific basis related to air quality and public health. The EPA was forecasting air quality by using PSIN100 at the different monitoring stations. The PSI included sub-indices for five majors [O₃, PM, CO, SO₂, and NO₂], which represent ambient pollutant concentrations to index values on a scale from 0 to 500. (15) Later, PSI was renamed to AQI in 1999 by consideration of addition breakpoint and 8 hours sub-index for O₃ (Ozone) and sub-index of 8 hours for PM 2.5 as well.

The index for measuring the individual pollutant is calculated by using the following linear interpolation equation, pollutant concentration data, and reference concentration.

The breakpoint concentrations of each pollutant have been defined by the EPA based on NAAQS (National Ambient Air Quality Standards) as shown in Table 2.1, and the effects of the epidemiological studies refer to the significant impact pollutants on the human body.

The official method for calculating the AQI according to EPA uses the following equations (13):

$$I_p = \frac{I_{Hi} - I_{Lo}}{BP_{Hi} - BP_{Lo}} (C_p - BP_{Lo}) + I_{Lo}$$

Where

I_p = the index for pollutant p

C_p = the truncated concentration of pollutant p

BP_{Hi} = the concentration breakpoint that is greater than or equal to C_p

BP_{Lo} = the concentration breakpoint that is less than or equal to C_p

I_{Hi} = the AQI value corresponding to BP_{Hi}

I_{Lo} = the AQI value corresponding to BP_{Lo}

An example to measure PM 2.5 for a for specific concentration make it more understandable. Let's calculate for 24 hours, PM 2.5 concentration found $35.9 \mu\text{g}/\text{m}^3$. This refers to the 3rd row column 3 from the left that fall between 35.5 –55.4 limits. In this case $35.9 \mu\text{g}/\text{m}^3$ value is found within 101 – 150 limits. Now, calculate Index of pollutants $I_{PM\ 2.5}$ according to the formula:

$$I_{PM\ 2.5} = \frac{150 - 101}{55.4 - 35.5} (35.9 - 35.3) + 102 = 102$$

Above value indicates the orange color and represents the category: Unhealthy for sensitive group.

Table 2. 1: Air Quality Index (AQI) and categories according to EPA (Environmental Protection Agency, USA)

Breakpoints of pollutants							AQI limits	Category	Color indicator
O ₃ (ppm) 8-hour	O ₃ (ppm) 1-hour ¹	PM 2.5 (µg/m ³) 24-hour	PM 10 (µg/m ³) 24-hour	CO (ppm) 8-hour	SO ₂ (ppb) 1-hour	NO ₂ (ppb) 1-hour	AQI		
0.000 - 0.054	-	0.0 – 12.0	0 - 54	0.0 - 4.4	0 - 35	0 - 53	0 - 50	Good	green
0.055 - 0.070	-	12.1 –35.4	55 - 154	4.5 - 9.4	36 - 75	54 - 100	51 - 100	Moderate	yellow
0.071 - 0.085	0.125 - 0.164	35.5 –55.4	155 - 254	9.5 - 12.4	76 - 185	101 - 360	101 - 150	Unhealthy for sensitive groups	orange
0.086 - 0.105	0.165 - 0.204	(55.5 - 150.4) ³	255 - 354	12.5 -15.4	(186 - 304) ⁴	361 - 649	151 - 200	Unhealthy	Red
0.106 - 0.200	0.205 - 0.404	(150.5 - 250.4) ³	355 - 424	15.5 -30.4	(305 - 604) ⁴	650 - 1249	201 - 300	Very unhealthy	Violet
(2)	0.405 - 0.504	(250.5 - 350.4) ³	425 - 504	30.5 - 40.4	(605 - 804) ⁴	1250 - 1649	301 - 400	Hazardous	Maroon
(2)	0.505 - 0.604	(350.5 - 500.4) ³	505 - 604	40.5 - 50.4	(805 - 1004) ⁴	1650 - 2049	401 - 500	Hazardous	Maroon

⁽¹⁾ Areas are generally required to report the AQI based of 8- hours ozone values. However, there are a small number of areas where an AQI based on 1-hour ozone values would be more precautionary. In these cases, in addition to calculating the 8-hour ozone index value, the 1-hour ozone value may be calculated, and the maximum of the two values reported.

⁽²⁾ 8-hour O₃ values do not define higher AQI values (≥301). AQI values of 301 or higher are calculated with 1-hour O₃ concentrations.

⁽³⁾ If a different SHL for PM 2.5 is promulgated, these numbers will change accordingly.

⁽⁴⁾ 1-hour SO₂ values do not define higher AQI values (≥200). AQI values of 200 or greater are calculated with 24-hour SO₂ concentrations.

Common Air Quality index (CAQI) followed by Europe

The CAQI (Common Air Quality index) was formed in 2006 as a sequence of the CITEAIR project (an INTEREG IIIC project, 2004-2007)(14). The index was established to compare the real-time air quality throughout European cities. It was developed to present comparable and understandable measurements, which were transformed into a single relative figure called the Common Air Quality Index. In the beginning, many cities used their own air quality index with different indices that made it difficult to represent an overall overview. The CAQI was developed to present comparable data to all cities in an accessible way. It focused mainly on two indices, the roadside and the background index.

The roadside index considers the traffic pollution including NO₂ and PM 10 as mandatory pollutants and PM 2.5 and CO as auxiliary pollutants. The later one monitor the city background sites including NO₂, PM 10 and O₃ as mandatory pollutants and PM 2.5, CO and SO₂ as auxiliary pollutants. In addition, a website for the purpose of comparing cities and coexist with any local indices by which people can easily understand was provided. Another reason was to protect the data from misuse by others authorities. The CAQI is designed to present and compare air quality in near-real time on an hourly or daily basis. It uses five levels with daily and hourly based measurement, using a value from 0 (minimum) to 100 (maximum) and color from light green to dark red. The CAQI is calculated depending on scale basis (shown in Table 2.2) between the class borders. Each pollutant has a sub-incidence that represents the highest and lowest value. Nevertheless, the choice of the classes for the CAQI is inspired by the EC (European Commission) legislation. The above method can be applied to make a comparative study of urban air quality in real time without facilitating or considering the spatial aggregation, pollutant aggregation, uncertainty measures and health effects (14).

Table 2. 2: Common Air Quality Index (CAQI) and categories according to EU (European Union)

Index class	Scale	Roadside Index						Background Index							
		Mandatory Pollutant			Auxiliary Pollutant			Mandatory Pollutant				Auxiliary Pollutant			
		NO ₂	PM 10		PM 2.5		CO	NO ₂	PM 10		O ₃	PM 2.5		CO	SO ₂
			1-h r	24-hrs	1-h r	24-hrs			1-h r	24-hrs		1-hr	24-hrs		
Very low	0	0	0	0	0	0	0	0	0	0	0	0	0	0	0
	25	50	25	15	15	10	5000	50	25	15	60	15	10	5000	50
Low	25	50	25	15	15	10	5000	50	25	15	61	15	10	5001	50
	50	100	50	30	30	20	7500	100	50	25	120	30	20	7500	100
Medium	50	100	50	30	30	20	7500	100	50	25	120	30	20	7501	100
	75	200	90	55	55	30	10000	200	90	50	180	55	30	10000	350
High	75	200	90	55	55	30	10000	200	90	50	180	55	30	10001	350
	100	400	180	110	110	60	20000	400	180	100	240	110	60	20000	500
Very high	>100	>400	>180	>110	>110	>60	>20000	>400	>180	>100	>240	>110	>60	>20000	>500

NO₂, O₃, SO₂: hourly value / maximum hourly value in µg/m³

PM 10, PM 2.5: hourly value / maximum hourly value or adjusted daily average in µg/m³

CO: 8 hours moving average / maximum 8 hours moving average in µg/m³

2.3 Global guideline and regulations for air quality

Recent studies reveal that air concentration contaminants with PM, NO₂, SO₂, particulate matter and so on, but among them PM has the most prominent health concern. Environmental impacts of PM include reduced visibility, increased atmospheric acid deposition, damage to crops and forests, increased corrosion of materials, depletion of the nutrients in the soil and adverse effects on the diversity of ecosystems. (16) The regulation was introduced based on the human health impact for PM 10 and PM 2.5 to reduce the concentration of particulate matter especially the fine particulate matter.

2.3.1 WHO regulations

The “Air Quality Guideline: Global Update, 2005” was published by WHO (World Health Organization) in 2006. The guideline conveyed the message to the national and international authorities as well as policy makers concerning the pollutant including particulate matter present in the ambient air. The guideline discussed the approach to reach the air quality target and focus the health risk assessment, scientific, socioeconomic issues (17).

2.3.2 EPA regulations

The standards address both PM 2.5 and PM 10 and require measurement of PM concentration for 24-hr and annual averages. The limits are set under primary and secondary standards with specific aims to protect public health and public welfare. The agency requires states to propose SIPs (state implementation plans). The complex rules involve several milestones to be met by a specific timeline spanning several years. According to the final rule published in April 2007, each state having a nonattainment area must submit to EPA an attainment demonstration and adopted regulations ensuring that the area will attain the standards by no later than 2015. (16)

2.3.3 European council

In the European Union, air quality is regulated under EU directives. Members are obligated to achieve this standard. Member countries have their air quality standards, which they follow to reach the EU derivatives. Directives focus on TSP (total suspended particles) from industries and vehicles, ambient air quality for PM 2.5 µm and PM 10 µm and reports to United Nations Economic Commission for Europe (UN ECE). European Union as a single body and all member states are responsible to report their particulate matter to the Emission Monitoring and Evaluation Program (EMEP) Core Inventory of Air Emission (CONAIR). Both PM 2.5 µm and PM 10 µm are included in these inventories with hourly, daily and yearly threshold level.

An overview of air quality standards from different nationalities is shown in table 2.3 and table 2.4 for PM 10 and PM 2.5 respectively. From the following comparison it is clear that developed countries made the specification of particulate matter concentration according to their development of ambient air quality. Countries from Asia have only developed regulations for PM 10, whereas the European Union and the United States trying to maintain PM 2.5 regulation. These assumed that, the developing

and least developed countries are still far away from the compliance of PM 2.5 which supposed to be more harmful than PM 10.

Table 2. 3: Standards and guidelines for particulate matter less than 10 µm (PM10)

Country	Limit value(µg/m ³)	Organization
China	150 µg/m ³ as 24-h average	AQSIQ SEPA
Hong Kong	20 µg/m ³ as 8-h average (Excellent Class) 1a 180 µg/m ³ as 8-h average (Good Class) 1b	HKEPD
Malaysia	150 µg/m ³ as 8-h average	DOSH
Singapore	150 µg/m ³ (in office) 2a	Institute of Environmental Epidemiology, SIAQG
Australia	90 µg/m ³ as 1-hr	NHMRC
US	150 µg/m ³ as 24-h average (Exposure) 3a	ASHRAE
	150 µg/m ³ as 24-hr (Exposure) 3a	US EPA
	150 µg/m ³ as 24-h average	US EPA
	50 µg/m ³ as 1-y average	US EPA
EU	40 µg/m ³ as 1-y average	EU
Others	50 µg/m ³ as 24-h average	WHO
	20 µg/m ³ as 1-y average	

1a Excellent class: Excellent level of indoor air quality (Hong Kong)

1b Good class: Good level of indoor air quality (Hong Kong)

2a Guidelines for good IAQ in office premises (Singapore)

3a Exposure: It means a continual and repetitive contact with the substance over a set period (US)

Table 2. 4: Standards and guidelines for particulate matter less than 2.5 µm (PM2.5)

Country	Limit value (µg/m ³)	Organization
Canada	100 µg/m ³ as 1-h average (Short-Term Exposure) 1a	Health Canada
	40 µg/m ³ as 8-h average (Long-Term Exposure) 1b	
United State	65 µg/m ³ as 24-h average (Exposure) 2b	ASHRAE
	35 µg/m ³ as 24-h average	US EPA
	15 µg/m ³ as 1-y average	
	60 µg/m ³ as 24-h average	US EPA
	15 µg/m ³ as 1-y average	
	65 µg/m ³ as 24-h average (Exposure) 2b	US EPA
EU	25 µg/m ³ as 1-y average	EU
Others	25 µg/m ³ as 24-h average	WHO
	10 µg/m ³ as 1-y average	

1a Short-term exposure: Exposure over a short period of time. It is usually less than 8 hours or 15 minutes to high levels of a substance (Canada)

1b Long-term exposure: Exposure over a long period of time. It is usually more than 8 hours (Canada)

2a Ceiling level: Highest possible allowed value for exposure (US, ACGIH)

2b Exposure: It means a continual and repetitive contact with the substance over a set period (US, ASHRAE)

3. HEALTH EFFECT

3.1 Deposition and excretion of particulate matter

The health hazard in the human body influenced by particulate matter depends on its chemical composition, localization and the method of deposition into the respiratory system where the particles are deposited. These characteristics are related to the particle size and inhalation method. However, the basic mechanism of filter activity or collection of the particle into the filter is comparable with the particle deposition in the human respiratory system but later one is much more complex including geometry, flow rate and direction of the cycle (18).

Human respiratory consists of three distinct sequences. The first part *head airway region*, also known as an *extrathoracic* or *nasopharyngeal* region, consists of nose, mouth, pharynx, and larynx. Inhaled air is heated and dehumidified in this region. Later air enters the second region called *lung airways* or *tracheobronchial* and is then then divided according to a successive bifurcation in the bronchial tree, then enters the bronchioles (with diameters of ~ 500 nm) (19). In the end, air comes to the pulmonary or alveolar (with diameters of ~ 200 nm) area having 50 m² surface area, where gas alteration takes place. A normal adult person inhaling $10 - 25$ m³ of air having 75 m² surface area (18). The deposition of the inhaled particle into the various locations of the respiratory system follows various deposition mechanisms including impaction, settling and diffusion. Nevertheless, the retention time and location depend on individual breathing system and particle size, shape and airway geometry (20).

The size and composition of the particulate matter present in the ambient air depend on the sources of generation. These characteristics also play an important role in particle deposition process, location and residence time into the respiratory system. Particles between 2.5 μm to 10 μm can deposit into the upper airways through impaction or sedimentation mechanism whereas particles below 2.5 μm can reach in the alveoli by following sedimentation and Brownian diffusion processes. The fine particle having diameter less than 1 μm can mainly penetrate into the lung by Brownian diffusion, and afterward these particles can be circulated into liver, spleen, heart or even can cross the blood-brain barrier through the systemic circulation. (8)

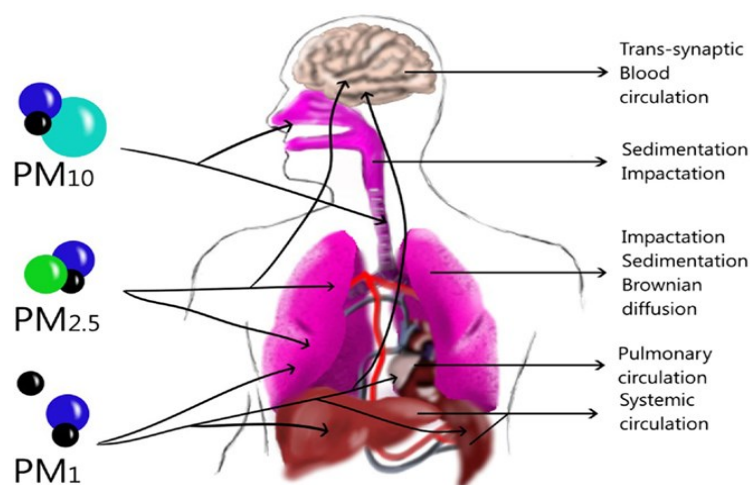


Figure 3. 1: Particles sizes and their deposition throughout the human respiratory and other tissues (8)

The residence time of a particle depends on the ciliary activity and rheological properties of mucus. Particles are generally removed within minutes or hours but sometimes it takes longer time for deeper particles to eject depending on the owing distance and slower rates of mucus transport. Particles are swallowed with the mucus and reach the stairway, hence cleared to the digestive tract or ejected from the mouth by expectorant.

Clearance is a slow process for the particles that go down into the deeper lung where alveoli lack the protection of cilia. Particles can remain with freedom for weeks, month or even years. Removal of these particles is associated with the white blood cells called “macrophages”. The engulfing mechanism of foreign particles is known as phagocytosis. Through this process, particles are cleared out from the alveolar by many routes (21). The schematic diagram in figure 3.2 illustrates the mechanism of phagocytosis. Particles can also enter through the pulmonary epithelium, bloodstream or the lymphatic system. Some particles also can dissolve in the lung fluid for their solubility and they can be removed without the involvement of macrophage.

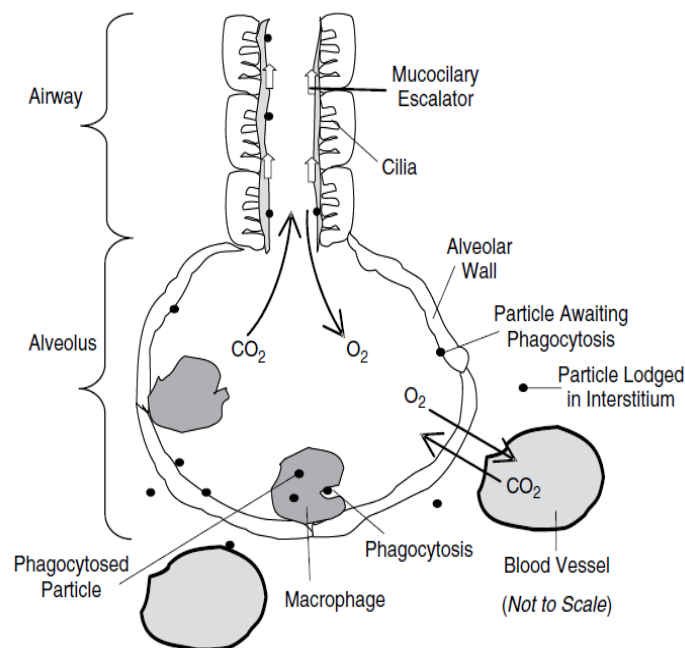


Figure 3. 2: The engulfing process of ultrafine particles. (19)

3.2 Induced diseases by particulate matter

The chemical composition of PM is divided into water-soluble and water-insoluble substances. Comparing both fractions, exposure to the water-soluble part is more detrimental, which produces ROS (reactive oxygen species) and increases the inflammatory cytokines concentration. The ROS generate free radicals responsible for cell dysfunction including cell signaling; activate inflammatory mediators and oxidative stress, which leads to DNA (deoxyribonucleic acid) damage. An in-vitro study using human BEAS 2B (bronchial epithelial) cells exposed to PM expressed that water-insoluble

inorganic elements and ions showed early stage oxidative events while PAH (polycyclic aromatic hydrocarbon) was associated with later oxidative damage and cytokine secretion. (8)

IARC (International Agency for Research and Cancer) categorized outdoor air as a group-1 carcinogenic level. Metal and PAHs are two major components emitted from the vehicle combustion present in the ambient air. Both components have mutagenic and carcinogenic properties. (19) The most discussed diseases in the history of the particulate matter are lung cancer, chronic bronchitis especially for those who are exposed occupationally to diesel exhaust (22). The dangers of soot's and tar, cigarette smoke are familiar for this reason but here PAH is the most cancer-causing agent (23). Both PAH and nitro-polycyclic aromatic hydrocarbon (nPAH) are a major part of PM exhaust from vehicles. When activated, it shows mutagenic action, the growth of tumors, and the increase of malignant neoplasms in lung cancer (6). Studies also demonstrate that PM show oxidative activity due to quinones and PAHs. This redox reaction can damage the macrophage, bronchial epithelial cell, and mitochondria (6).

The chemical reaction of the exogenous carcinogenic agent with the encoded information of DNA is anyhow corrupt onto its information structure; the breed up of mutated cells might become proliferate out of control (24). PAH has the same nature as a carcinogenic agents and it might be showing more effect when it is inhaled as a particle sorbate than vapor. Because this can be, remaining for prolonged action, it is more significant than the real aspirated amount. In contrast, the organic compound is less bioavailable and nonreactive if the molecules are not fixed with the surface of the particle. When the PAH adheres with the surface, it also reduces the release of other organic compounds.

The presence of organic compounds does not act as a carcinogenic agent unless it is metabolized and interaction with other compounds to act as a promoter. PAH and their metabolites are chemically reactive intermediates that can bind covalently macromolecules like proteins, DNA, RNA (ribonucleic acid) (25). Studies done by different researchers illustrated that this adduct plays an important role to the people who are occupationally exposed to the diesel exhaust and associated with the cell mutations (26).

The substituents of fine and ultrafine particles lead to modification of epithelial cell permeability influenced by ROS-Oxidative mediated stress. (8). Another study shows that oxidative substances are produced by quinones, which is the major compound of PM toxicity (27). Many studies observed that DEP (diesel exhaust particles) have a significant impact on oxidative cellular damage by producing Oxygen free radicles (e.g. OH, O₂) and ROS, which leads to lipid peroxidation and oxidative DNA damage (6). Studies also indicate that oxidative stress can change the immune response from Th1 (T helper cell 1) to Th2 (T helper cell 2) dominance (28). Heavy metals (such as Fe, Cu, Ba, Sb) originated from brake and tires induce an oxidative reaction. During winter, the PM concentration becomes increased when the road dust is an important factor. Studies showed that exposure to road dust below 2.5 µm increased 7% of cardiovascular mortality in Barcelona (29). A study reported that exposure of the DEP, 300µg/m/h to an adult enhance the neutrophils, B and T lymphocytes, which is the cause of lung inflammation (8).

A study conducted in hospital environment observed that cardiovascular problems raised 0.5% due to increase 10µg/m³ particular matter (6). Hemostasis and thrombosis or blood clotting are suspicious due to the particle penetration into the systemic circulation, which leads to heart attacks in the coronary arteries and strokes in the cerebral microcirculation. Two assumed mechanisms are drawn

in figure 3.3 (19). One reason is the PMN (polymorphonuclear neutrophil leukocytes), which have a slightly larger size (7 μm) than alveolar capillaries (5 μm) that needs longer duration for microcirculation and these prolongation leads to accumulating at various point (30). This condition deteriorates during inflammation of oxidative stress. Fibrinogen is accused of for the second mechanism, which is the controlling factor for blood viscosity and coagulability.

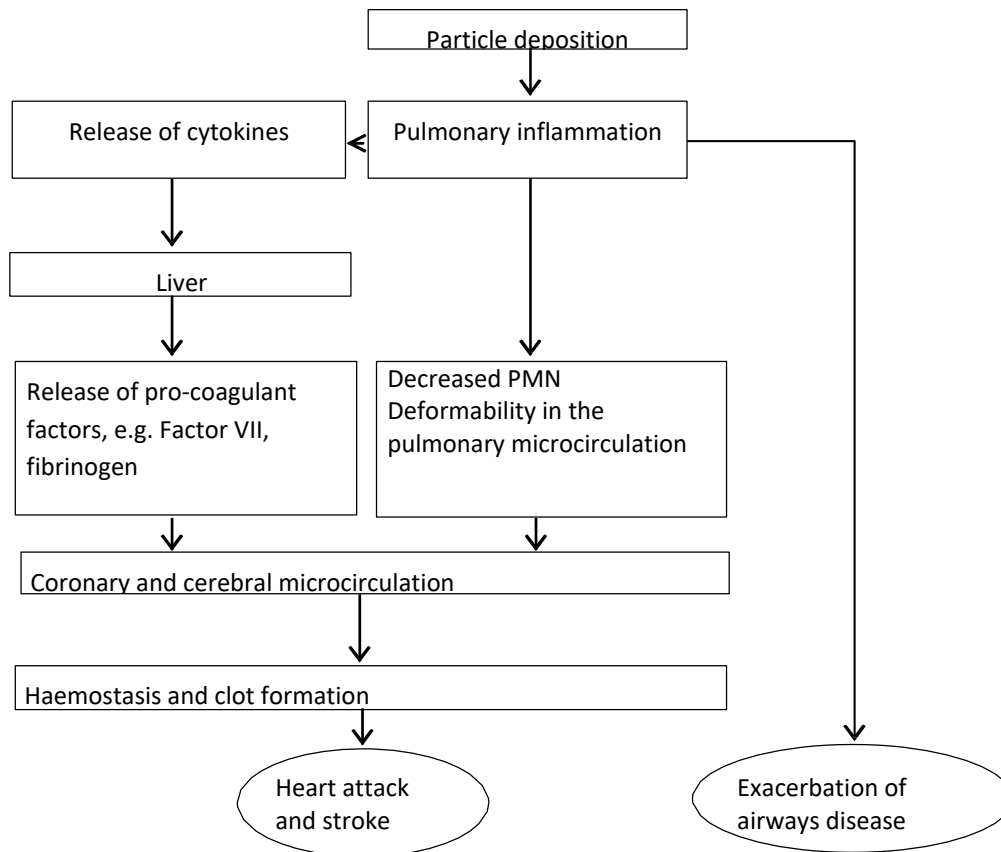


Figure 3. 3: Hypothetical fate of particulate matter into the cardio vascular system. (19)

Three common diseases named asthma, bronchitis and COPD (chronic obstructive pulmonary disease) concerned with the particulate matter infected mainly in the upper airways. Comprehensive studies surveyed on 38 million hospital people living in 6 European cities showed asthma and COPD increase of 1.0% for each 10 $\mu\text{g}/\text{m}^3$ increase of PM10 for old people age more than 65 years (6). Some reports found that the exposure to DEP activates Th2 response and leads to the production of IL-17A (Interleukin 17A) (75) and mucous in the bronchiolar epithelium

Asthma is an allergic inflammatory disease, which causes shortness of breath, wheezing and panting. Hypersecretion of mucus by histamine and musculature contraction of airway increase the resistant that leads to the inflammation of the bronchial tree. Studies found that TH2 stimulates DEP exposure, which is promoting to Interleukin- 17 protein and mucous production in the epithelium cell (8). Particulate matter increases the IgE (Immunoglobulin E) secretion, an antibody that concerned with the allergic reaction (31). PM can also increase acute airway inflammation that can lead to asthma flares (32).

Bronchitis is the second disease that causes persistent coughing syndrome and produces sputum expectoration. The severity of bronchitis can cause reduction of ciliary action (30). Release of ROS and cytokine followed by PM penetration leads to reduce the mucociliary action. (8)

The COPD represents the overall lung dysfunction emphasize chronic bronchitis, emphysema, and diseases related to airways (30).

4. SOURCES OF PARTICULATE MATTER

4.1 Sources of particulate matter in the ambient air

According to US EPA, particles with less than 10 μm in diameter, having both liquid and solid phase called airborne particulate matters, moreover particles with a diameter less than 2 μm or 2.5 μm are called fine particles, while others are called coarse particles. (13) This PM is generated from both in natural and artificial source distributed throughout the atmosphere. However, besides its classification according to size, PM is classified into primary and secondary particles based on its sources generation.

Naturally, formed PM is a component of polluted air, which can blow away from one place to another with the help of environmental medium, for example sea salt, can pass a hundred kilometers; a volcanic eruption can spread out miles after miles. Development of modern industries also contribute many ashes and Sulfur dioxide (SO_2) which are produced from petroleum with photochemical reaction. Reaction between nitrogen and hydrocarbon exhausted from combustion engines also contribute to the photochemical reaction, which produce Ozone, Peroxyacyl nitrate. These substances produce a kind of toxic smoke through the radiation of solar ultraviolet. By using diesel engines exhaust gases, photochemical reaction might be reduced but still smoke formed (33). Emission from vehicles also contains carbonaceous materials in both solid and gaseous phase. Potentially carcinogenic components PAH (polycyclic aromatic hydrocarbon) and trace metal are also a source of traffic emission (34).

According to international regulations such as EPA, EU or WHO, indoor air quality regulations have defined already a minimum concentration value for both coarse and fine particulate matter. However, it also differs according to spatially. The Asian region is trying to meet the value of the PM 10, whereas European Commission and US EPA are taking the plan to reach the optimum level for PM 2.5 μm . A comparison has been done in table 4.1 with the help of annual measurement of WHO Database (35). The studies are based on annual concentration level of PM in cities around the world. Few megacities have five times more concentration for PM 2.5 and PM 10 respectively than official limit of WHO including Karachi, Dhaka, Delhi, and Beijing.

Table 4. 1: Mass concentration of Particulate Matter throughout few mega cities.

Country	City/station	Annual mean, $\mu\text{g}/\text{m}^3$	Year	Annual mean, $\mu\text{g}/\text{m}^3$	Year
		PM10	PM10	PM 2.5	PM2.5
Pakistan	Karachi	273	2010	117	2010
Bangladesh	Dhaka	180	2013	86	2013
India	Delhi	286	2010	153	2013
China	Beijing	121	2010	56	N/A
Austria	Graz	30	2011	23	2011
Austria	Wien	27	2011	19	2011
Germany	Berlin	24	2011	20	2011
Finland	Helsinki	13	2011	8	2011
United States of America	New York- New Jersey-Long Island	23	N/A	14	2012
Australia	Sydney	9	N/A	5	2010

Much research has been done for source apportionment of PM using different methods such as receptor model, source-oriented model or emission inventories. These are used to illustrate the real-world measure measurement (36). A scientific publication studied source apportionment by using receptor models to show the comparison of emission sources. The research was done between 1990 to 2014 (publication year) with the help of the WHO database (35). Six main sources were identified throughout the all-scientific studies and grouped them by using receptor model. The traffic source is categorized by PM emission from the exhaust, organic and inorganic gases, wear of brake, linings clutch and tires (37).

Emissions of PM from traffic sources substantially differ from one location to another. Air pollution in the urban area are considered mostly by traffic contribution. Most studies measured traffic emission, for example, diesel soot and non-exhaust emission as a primary source of PM generation but do not consider the secondary inorganic sources of PM.

In some cities, traffic is the main contributor of PM throughout the urban and residential area especially in southeast Asia. Urban area also has a contribution of PM from traffic in Europe compared to other sources.

4.2 Particulate matter emitted from vehicles

Particulate Matter (PM) generated from traffic sources is significantly increasing nowadays in the urban and industrial area. The contribution of PM from the traffic sources can be divided into two different components:

- Primary and secondary particles from the exhaust
- Primary and secondary particles from non-exhaust sources (road, tire, and breaks including resuspension particle due to abrasion and resuspension) (34) (38)

The differentiation between exhaust and non- exhaust is quite difficult to distinguish as PM also form in the environment during fuel consumption and other operations of vehicles emit different groups of the particles. Therefore, not all sources of particles contain the same substances. The PM generated from exhaust systems is considered as that from the fuel combustion and has a legislative regulation. Non-exhaust emission, on the other hand, are disintegrated from the road, break, tires and surface abrasion (38).

PM emitted from the exhaust sources contain different hydrocarbons that are mainly ultrafine particles, contribute less in particle mass concentration (39). On the other hand, non-exhaust particles are composed of heavy metal including Zinc (Zn), Copper (Cu), Iron (Fe), Lead (Pb), which contain most of the particulate mass in PM 2.5 μm (40). In recent years, many local and international legislation make effort to reduce the exhaust emission (41). PM was added into the AQI (air quality index) list when it seemed the exhaust emissions from diesel cars seemed to be a major source of PM(42). As a result in the European Union region, where diesel vehicles are mainly popular, it came up with the regulation of DPF's (diesel particulate filter), which claimed to reduce the emission 99.3 % according to mass (43). New Euro 6 regulation commands that new diesel and petrol cars have to exhaust less than 5 mg/km (44). It is expected within next decade that the combustion engines might comply the regulations but the contribution of PM from non- exhaust sources is still a discussion topic. A review

has been done on 2016 predicted PM emission, which suggests that it might be increased more than 80 % in the next couple of years (41)

Generation of PM from the traffic pollution concerns many factors as there are a lot of sources of emission and also formation follows multiple steps and its surrounding effects. A study conducted in the Houston, USA demonstrated that organic and inorganic substances are generated from diesel and gasoline engines. Carcinogenic Polycyclic aromatic hydrocarbon (PAH), n- alkanes, and biomarkers are major parts of organic parts, whereas Zinc(Zn), Copper (Cu) and Barium (Ba) come as an inorganic component (7). A research group in California, USA noticed that large vehicles operated by a diesel engine are a major source of lighter PAH whereas light-duty gasoline vehicles were dominant sources of higher molecular weight PAH. Ultrafine size (<0.12 µm) and accumulation mode (0.12-2 µm) PAH is generated from diesel engines, whereas gasoline engines produced mostly ultrafine particles (42).

The contribution to quantify the exhaust and non-exhaust particles depends on the different receptor models or tools aimed to figure out source contributions from different sources of PM pollutants. Many authors identified road traffic as a source of exhaust emissions, whereas the crustal materials counted for the road dust or non-exhaust sources. A review study accounted different cities throughout the European region and interprets the variety of road traffic emissions, where only the traffic volume was considered rather geographical influences. The table 4.3 demonstrates the sources apportionments of exhaust and non-exhaust PM 10 and PM 2.5 in urban and rural areas. (34)

Table 4. 2: Sources attribution of PM from traffic sectors in different cities

City	Area	PM Size	Sources	(%) Mass contribution
Zürich	Urban	PM10	Exhaust	41
			Non-exhaust	38
Duisburg	Urban	PM10	Exhaust and non-exhaust	36
Barcelona	Urban	PM10	Exhaust	30
			Non-exhaust	16
Thessaloniki	Urban	PM10	Non-exhaust	28
			Exhaust	38
Athens	Urban	PM10	Exhaust	19–27
			Non-exhaust	25–34
Dresden	Urban	PM2.5	Exhaust and non-exhaust	43
Barcelona	Urban	PM2.5	Exhaust	43
			Non-exhaust	8
Birmingham	Urban	PM2.5	Exhaust and non-exhaust	35
Athens	Urban	PM2.5	Exhaust	27– 34
			Non-exhaust	18–27
Amsterdam	Urban	PM2.5	Exhaust and non-exhaust	30

4.2.1 Particulate matter from exhaust sources

Exhaust emissions are one of the major sources of PM and fine PM in the atmosphere (45). The sources of the particle are not always the combustion in the engine chamber, but heated vehicle tailpipes (due to exhaust gas after treatment) are also a source of particulate generation. Many more reaction processes take place behind the initial particulate generation and its emission.

Formation of particulate matter

The figure drawn below is a conceptual overview of particles emitted from engine exhaust and collected by the filter during passing through on it. It explains three most immediately striking aspects of particle formation labeled 'nucleation mode', 'accumulation mode' and 'coarse mode'. Particles from the atmosphere and motor vehicle emissions both exhibit tri modality properties. Coarse particles are changing their nature, as this mode includes, also, atypical rust and scale from the exhaust system, and mostly they are not emitted directly as such, but they can be formed by other two modes, they likely consist of a solid core with an outer layer of volatile material. (19)

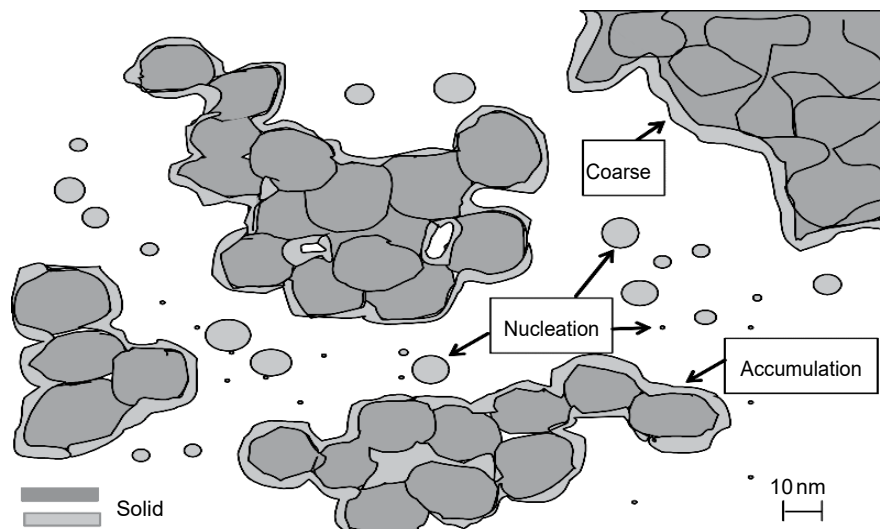


Figure 4. 1: The conceptual formation of PM from internal combustion engines including three layers of particle size. Coarse mode, accumulation mode, nucleation mode. (19)

Particles emitted as nucleation-mode look ambiguous, although admittedly this situation is unstable and changing rapidly. While some researchers suggest that nucleation-mode particles contain volatile material, others assume that the nucleation-mode is probably in solid form but this topic still has controversy and depends on the sources of the generation. (19)

The accumulation of mood particles formed by agglomeration of multiple primary particles is getting more attention nowadays because of its stable character. These primary particles are known as spherules, which resemble spherical but not exactly like that and having 20 nm to 50 nm diameter in size. These are known as building blocks of accumulation mood particles (19), which give the structure of accumulation mood particles. The accumulation could not be happened among a few numbers to thousands of particles. A viscous volatile or semi-volatile layer is coated over it, which can enter between the internal void spaces. These layers finally define the particulate's nature itself. The high

temperature is a convenient environment for the chemical reaction of various particles emitted from the engine exhaust until the end of the tail pipe. However, the rapid drop of temperature from the exhaust of the engine combustion to ambient air through tail pipe converts the volatile, liquid or gaseous component into the particular phase.

4.2.2 Particulate matter emitted from non-exhaust sources

Non-exhaust particles can be degenerated through a combination of thermal and mechanical stress, erosion, abrasion, friction and corrosion within tire, road and braking system, known as “wear”. These particles inherently have different chemical compositions than particles generated from the engine combustion. The friction of different stress among tires, breaks and road surface produces dissimilar particles ranging from fine particle to coarse size (19). Coarse particles present in the atmospheric aerosols that are more disposed to gravitational settling because of relatively less itinerary, but the contribution of road dust is increasing due to the frequent friction or agitation of a passing vehicle.

Roads

Repeatedly friction of the road surface by motor vehicles generates road-wear particle. These particles are identical then the road debris, which contain diversified particles dissected from non-road materials such as tire wear particles, by-products from combustion such as soot materials or PAH (polycyclic aromatic hydrocarbon) (46), road salt (47) and Lead (48). The frequent grounding by the wheels of passing vehicles and accumulated dust on asphalt makes a synergistic effect to enhance the concentration of particulate matter into the ambient air. One natural source of PM, especially during winter and autumn, is leaf fall. Most of these particles suspended cheerfully but frequent compounding by passing vehicles raise it. Therefore, gradual accumulation occurs at less agitated places such as road shoulder, alongside kerbs. Most of the coarse particles enrich the urban atmosphere from suspended particles, especially through the heavy-duty traffic, as the combustion is not the only source that is account for PM generation present in the street (49). During the winter studded tires and traction sand are also responsible for PM generation (50). These particles anti-skid and friction have few microns in size (51). A study has shown the controversy with continuous dust enhancement by friction rather they found the braking intensity also has an impact on PM contribution into the ambient air. The study observed the minor emission rate contributed from brake wear into the kerbside sampling where heavy braking at passenger cars generated 140 – 780 mg/km and 2-25 mg/km for PM 10 μm and PM 2.5 μm respectively (52).

Both bitumen and diesel combustion particles are simultaneously distinguished in urban streets (53). The bitumen consists of saturates, resins, aromatics, and asphalts. Asphalts are (53) black concrete layered with resins and desecrated into the oily mix (54). The composite mixture has a high molecular weight consisting of aromatic hydrocarbon, which also contains Sulfur (S), Nitrogen (N) and minerals at concentrated state.

Brakes

The braking system of a vehicle produces friction between the metallic disk and a polymer brake pad. The pad consists of polymer matrix infused with hard particles into it. When the pad grasps the metal disk during brake, it causes heavy friction between two surfaces and these solid particles are grinding and spread into the ambient air (55). There are also few factors that regulate these particle emissions including the wear moods, for example, the heat due to the degradation (56) and braking behavior like the grasping force and time (57). Copper (Cu), Barium (Ba), and Lead (Pb) are used as a metal for braking pads where Barium (Ba) is used as a filler. Other metals found from the brake wear dust is Silicon (Si), Aluminum (Al), Iron (Fe), and Carbon (C). A concentration of Lead (Pb) is supposed to have a carcinogenic effect (56).

Tires

Tires are composed of organic & inorganic compounds where the composite of styrene-butadiene rubber (SBR), polybutadiene and natural rubber make an elastomeric polymer that is implanted with carbon black (58). A study conducted in a tunnel traced <2.5 % of SBR in ambient air and surface of the tunnel (59). The organic compounds used as tire wear having less molecular weight than diesel and bitumen (53) and in studded tires contains tungsten in the winter area (60). Inorganic materials Sulfur(S), Zinc (Zn) and Silicon (Si) used as a combined solution for the tire. Sulfur (S) is used through vulcanization of rubber. Zinc (Zn) and Silicon (Si) are added later on as a cross-linked compound of Sulfur (S) supporting filler during these processes. (61).

During the friction between road surface and tire, apparently 10 % of the tire and 30 % of the tire tread are dissected into the ambient environment (58). The rate of erosion depends on the driving style and during the turning or acceleration when maximum friction happens, but the wearing away depends on many factors that variate the range from 10 µg/km to 70 µg/km referenced to a study group (62). Another study group found a correlation between the discharge of accumulation or nanoparticle plausibly when the tires heated, after continuously repeated friction.

5. CHARACTERISTIC OF AEROSOL PARTICLES

5.1 Chemical composition of particulate matter

The chemical composition of aerosol particles is not well established. A four-layered conceptual model is discussed in figure 2. In the beginning, the filter can capture almost everything when the exhaust gas is passing through it, except the condensed water; this is the legislative definition of 'particulate'. Water droplets contain minute solid particles and absorb soluble combustion products such as aldehydes and ketones. While heated, some material evaporates, and some does not; or in other words, some material dissolves in certain solvents, and some don't. This divides the particulate matter into two different groups. One that is volatile or soluble, and another, which is nonvolatile or insoluble. Afterwards, there are five subgroup names: Sulfates, Nitrates, Carbonaceous, Organics and Ash (19). As shown, the chemical composition figure 5.1 corresponds to a large degree to the physical representation.

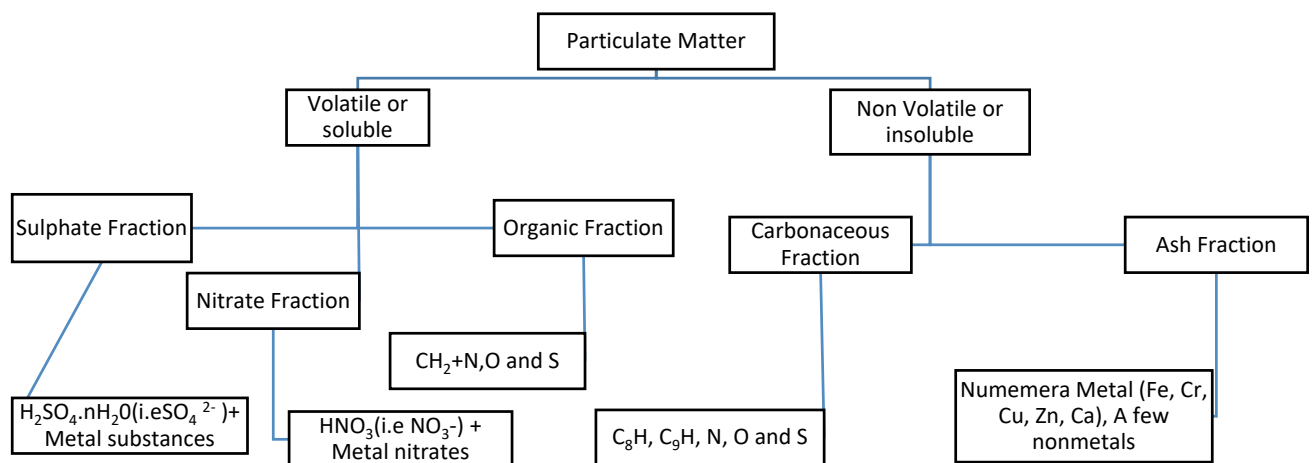


Figure 5. 1: Chemical composition of PM likely from conventional engines.

Among the mentioned five fractions, two of them, Ash and Carbonaceous, are produced within the engine; the other materials form later, in the exhaust system or, more probably, when the exhaust mist enters the surrounding air, though, of course, important precursor reactions must first take place within the engine.

5.2 Size, shape & diameter of particulate matter

Particle size determines the behavior of an aerosol particle, whereas some of them are strongly related to these properties. This is not only defining their physical properties but regulates their characteristics that are changed according to their particle size. For measuring the particle size, particle diameter or particle radius is considered. In general, the unit micrometer (10^{-6} m) is used for measurement, but nanometer is also used for particle sizes less than $0.1 \mu m$. The particle diameter is expressed by the symbol d_p . Different sources of particles have different sizes. Figure 5.2 illustrates the particle sizes ranges from $0.001 \mu m$ to $1000 \mu m$. It includes the invisible gas molecules to visible millimeter sized particles. The aerosol particles are shown in this figure between $0.01 \mu m$ to $100 \mu m$ ranges. Ultrafine particles cover the range from $0.001 \mu m$ to $0.1 \mu m$. Particles having a diameter less than $50 \mu m$ are called nanoparticles. The largest aerosol particle type is visible grain, which is visible

under normal condition and has a size range of 50 – 100 μm (18). For better understanding of particle size, figure 5.3 expresses a comparison between a human hair with particulate matter PM 2.5 μm . The average human hair become 70 μm in diameter, which is 30 times larger than PM 2.5 μm .

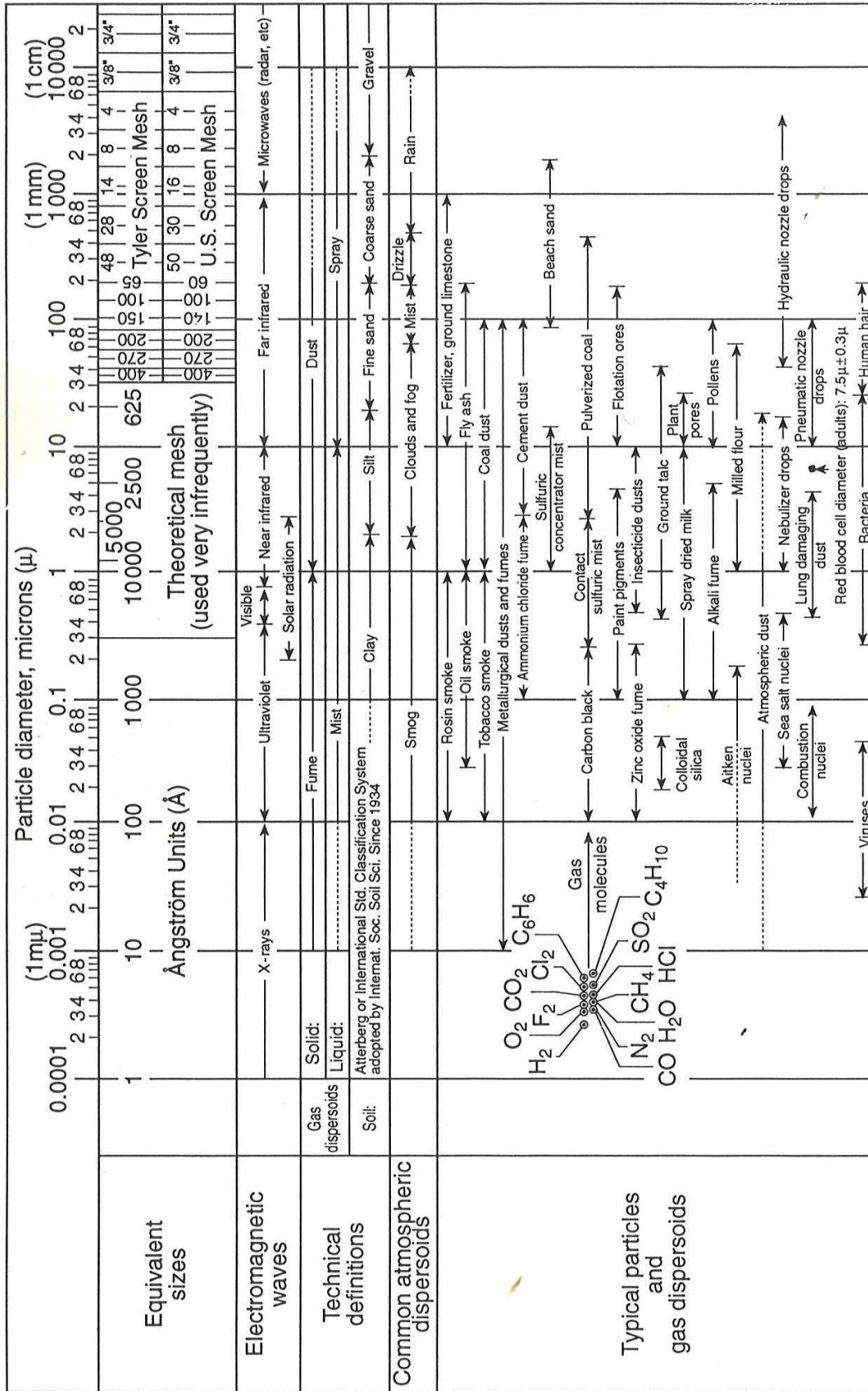


Figure 5. 2: Particles and their size ranges. (18)

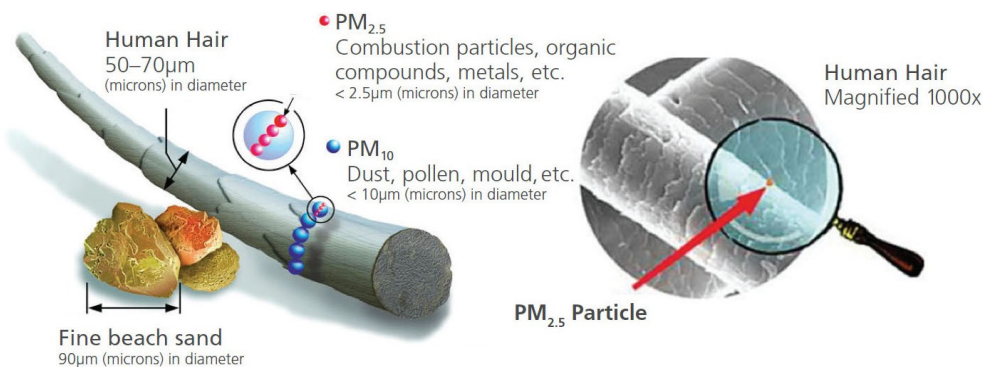


Figure 5. 3: Comparison of particle diameters with a human hair. (63)

Liquid particles have an almost spherical shape and diameter but solid particles have numerous dimensions and uniformity that makes it very difficult to categorize their properties and behavior. A strategy is to consider each particle as a sphere shape and measure its diameter thereon. The aerodynamic diameter is the key characteristics of particles for determining filtration, respiratory deposition and mostly required for air cleaning strategies. This is not decided always by geometrical diameter, but particle behavior when forces are applied to it. It is more important to know the size and shape to access characteristics rather only examine their appearance under electronics microscope.

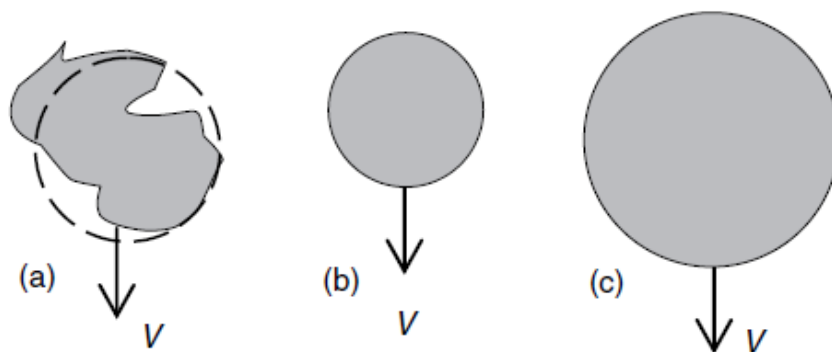


Figure 5. 4: (a) An irregular shaped particle superimposed equivalent diameter, (b) Stokes equivalent diameter, (c) aerodynamic equivalent diameter (spherical shape with unique density). (18)

Different particles come in an infinite variety of shapes. Therefore, there have been numerous proposals on how to uniformly describe and categorize a particle. A common practice is to consider each particle as a perfect sphere, defined by its diameter d_p . For liquid particles, this is usually a valid assumption, as they nearly always come in spherical droplets. Solid particles, however, come in the most complex shapes, making it hard to describe them uniformly.

Equivalent diameter estimates ideal properties for particle behavior measurement. Figure 5.4 describes different particle shapes and their influences. In figure 5.4 (a), an irregular shaped particle

is superimposed by volume-equivalent diameter. In figure 5.4 (b), the Stokes equivalent diameter is shown that follows the same density and settling velocity as the particle, whereas the electrical-mobility diameter refers to the velocity of a charged particle when moving in an electrical field, as referenced to the strength of that field. Figure 5.4 (c) shows the aerodynamic diameter, which has the same settling velocity as Stokes equivalent diameter but has the unit density. The aerodynamic diameter defined as the diameter of a spherical particle d_p with a density of 1000 kg/m^3 and settling velocity like the density of a water droplet. The standard bulk density ρ_0 is defined as the density of water with 1000 kg/m^3 . (18)

To calculate the aerodynamic diameter from the particle diameter used, the following formula can be applied:

$$d_a = d_p \left(\frac{\rho_p}{\rho_0} \right)^{1/2} \quad (5.1)$$

Where,

d_a = aerodynamic diameter (m)

d_p = particle diameter (m)

ρ_p = particle density (kg/m^3)

ρ_0 = standard particle density (density of a water droplet) (kg/m^3)

5.3 Transportation of aerosol particle

5.3.1 Reynold's number

Reynolds number is a dimensionless number that explains the characteristics of aerosol particle into the airstream. It is defined as the ratio between inertial forces of the aerosol particles to the viscous forces of the gas molecule (18). So, the Reynolds number Re can be written as:

$$Re = \frac{\rho v d}{\eta} \quad (5.2)$$

where,

Re = Reynolds number (dimensionless)

ρ = density of the gases (kg/m^3)

v = velocity of the gas molecules (m/s)

d = diameter of aerosol particle (m)

η = Viscosity of gas molecule ($\text{kg/m}\cdot\text{s}$)

The Reynolds number provides information of the aerosol flow pattern, whether a flow of aerosol particles through the gaseous medium would be laminar or turbulent. The ratio indicates the flow

resistance equation for a given situation. It explains the pattern or path equality of the gas flow surrounded by an object.

The Reynolds number depends only on the relative velocity between an aerosol particle and the surrounding gas molecule (18). To describe the flow regime, if the Reynolds number is $Re < 1$, the flow would be laminar, whereas high Reynolds numbers represent the turbulent flow. Laminar flow is characterized by negligible inertial forces and thus referred to as viscous flow, while on the other hand turbulent flow is called inertial flow.

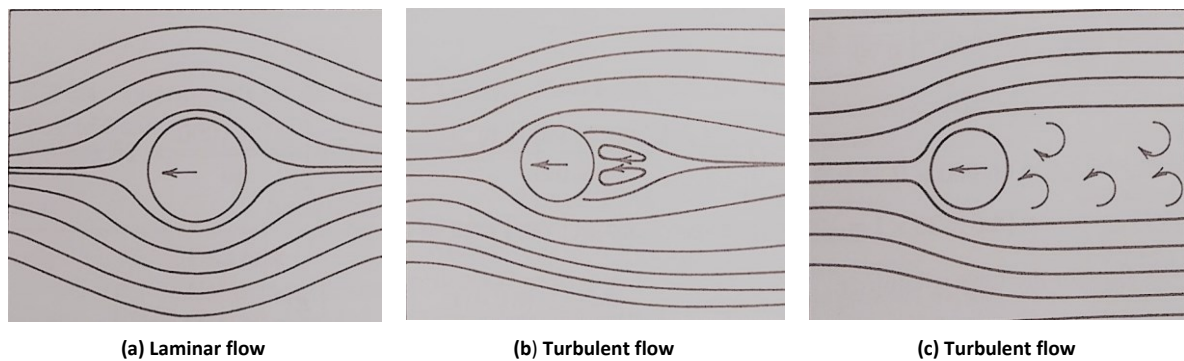


Figure 5.5: Explanation of Reynolds number (18)

Above figure illustrates the flow following the Reynolds numbers of (a) $Re = 0.1$, (b) $Re = 2$ and (c) $Re = 250$.

5.3.2 Settling velocity

When a particle starts settling down through the free air, the gravitational force is applied to the particle and the velocity increases. In time, the gas molecules start drag forces against the gravity, which acts against the free flowing of the particle. When these two forces become equal to each other, the net velocity is reached at zero and the velocity gets constant. This phenomenon is defined as the settling velocity (18). If the drag force against the particle F_d , is equally, same and opposite to the gravity force F_g , then settling velocity can be written as

$$F_g = F_d = mg$$

Usually, the gas molecule has a negligible density compared with the particles present in the air. For a free flowing particle, by applying the Stokes dragging force, the terminal settling velocity is defined as

$$V_{TS} = \frac{\rho_p d_p^2 g}{18\eta} \quad (5.3)$$

where,

V_{ts} = terminal settling velocity (m/s)

ρ_p = particle density (kg/m^3)

g = gravitational force (m/s^2)

d_p = particle diameter (m)

This condition can be explained by the Reynolds number when it is $Re_p < 1.0$. Usually, the aerosol particles encounter with the dragging force when it is $Re < 1.0$.

5.3.3 Peclet number

The Peclet number provides the information of particle transport process through a fluid. The Peclet number is defined as the ratio between mass transports due to the advection of particles to the mass transport to diffusion of particles. The term advection defined as the bulk flow of aerosol stream in a characteristic length is determined by the product of flow velocity and length. According to Hinds (18) the Peclet number is defined as,

$$P_e = \frac{d_f U_o}{D} \quad (5.4)$$

where,

P_e = peclet number (dimensionless)

d_f = characteristic length (diameter) of fiber (m)

U_o = free stream velocity (m/s)

D = diffusion coefficient (m^2/s)

5.3.4 Slip correction factor

It is assumed from the Stokes law that the relative velocity of the air at the particle surface is exactly zero when the medium is continuous. When particles getting smaller, the gas molecules are moving around the particles and possibly missed the friction with the particles, which is called "slip". As the particles are getting no collision with the air molecules, the velocity of the air at the particle surface is no longer zero. Such particle settlement is faster than those according to the predicted resistance law. If the particle size is smaller than the mean free path $< 1\mu m$, then the slip factor is significant. The drag force then decreases, whereas the settling velocity increases (18). This effect can change the settling velocity and drag force and is considered by adding a slip correction factor.

For drag force,

$$F_D = \frac{3\pi\eta V d_p}{C_c} \quad (5.5)$$

F_D = drag force (N)

V = velocity of particle (m/s)

d_p = particle diameter (m)

η = viscosity of gas molecule (kg/ m. s)

C_c = Cuningham correction factor

And settling velocity,

$$V_{TS} = \frac{\rho_p d_p^2 g C_c}{18\eta} \quad (5.6)$$

where

V_{TS} = settling velocity (m/s)

d_p = particle diameter (m)

η = viscosity of gas molecule (kg/ m. s)

ρ_p = particle density (kg/m³)

C_c = Cuningham correction factor

For both formularies, Cuningham correction factor is applicable when Reynolds number $Re > 1$.

5.3.5 Brownian motion and diffusion coefficient

When aerosol particles are in wiggling motion throughout the still air due to random variation in the relentless bombardment of gas molecules, this is called Brownian motion. Diffusion is defined as transportation of particles from higher concentration to lower concentration. Both of these methods are characterized by the particle diffusion coefficient D . This constant is directly proportional to the number of particles traveling through the unit area. Diffusion of aerosol particles is defined as the net transport of particles in between regions of different concentrations. To characterize this transport process, the diffusion coefficient D was introduced. A high value of D implies the intense of Brownian motion and a rapid mass transfer from a region of higher particle concentration to a region of lower particle concentration. A practical way to obtain the diffusion coefficient is the Stokes-Einstein equation that can be expressed as:

$$D = \frac{kTC_c}{3\pi\eta d_p} \quad (5.7)$$

Where,

D = diffusion coefficient (m²/s)

d_p = particle diameter (m)

T = absolute temperature (°C)

K = Boltzmann's constant (J/K)

C_c = Cuningham correction factor

The above equation represents a proportional relationship between the diffusion coefficient with the temperature and the slip correction factor. A higher temperature T stimulates the particle movements within the gas medium. The particle diameter is inversely proportional to the diffusion coefficient, which means that the smaller particles have greater influence of diffusion properties. The slip correction factor gets less on smaller particles, which has a proportional relationship with the diffusion coefficient.

5.4 Particle size distribution

Particle size distribution is a method, which illuminates the spread of different sizes of particles according to their characteristic value like number, mass or volume. As a number of a particle population with different sizes is large and complex to evaluate, particle size distribution breaks down the total number into different size intervals or classes that are calculated based on the frequency of occurrence. (33)

It is quite rare that particles are found in uniform size except they are prepared intentionally in the laboratory. On the other hand, an aerosol containing more than one particle size is called polydisperse. These are particle distributions as present in the ambient air. In order to explain the particle behavior and characteristics of their size distribution, it is necessary to use mathematical expressions properly. Monodispersed particles have narrow spread like 10- 20% with a geometric standard deviation $\sigma_g < 1.2$ (64), whereas polydisperse aerosols maintain geometric standard deviations $\sigma_g > 1.2$ (65).

In order to characterize polydisperse particles, three different size modes were developed according to Whitby (1978) named nuclei, accumulation and coarse mode (64). Each mode interprets distinct formation and characteristics of particles.

The nuclei mode particles contribute to the least particle size and mass concentration. The usual particle size ranges between 0.005 – 0.1 μm . This class encompasses the highest number of unstable particles with the lowest number of mass concentration.

The accumulation mode particle class lies between 0.1 – 2 μm . Particles in this mode are structured and stable, which contribute to the main particle mass of the fine particles (64). Mostly anthropogenic combustion produces the accumulation mode particles. Two intermediate mode particles named condensation and droplet mode having diameter 0.2 μm and 0.7 μm respectively. When gases molecules condense, the nuclei mode particles start coalescences with each other. These phenomena are continuing till the particle size reaches 0.2 μm . Another mode is called droplet because it shows humid in nature having an average diameter from condensation mode to 0.7 μm (66). The PAH (polycyclic aromatic hydrocarbon) and elemental carbon emitted from the vehicles are present in this size range nearly 0.1 μm and 0.7 μm respectively (67).

The average coarse mode particle diameter stated in Whitby and Sverdup study is $6.3 \pm 2.3 \mu\text{m}$ (64). However, particles larger than the mentioned size are called giant coarse mode in this study, but another research group has a controversy with average coarse diameter. They measure an average coarse mode diameter of 20 μm (68) μm , but it is agreed that the particles of more than 2 μm diameter are considered as coarse particles. These particles getting less interest because the respiratory

cutpoint diameter is close the accumulation mode particles and the sampling problem for their inertial characteristic (64).

In order to express the particle behavior, many statistical methods are available. Polydisperse particles present in the environment are seldom symmetrical, but normally have a wide range of distribution and positively skewed shaped with a long tail. The normal (or gaussian) distribution is a supreme choice for expressing any measurement uncertainties that could have both positive and negative values. This distribution is only suited if the all particles are nearly similar size like monodisperse aerosol (64). Contrariwise, the polydisperse aerosols do not follow the normal distribution method because obviously the particle size would not have negative values. The universal method for illustrating is the log-normal distribution (19) (64) (33) (65), which supports specific coagulation from smaller objects into the larger ones (69). The log-normal distribution is a mathematical expression by geometric mean diameter d_g and geometric standard deviation σ_g , geometric mean diameter can be defined as follows:

$$\log(d_g) = \frac{\sum_{i=1}^N n_i \log(d_i)}{\sum_{i=1}^N n_i} \quad (5.8)$$

where,

d_g = geometric mean diameter

d_i = midpoint of particles diameter of the i_{th} class.

N_i = number of particles in a group i having midpoint size

N = total number of particles in an interval

And geometric standard deviation:

$$\log(\sigma_g) = \sqrt{\frac{\sum_{i=1}^N n_i (\log(d_i) - \log(d_g))^2}{\sum_{i=1}^N n_i - 1}} \quad (5.9)$$

where,

σ_g = geometric standard deviation

d_i = midpoint of particles diameter of the i_{th} class.

n_i = number of particles in a group i having midpoint size

N = total number of particles in an interval

5.5 Particulate mass concentration vs particulate number concentration

When all regulation regarding air quality getting worried about particulate mass concentration, there is a lack of defined specifications concerning particulate number concentration (70). A study examined that the density of particle number concentration was much higher to the vicinity of highway and reducing the density when the increase of the distance from the highway. The presence of nucleation mood particles with a mean diameter of 13 nm was dominating at the highway and disappear just after 90 m with domination of the larger particles (71).

The fact of hazardness PM is due to the smaller diameter. The increasing awareness regarding traffic emission is about PAH (polycyclic aromatic hydrocarbons), which are directly or indirectly responsible for carcinogenic effects in the respiratory system. This PAH is the fine particulate matter that does not represent the actual quantity when measuring the particular mass concentration. The increase of the particular mass concentration is a consequence of reducing the air transparency (70).

The correlation between particle mass and their number is interesting and could slightly differ because of the measurement method, sampling technique. Nevertheless, it is agreed by a study group that for determining the correlation only one methodology should be used. The particle density for the aerodynamic diameter is 1 g/cm^3 and only this criteria is well established and accepted (18). A study was performed to show the relationship between mass and number in a static condition (70).

Table 5. 1: Relation between particle mass and particle number concentration (70)

Particle Mass (g)	Particle Diameter (μm)	Particle Number (millions)
1	1000	0.002
1	100	2
1	10	2000
1	1	2000000
1	0.01	2000000000

The important perception between the mass and number correlation illustrates that the maximum number of particles exists in the nucleation mood, though the accumulation particle contains the majority of mass. The transportation of these nucleation mood particles follows the diffusion mode, whereas the accumulation of mood particles follow the inertial method. More details regarding the particle movement and deposition are discussed in chapter 6: Filtration mechanism. In this way, the fine and ultrafine particles should be getting more concentration as this reflects much harmful effects. (19)

However, the nucleation mood particles have a higher quantity than the accumulation or coarse particles, but the only measurement of number concentration of nucleation mode particles can overwhelm an experimental value. Indeed, only the measurement of the notoriously volatile and ambiguous structure of nucleation particles does not always express a meaningful and trustworthy overview of a polluted environment. On the other hand, the solid structured accumulation mode particles more likely reflect the consistent impression. (19)

6. FILTRATION MECHANISMS

The filtration process of aerosol particles has been the topic of extensive research in the past. However, even though the basic underlying principles are well understood, there is still a remarkable gap between theory and reality. Considering atmospheric aerosol concentrations, the most efficient, inexpensive and simple means to achieve a high capture rate are fibrous filters. However, as they also implicate a high-pressure drop in order to achieve a high filter efficiency, a recent practice is to additionally apply an electrostatic charge on the fibers, combining mechanical and electrostatic filter effects. Using this technique, it is possible to get rather high capture rates at low-pressure drops. The main disadvantage of this practice is that, in contrary to the mechanical collection efficiency, the electrostatic collection efficiency decreases during lifetime. It is very complex to accurately measure the electrostatic filter effect, as it is influenced by many parameters.

6.1 Types of filters

6.1.1 Fibrous filters

For filtering the aerosol particles, fibrous and porous membrane filter are mostly used. Most common types are cellulose fibers (wood fibers), glass fibers, and plastic fibers. They are consisting of fibrous and are arranged perpendicularly to the direction of airflow. The fibers range in size from submicrometer to 100 μm having porosities from 70% to more than 99%. The air velocity through high-efficiency filters is usually quite low, about 0.1 m/s. (18) Filtration through this microscope sieve does not mean that the hole only retains the particles larger than the pore size during the particles pass through it. This might be fulfilling the concept of liquid filtration of solid particles but does not explain how aerosol particles pass through the filter. Fibrous filters capture particles rather by collision and adhesion. Each fiber has a certain probability of capturing particles, depending on numerous characteristics of the aerosol and the fiber itself.

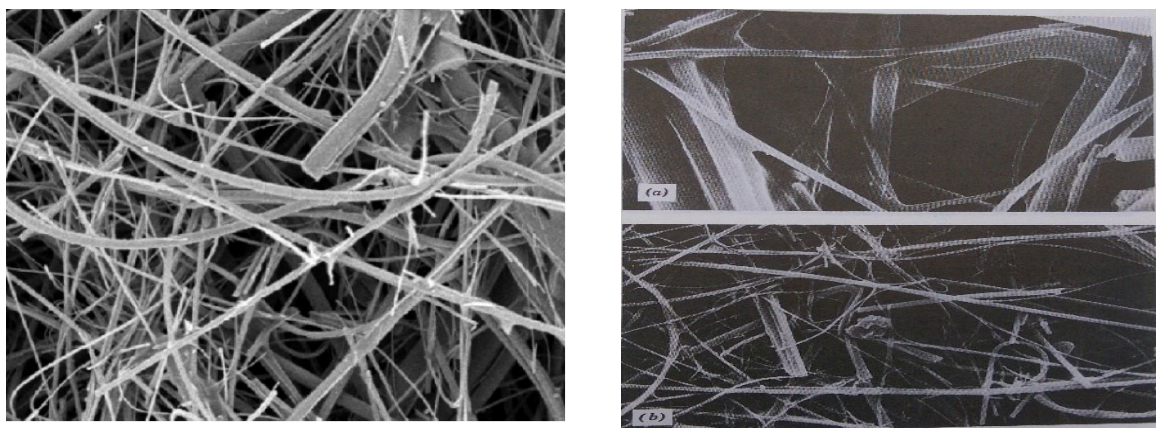


Figure 6. 1: Microstructure of a glass fiber filter taken by Electronic microscope(18)

6.1.2 Membrane filters

Membrane filters are structurally different with fewer pores than a fibrous filter. A gel-like material made from nitrocellulose acts as the main part of the filter. The combination of ether alcohol and nitrate esters formed a gel-like colloidal solution which provides relatively uniform tortuous pores structure throughout the filter (33). Series of layers are overlapped to provide its construction. The filter composed of cellulose esters, polyvinyl chloride, Teflon, sintered metal and other plastics. The usual pore size is $0.02 - 10 \mu\text{m}$ with thickness range $0.05 - 0.2 \text{ mm}$ (64). The porosity is less than 85 % of its structure which is 50 to 90 % less than a fibrous filter. Due to its structure, the pores aren't regular shaped and air flow through the filter doesn't follow a regular path. Though this filter has high-efficiency rate but not recommended to use due to high pressure drop and low tensile strength.

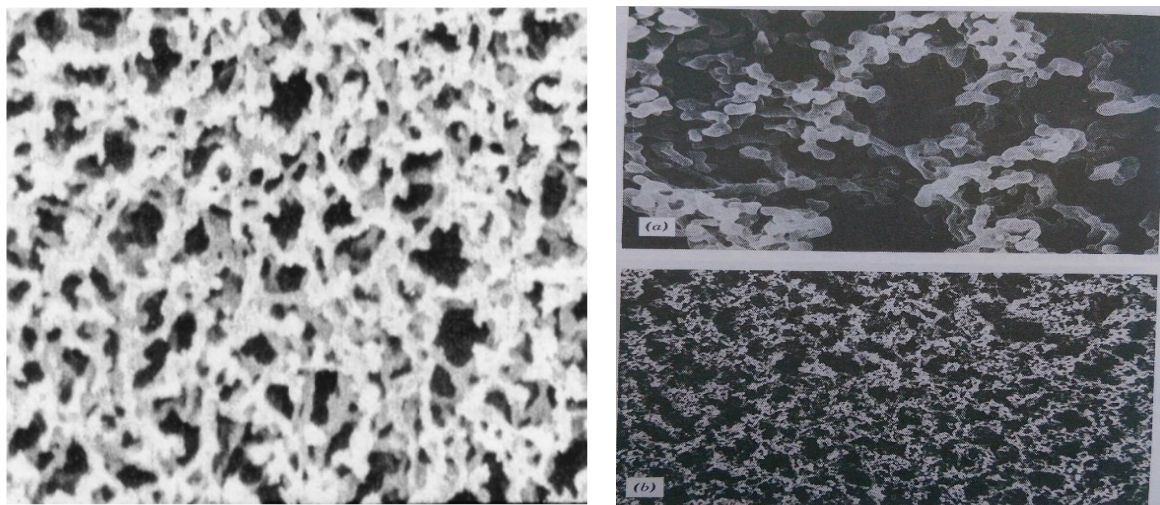


Figure 6. 2: Electron micrograph of a membrane filter(18)

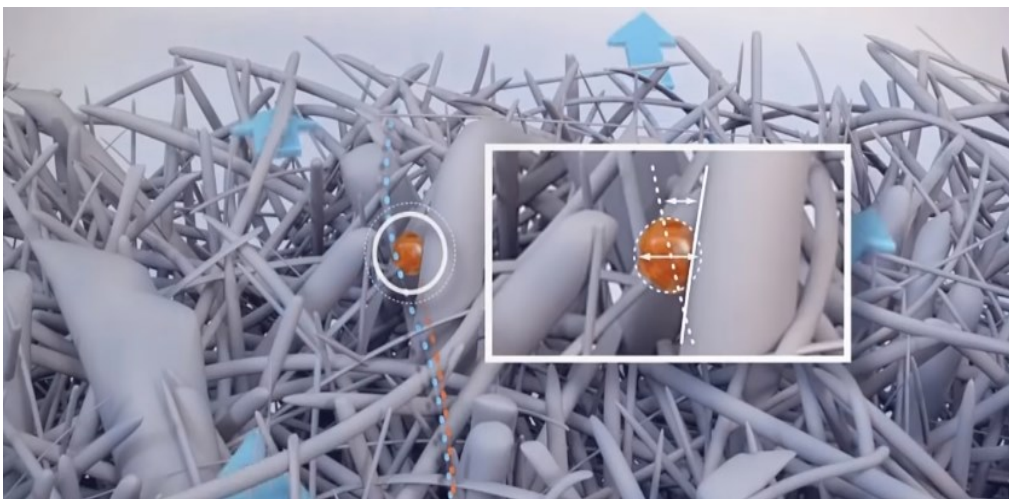
6.2 Deposition mechanism and efficiency of fibrous filters

To elucidate the deposition mechanism of the filter, a set of mathematical equations is used to represent the characteristics – in all types of applications, if it is in the lung, in a simple tube or the air cleaner. In all situations, these principles express the same methodology. These are divided into two groups, one called mechanical collection group and another one electrostatic attraction. (18)

1. Interception
 2. Inertial impaction
 3. Diffusion
 4. Gravitational settling
 5. Electrostatic attraction
- } Mechanical effects

6.2.1 Interception

Fibers are arranged randomly inside a fibrous layer. Particles having larger radius than the fibrous pore and thus are captured by sieving effects. However, this is not the actual work filter always does. Nevertheless, if the particles are light enough to follow the streamline, but their radius is larger than the distance between the fibrous layers, they are captured by the fibers. This effect is called interception deposition (33). Figure 6.3 illustrates the interception mechanism of a particle on the fiber surface. The shape of fibers inside the fibrous layer is considered as cylindrical. So, interception is effective when particles size is getting larger. In figure 6.3, r_f and r_p is the fiber radius. Particles present between r_f and r_p+r_f are presumably to retain within filter media.



(a)

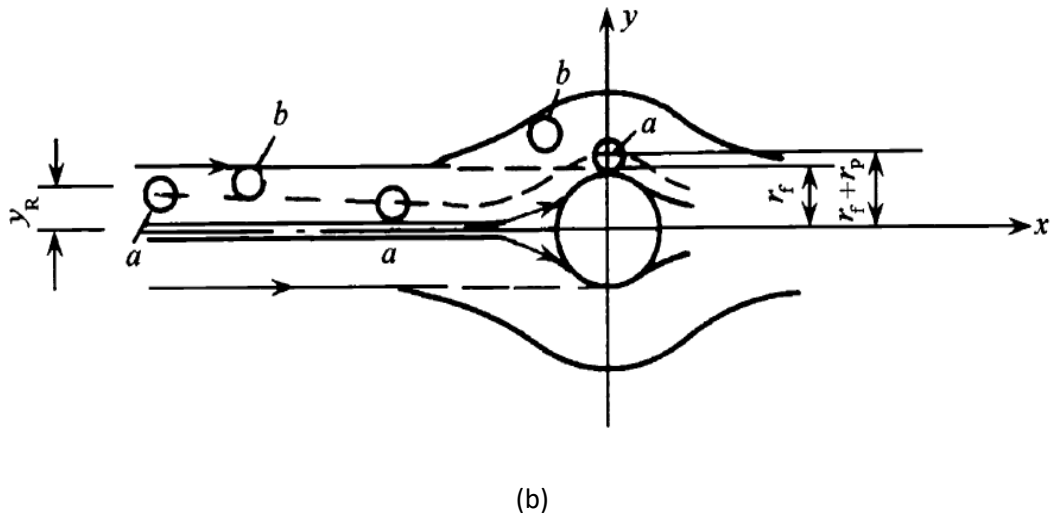


Figure 6. 3: Interception mechanism of the fibrous filter a(72) , b(33)

As the width of the airstream above, the fiber is smaller than the width of the air stream fiber faced. The interception efficiency R is the ratio between particle number per unit time present in the unit length of the fiber surface and total particle number in the streamline heading to the fiber.

$$E_R = \frac{y_r}{r_f} \quad (6.1)$$

Where

E_R = interception efficiency

y_r = the distance between fiber axis and the effective particle trajectory at infinite, where particles presumably are captured (m)

r_f = fiber radius (m)

So, normally the interception efficiency presumably less than 1, but could be 1, if the ratio between the particle concentration in air stream becomes equal with the flow rate. This is considered as the 100% interception efficiency.

6.2.2 Inertial impaction

The air stream flows frequently around the complex fibrous layers. When the particles have larger masses, by virtue of their inertia, they get the higher velocity and could not change the direction rapidly with the air stream around the fiber. Consequently, those particles are departed from the streamline and collide due to the particle momentum with the fibers layer and tend to deposit on it. If the inertial efficiency is increased, the interception efficiency is increased as well. (18) The dimensionless parameters, which are known as Stokes Number can explain the inertial effect of particles with

$$Stk = \frac{\tau U_o}{d_f} = \frac{\rho_p d_p^2 C_c U_o}{18 \eta d_f} \quad (6.2)$$

where,

S_{TK} = Stokes number (dimensionless)

d_p = particle diameter (m)

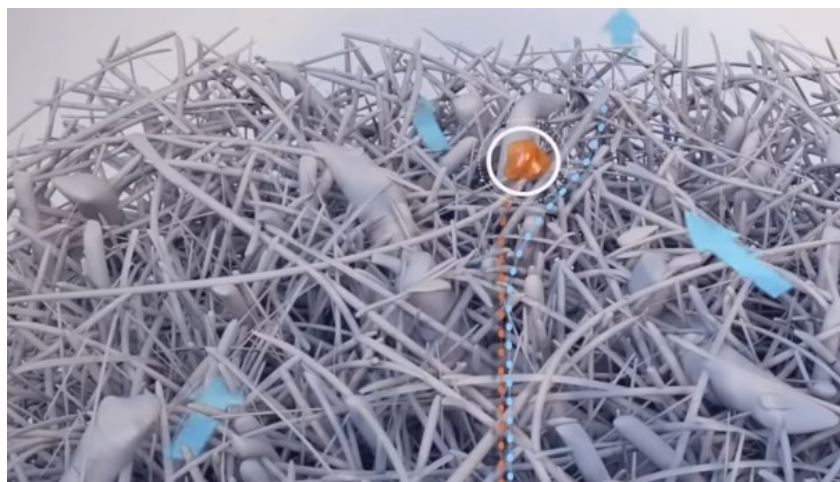
η = Viscosity of gas molecule (kg/ m. s)

ρ_p =density of the particle (Kg/m³)

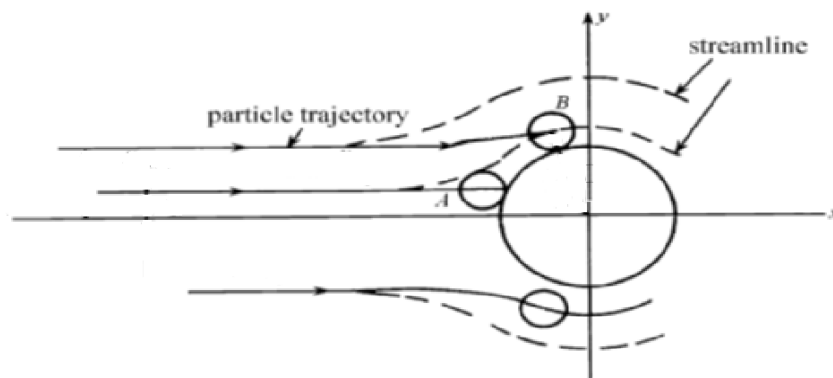
U_0 = free stream velocity (m/s)

d_f = fiber diameter (m)

C_c = Cuningham correction factor



(a)



(b)

Figure 6. 4: Inertial impaction of the fibrous filter a(72), b(33)

The Stokes constant Stk is a dimensionless number, which is proportional to particle diameter, air velocity and density. Therefore, the inertial efficiency is increased when particle diameter, air velocity and density are increased. If no inertial force is ($Stk = 0$) implicated on the particle flow, the particle will follow the airstream accordingly. When the inertial force is small enough, which is unable to

distract the particle from the air streamline and settled into the fiber surface, inertial efficiency would be close zero. Less fiber diameter become distort due to the air velocity, which is explained by the Kuwabara hydrodynamic factor. The single-fiber collection efficiency due to inertial impaction (E_I) is described by Hinds (18):

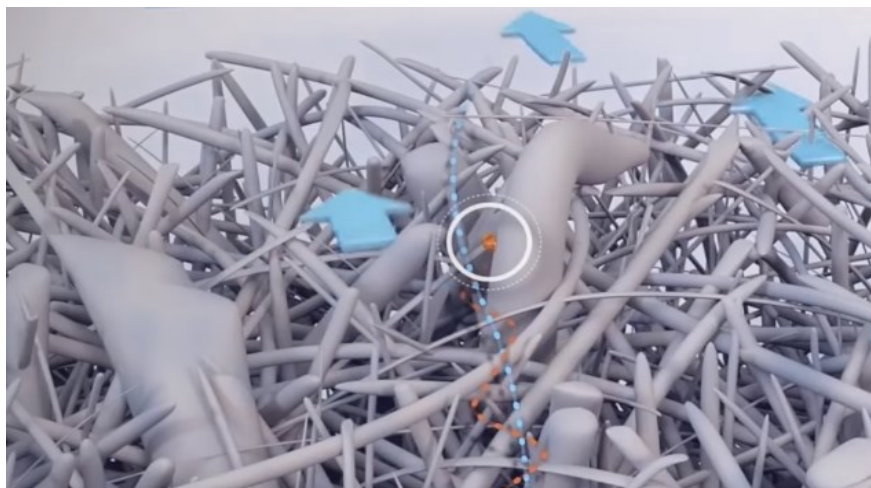
$$E_I = \frac{(Stk)J}{2Ku^2} \quad (6.3)$$

Where, $J = (29.6 - 28 \alpha^{0.62})R^2 - 27.5R^{2.8}$ for $R < 0.4$. The value of J is defined, but when $R > 0.4$ it becomes critical for calculation. In this case, $J=2$ is recommended according to Hinds (18).

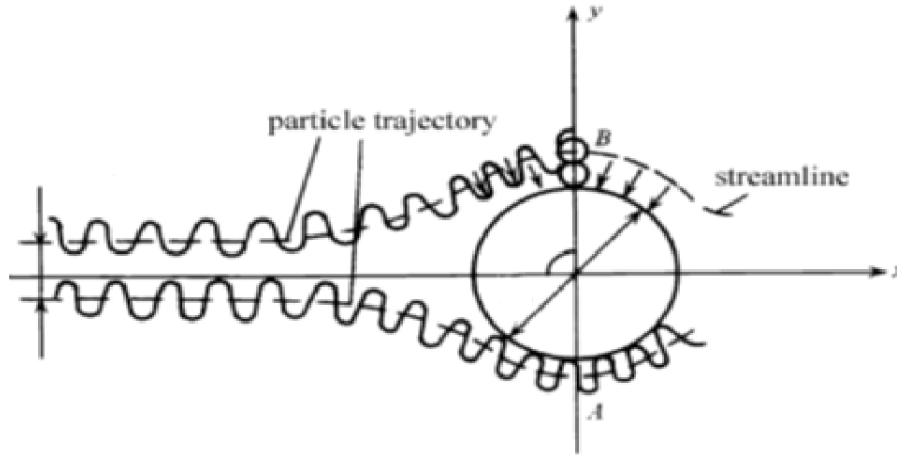
Ku = Kuwabara hydrodynamic factor explains the distortion of the fiber field.

6.2.3 Diffusion

As impaction and interception apply to particles of adequately high inertia, they are still insufficient in describing the movement of particles subject to Brownian movement (discussed in 5.3.5). Similar to highly inert particles, small particles are not able to follow their streamlines always (18). The inertia of smaller particles influences them to deposit on a single fiber by Brownian motion. The random movement of smaller particles enhances the probability of collision with the fiber and hence the deposition. The deposition is inversely proportional to the particle diameters. The diffusion efficiency E_D for a single fiber can be derived from the dimensionless Peclet number (Pe) (explained in 5.3.3), which describes the ratio between the advection of the aerosol transport due to the diffusion. The term advection is defined as the transfer of the aerosol flow by its motion. This behavior increases their probability to be captured by a fiber.



(a)



(c)

Figure 6. 5: Diffusion mechanism of the fibrous filter a(72), b (33)

Using the concept of the Peclet number with respect to the fiber diameter, the Peclet number is calculated as:

$$Pe = \frac{d_f U_o}{D} \quad (6.4)$$

To get the single-fiber efficiency due to diffusion E_D , Kirsch and Fuchs proposed the following expression (18):

$$E_D = 2Pe^{-2/3} \quad (6.5)$$

Peclet number (Pe) increases with higher flow velocities; particle collection due to diffusion is more likely to happen at lower face velocities. From the equation 6.5, the diffusion efficiency is increased when Peclet number (Pe) and particle size d_p decrease. This is the only filter efficiency that increases if the particle sizes decrease. The particle does not deviate from the air streamline like other efficiency, but deposit only through diffusion effect. However, the diffusing particles are also more likely to be captured by interception. The flow towards the fiber make distortion and passes around the fiber surface. The dimensionless Kuwabara hydrodynamic factor explains the effects of distortion of the fiber due to airflow on the fiber surface. So, the interaction term has to be included to calculate the total diffusion efficiency. Then equation could be written as follows (18).

$$E_{DR} = \frac{1.24R^{2/3}}{(ku Pe)^{1/2}} \quad (6.6)$$

Where

E_{DR} = the collection efficiency for enhance diffusion on to the fiber

Ku= Kuwabara hydrodynamic factor explain the distortion of the flow field

R = interception efficiency

Pe = Peclet number

6.2.4 Gravitational settling

Compared with the other deposition mechanisms, particles are less likely to deposit following Gravitational mechanism. Particles show settling effect only when they have larger particle diameter d_f and less particle flow. However, if the particle has a velocity of more than 0.1 m/s, impaction deposition has dominant effect above settling effect. The dimensionless number that represents the number of deposition due to gravitational settling is G , which is the ratio between settling velocity and airflow velocity. (18)

$$G = \frac{V_{TS}}{U_o} \quad (6.7)$$

where,

G = gravitational settling parameter

V_{TS} = terminal settling velocity (m/s)

U_o = free stream velocity (m/s)

The overall gravitational velocity was then calculated by Fuchs in addition to the interception deposition along with Gravitational deposition. Depending on the geometry, U_o and V_{TS} are oriented towards each other in a certain way. Downward airflow means they are in the same direction. The single fiber efficiency for settling E_G is

$$E_G = G(1 + R) \quad (6.8)$$

For airflow goes from opposite direction or upward to V_{TS} ,

$$E_G = -G(1 + R) \quad (6.9)$$

6.2.5 Electric filters

This mechanism is completely different from the mechanical deposition because it works by the charges between particles and the fibers. This creates an electrostatic effect, which attracts the particles to the fibrous filter. The charges generated from the friction between particles and fibers are not such strong and lasting for prolonged time unless the intentional charge is applied to the fibrous media. The theory of the electric filter is to charge the particles and oppositely charge the fiber. This creates a coulombic attraction between the oppositely charged particle and fiber. The neutral particles can also be captured by charged fiber. The charged fiber generates a dipole into the particles. These particles then get captured by randomly charged fibers (18).

6.2.6 Efficiency of an isolated fiber filter

The efficiency that calculates the fraction of particles towards one single fiber is stated as E_Σ , which is the ratio between actual particle number deposited in the fiber in one second and the theoretically total particle number pass through in one second. The airflow approach to a single fiber is considered

as perpendicular to the middle of the fiber. Particles flowing into the air stream are considered to remove permanently through deposition mechanism. The laminar airflow becomes distort due to the filter influences and the particle number within these projected area vicinities to the single fiber. The overall efficiency of an isolated filter is taken in to account as the four mechanical deposition mechanism are performed by a single fiber. The single fiber efficiency can be calculated as:

$$E_{\Sigma} = E_R + E_I + E_D + E_{DR} + E_G \quad (6.10)$$

6.2.7 Total collection efficiency of a filter

The filter efficiency is calculated based on the above mentioned deposition mechanisms. All fiber units arranged perpendicularly to the airflow act against the particle deposition. The efficiencies E_n and E_m are the ratio between intake and outgoing particles by calculating their number and mass concentration respectively. According to Hinds, the efficiency of filter can be calculated as (18).

$$E_n = \frac{N_{in} - N_{out}}{N_{in}} \quad (6.11)$$

$$E_m = \frac{C_{in} - C_{out}}{C_{in}} \quad (6.12)$$

where,

E = efficiency

N_{in} = quantity or mass of the intake particles

N_{out} = quantity or mass of the outgoing particles

If P is characterized by the fraction of penetrating particle into the filter, then efficiency can be written as

$$E = \frac{N_{out}}{N_{in}} = 1 - P \quad (6.13)$$

Considering the combination of all fibers, Hinds (18) calculated the efficiency a fiber as follows

$$E = e^{-\gamma t} \quad (6.14)$$

Where,

γ = the fraction of particle in the specific fiber thickness

t = average thickness of the fiber layer (m)

When all fibers present in the filter have the same diameter, the fibers contain uniform volume and thickness, and the fibers have uniform density or solidity, then according to Hinds (18), the fractional capture of particle per unit thickness γ is represent as

$$\gamma = \frac{4\alpha E_{\Sigma}}{\pi d_f} \quad (6.15)$$

where,

γ = fractional capture of the particle per unit thickness

α = ratio between fiber volume and total volume

d_f = average diameter of the fiber (m)

So, Overall filter efficiency can be calculated by the following equation.

$$E = \exp - \frac{4\alpha E_{\Sigma}}{\pi d_f} t \quad (6.16)$$

From the discussion above it is clear that the efficiency of filters is inversely proportional to their thickness. The particle capacity not always depends on the filter thickness; particle size, face velocity and solid factor have also great influence. Although the equation for filter efficiency is often used and accepted worldwide, but there are few limitations as well. Fibers are not arranged perpendicularly always. The thickness and solidity also differs sometime from fiber to fiber. In addition, the airflow on the fiber surface changes sometimes due to neighbor fiber influences.

6.3 Factors affecting filters efficiency

The deposition mechanism and filter efficiency depend on many factors. The fibers interact with the particles depending on the filter type and particle properties.

6.3.1 Influence of particle size

The deposition mechanism of a fiber filter depends on the particle size. Smaller particles settle down on the fiber surface through diffusion mechanism. On the other hand, with the increase of the particle size, both inertial and interception effects increase. The particle size with the minimum efficiency rate is difficult to capture. In the ambient air, polydisperse particulate matter is present that show different diffusion, inertial and interception mechanisms according to their size. Therefore, the efficiency of the filter is proportional to the diffusion, interception and interception mechanism (33). It is not true that the same particle type always shows the same penetration or efficiency rate. During tests of different filter efficiency, it was noted that the results vary with the different conditions like fiber diameters, filtration velocities and so on (33).

6.3.2 Influence of particle type

Filters do not show a similar efficiency for both solid and liquid phase particle phases. Agglomeration of solid particles increases the filter load, which reduces the penetration rate and increases the filter efficiency. Additionally, solid particles can also increase the electrostatic force that increases the dust holding capacity. On the other hand, liquid particles deteriorate the filter strength, which reduces the filter efficiency as well (33).

6.3.3 Influence of particle shape

In most cases, particles that are used for filter tests are generated artificially and considered as uniform spherical in shape. However, real particles have irregular surface that has better adherence possibility with the filter media. Therefore, the deposition rate is better with the spread particle distribution. (33)

6.3.4 Influence of fiber size

The reduction of fiber size increases the filter efficiency through the increase of cross-section area and surface area that grasp the particle more effectively. Although the pressure drop slightly increases with this method. (33)

6.3.5 Influence of filtration velocity

The filtration velocity also has influences on filter efficiency, which is proportional to inertial and interception effect but inversely proportional to the diffusion effect. Therefore, the penetration of smaller particles increases with the decrease of filtration velocity. However, the total efficiency is increased over the filter but it only works with the larger particles. (33)

6.3.6 Influence of solid fraction

Solid fraction of a fibrous filter is the ratio of the volume of fiber surface and the total volume of the filter. Therefore, it is assumed that filter efficiency is proportional to the fiber volume. When layer become dense, they can easily capture the larger particles, which is effective in inertial and interception mechanism. On the other hand, it decreases the diffusion mechanism that increases the penetration of finer particles. The overall filter efficiency increases, however, the pressure drop also increases in a larger proportion. (33)

6.3.7 Influence of air temperature

Elevation to optimum temperature can remove the vapors from the air. It reduces the pressure drop and increases the filter efficiency. The optimum temperature is recorded in a study between 15 to 20 °C. The dry air is comparatively lighter and can easily stream through the filter fiber. Both inertial and diffusion efficiency increase through these effects (73).

6.3.8 Influence of air humidity

Air humidity increases the particle penetration through reducing the electrostatic effect, Brownian motion (details in chapter 5.3.5) and overall filter activity. Figure 6.6 displays the humidity effects where the humid air elongates the retention time of particles on the filter surface, which leads the penetration into deeper surface (33). Bacteria present in the ambient air can also penetrate the higher humidity.

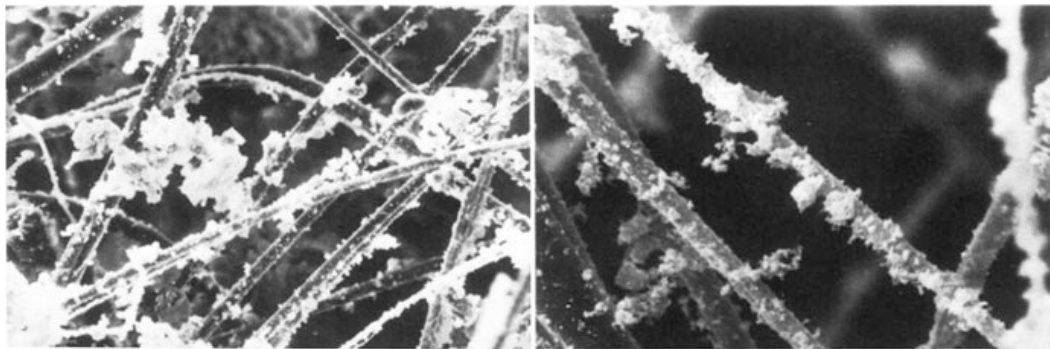


Figure 6. 6: Particle coagulation on filter medium (33)

6.3.9 Influence of airflow pressure

Air pressure is proportional to the air density and inversely proportional to the slip correlation factor (details in chapter 5.3.4). Increase of the pressure also increases the holding capacity for both fine and coarse particles. However, these efficiency is reduced if temperature increases additionally with the pressure (33).

6.3.10 Influence of dust holding capacity

Fiber filters have multiple layers on them and dust or particle are adhering on the fiber surface. Therefore, these dust particles increase gradually and have an impact on overall filter performance. As the particles are deposited like snow and ice crystal, this method is most familiar as dendrite crystal model (74). Filtration efficiencies increase according to the deposition of the loaded particles. Comparatively this property is common for the small fibers and large particles that are presented in the figure 6.7 (from c – f). However, in case of smaller particles and large fibers, these phenomena are rarely found, which is present in figure 6.7 (a-b), it seems a rough tree rind. As the loaded dust makes

a blockage over the fibers, it increases the pressure drop accordingly of the filter. Though the particle capturing capacity is increased only in the upstream of the filter, it increases the efficiency over the time. These accumulated dusts block the airflow path, which increases the pressure drop and makes filter rigid. It also decreases the lifetime of the filter. (33)

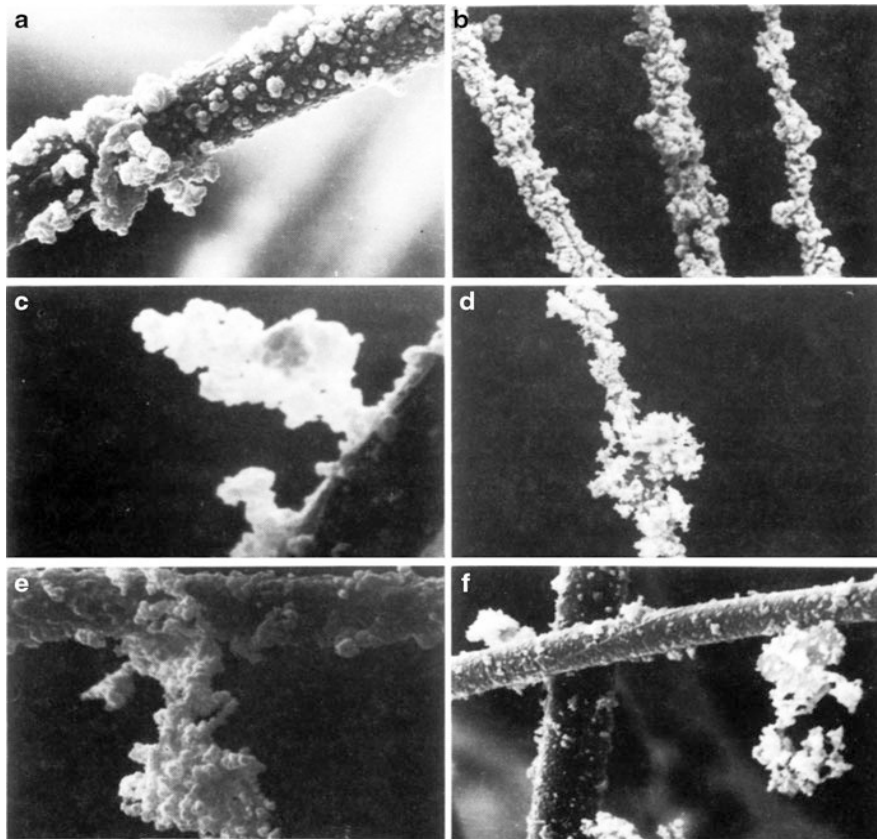


Figure 6. 7: Dust adherence of particles into the filter fiber (33).

6.4 Conclusion of theoretical studies

From the discussion above, it can be concluded that the air filtration is equally important for both the filter media and the particles present in the airstream. In addition, the aerodynamics attributes on the filter media, environmental factors like humidity and temperature can greatly influence the filtration mechanism. However, the properties of the particles present in the air stream also change the filtration efficiency as filter media directly contacted with them. In this master thesis, the influencing factors were investigated to monitor and assess the filter activity by a comparative study.

7. COMPARATIVE EXPERIMENTAL AND ANALYSIS OF MEASURING DATA

7.1 Overview of experimental plan

The aim of this experiment was to find out the PM mass concentration and PM number in a passenger cabin under multiple environment-related conditions. Three different HVAC conditions were selected to get the different environmental effects in three different locations for example urban, freeway and tunnel. The tests focused on to collect particulate number and particulate mass concentration by altering environmental situations and how the filtration system of the test vehicle works against it. Two different types of filters were used alternatively in the same test conditions. The differences of measuring data were observed and recorded throughout the experiment.

The tests were carried out in two different modes, static or parking mode and motion or driving mode.

1. Idling or parking mode: for the stationary condition, the vehicle was idling with the minimal stable engine revolutions (rpm) as declared by the manufacturer.
2. Driving mode: the steady state driving speed was dependent upon the street condition. The minimum speed in freeway was 80 Kmph, so the car tried to keep in mentioned speed. In the tunnel, the speed limit was also 80 Kmph.

7.1.1 Test procedure

A. Preparation for testing

1. Checked and recorded the informations of the reference vehicle and HVAC system that undergoes to the testing. Recorded the complete information of both filter (HEPA filter & micro filter).
2. A visual evaluation was done to confirm the conditions of the passenger compartment, filter and/or air cleaning systems as well as of the internal and external surfaces of the bodywork, sealing of the glasses, hatches, doors and exhaust path.
3. All measuring equipment found properly mounted and operated.
4. The sampling tubes and probes were properly connected and placed sampling zone.
5. Before performing the test, the complete passenger compartment with filter and air cleaning system were checked according to testing requirements. The following features were confirmed before testing.
 - Air conditioning system.
 - All modes and parameters of HVAC operation.
 - All ducts and flaps were working.
 - The blower unit worked properly.
 - The passenger compartment filters, filtration unit worked properly.
 - The exhaust pipe in relation to the bodywork (driver's cab) of the motor vehicle was checked.
6. Sufficient fuel filled up before the test drive.

B. Test procedure

After completion of test preparation, testing the environmental condition of the passenger cabin and filtration efficiency of the purified filter was performed according to the following sequence.

Test Location: Parking lot (less traffic density)

- The test was carried out at an open parking place.
- Both filters were installed according to the experiment plan.
- Three consecutive experiments were done according to three identical HVAC settings. During experiments repeatedly measurements were performed for both micro filter and HEPA filter.
- For each experiment, two consecutive samples were collected with the same settings and parameter.
- The engine was switched on during the experiment to ensure that all functionalities are working properly.
- The outside ambient environmental condition was measured with ventilation meter according to the experimental plan and recorded.
- The HVAC system was set according to the HVAC plan.
- After changing every HVAC setting, 1-minute intermediate was allowed for climate saturation and uniform mixing of the air inside the cabin.
- The sample was taken for 1 min by running dust collector and particle counter simultaneously.
- The climate control of the cabin was also recorded with ventilation meter throughout the operation.
- All measured values were recorded and transferred digitally for further calculation and evaluation.

Test Location: Freeway & tunnel (high traffic density)

- The test was carried out in both urban freeway and tunnel (Plabutsch Tunnel near the city of Graz). The direction of the test vehicle was kept from south to north, as much traffic was available in this direction.
- Both filters were installed according to the experiment plan.
- Two representative samples were taken repeatedly for each sample point.
- The vehicle speed was at kept 80 ± 10 kmph in the freeway test drive.

All samples were measured from inside the cabin and outside environmental conditions according to the experimental plan.

7.1.2 Data analysis

1. Particle number concentration inside the cabin using both filter and ambient location.
2. Standard deviation inside the cabin using both filter and ambient location.
3. Particle size distribution for all HVAC setting.
4. Particle mass concentration and mass- number correlation.
5. Filter efficiency.
6. Cabin pressure measurement for defined HVAC setting by using both filters.

7.2 Experimental setup and planning of measurement

The test vehicle was equipped with a particle counter with isokinetic probe, a ventilation meter, and an aerosol dust monitoring as shown in figure 7.1. The isokinetic probe of the particle counter was installed in the driver breathing zone as this zone was susceptible to driver inhalation. A silicone tube was used to connect the probe with the particle counter, which was placed inside the cabin. Another probe was connected in the same direction exactly at the inlet of the fresh airflow to measure aerosol dust mass concentration. The ventilation device was installed for measuring the cabin environmental conditions. During the measurement of airflow velocity, the probe of ventilation meter was close to the air supply duct. Two different filters installed alternatively and all measurement was done in the same direction and the same HVAC conditions. Schematic diagram drawn in figure 7.1 explains all test set up in the test vehicle.

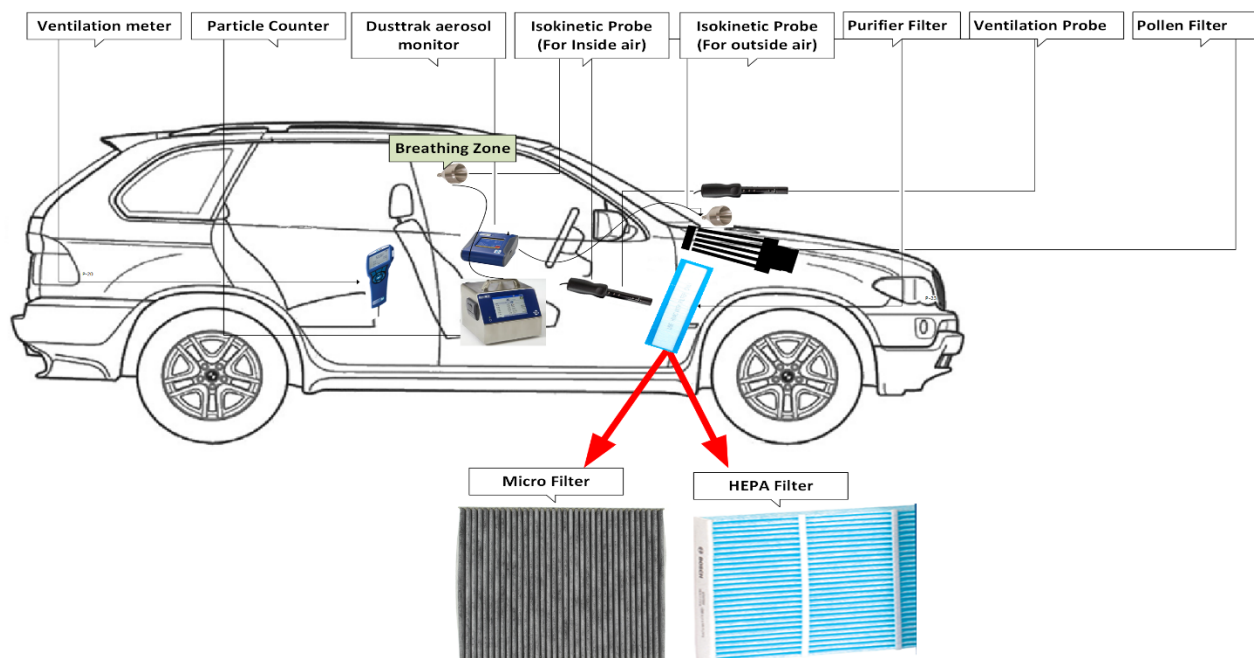


Figure 7. 1: Test vehicle installed with required equipment

The experimental plan was prepared by altering the factors that could have influences on the filter activity. Table 7.1 includes the possible testing parameters that were taken into account throughout of this experiment. Between the measurement, one-minute recovery time was allowed for saturation inside the compartment. Table 7.1 depicts testing conditions including all the parameters.

Table 7. 1: Experimental plan and set up for test-drive and sample collection.

Test Condition	Location	Traffic Condition	Test mode	Filter type	HVAC setting	Engine condition	Cabin condition	Passenger number	Sampling point
Test -1	Rural environment (Parking lot)	Light Traffic impact	Parking mood	Micro filter HEPA filter	(HVAC Setting 1) Recirculation (AUC): OFF (only outside air inlet) AC: Off Temp: ambient Blower speed: off Duct open: full	On	Completely closed	2	Drivers breathing point Outside air
Test - 2	Rural environment (Parking lot)	Light Traffic impact	Parking mood	Micro filter HEPA filter	(HVAC Setting 2) Recirculation (AUC): M (only cabin air recirculated) AC: On Temp: 16 Blower speed: min Duct open: full	On	Completely closed	2	Drivers breathing point Outside air
Test - 3	Rural environment (Parking lot)	Light Traffic impact	Parking mood	Micro filter HEPA filter	(HVAC Setting 3) Recirculation (AUC): M (only cabin air recirculated) AC: On Temp: 25 Blower speed: max Duct open: full	On	Completely closed	2	Drivers breathing point Outside air
Test - 4	Urban Environment (Freeway)	Medium Traffic impact	Driving at 80±kmph	Micro filter HEPA filter	(HVAC Setting 1) Recirculation (AUC): OFF (only outside air inlet) AC: Off Temp: ambient Blower speed: Off Duct open: full	On	Completely closed	2	Drivers breathing point Outside air
Test - 5	Urban Environment (Freeway)	Medium Traffic impact	Driving at 80±kmph	Micro filter HEPA filter	(HVAC Setting 2) Recirculation (AUC): M (only cabin air recirculated) AC: On Temp: 16 Blower speed: min	On	Completely closed	2	Drivers breathing point Outside air

					Duct open: full				
Test- 6	Urban Environment (Freeway)	Medium Traffic impact	Driving at 80±kmph	Micro filter HEPA filter	(HVAC Setting 3) Recirculation (AUC): M (only cabin air recirculated) AC: On Temp: 25 Blower speed: max Duct open: full	On	Completely closed	2	Drivers breathing
Test - 7	Urban Environment (Tunnel)	High Traffic impact	Driving at 80±kmph	Micro filter HEPA filter	(HVAC Setting 1) Recirculation (AUC): OFF (only outside air inlet) AC: Off Temp: ambient Blower speed: Off Duct open: full	On	Completely closed	2	1. Drivers breathing point 2. Outside air
Test - 8	Urban Environment (Tunnel)	High Traffic impact	Driving at 80±kmph	Micro filter HEPA filter	(HVAC Setting 2) Recirculation (AUC): M (only cabin air recirculated) AC: On Temp: 16 Blower speed: min Duct open: full	On	Completely closed	2	1. Drivers breathing point 2. Outside air
Test - 9	Urban Environment (Tunnel)	High Traffic impact	Driving at 80±kmph	Micro filter HEPA filter	(HVAC Setting 3) Recirculation (AUC): M (only cabin air recirculated) AC: On Temp: 25 Blower speed: max Duct open: full	On	Completely closed	2	Drivers breathing

Figures 7.2, 7.3 and 7.4 describe the imaginary traffic conditions of the test environment. In figure 7.2, the test vehicle is parked in minute traffic density area. On the other hand, figure 7.3 and figure 7.4 illustrate the high traffic density areas in the freeway and in the tunnel respectively. Steady speed was tried to maintain during the test drives.

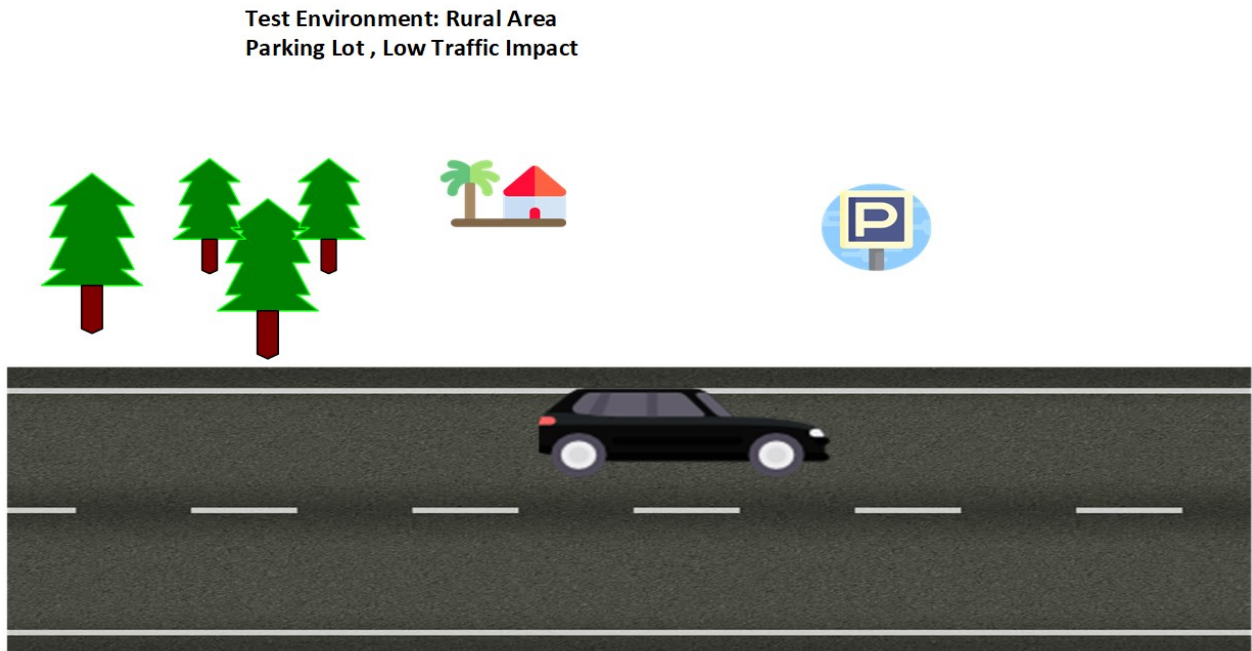


Figure 7. 2: Experimental model of the parking area.

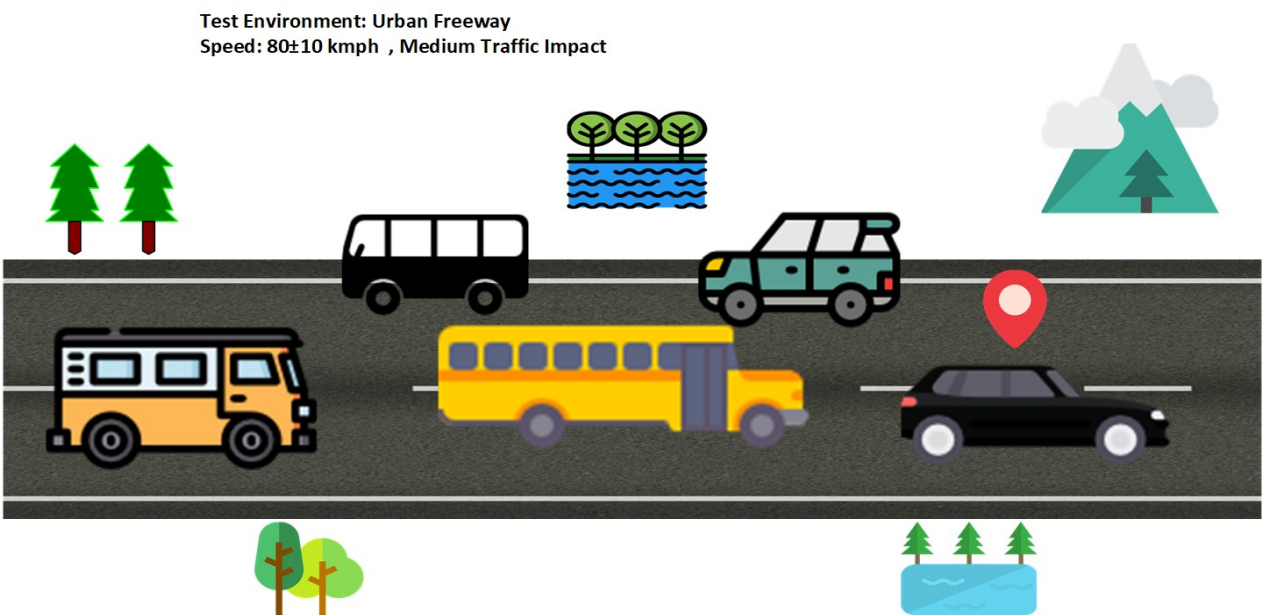


Figure 7. 3: Experimental model of test drive in freeway.

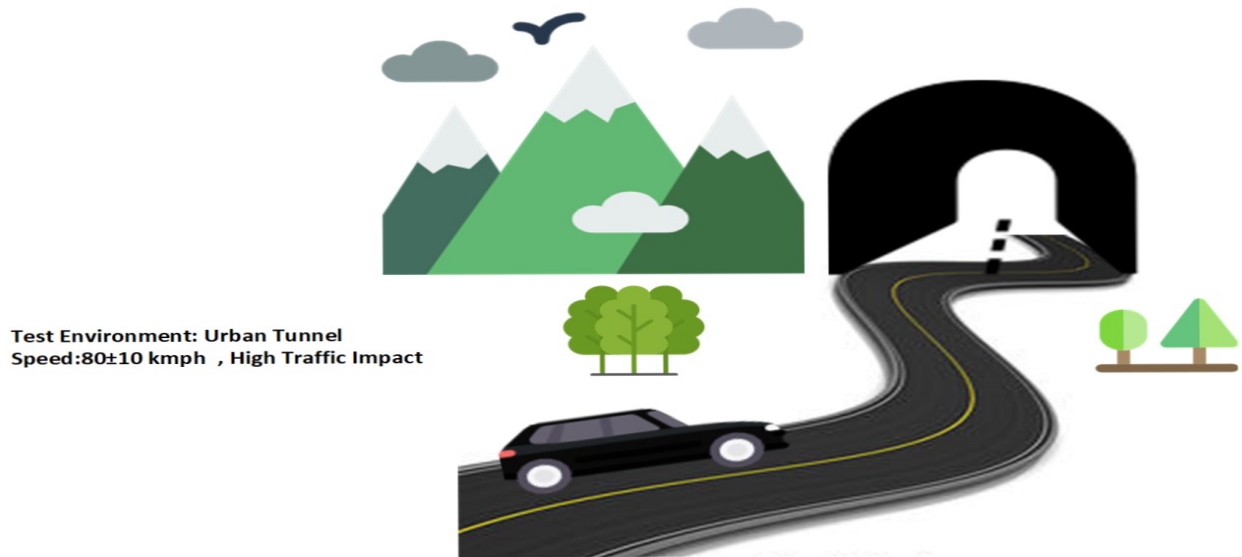


Figure 7. 4: Experimental model of test drive in tunnel.

7.3 Test environment

The experiment in this study was carried out in the beginning of October 2018 from morning to afternoon. Test drives were done within two days in three different locations. At the first day, the parking mode and the test drive in the freeway were completed. The second day was spent to measure the tunnel drive. As the tunnel was about 10 km long, the test drive was planned repeatedly to collect the test sample by maintaining the same test conditions. All test drives were conducted under real traffic conditions to measure the real ambient value. Based on literature research, it was assumed that the properties and characteristics of particulate matter depend upon source and surrounding ambient environment (5). For example, tunnel or freeway were major sources of nucleation size particles of combustion engines, whereas the rural area had the coarse particulate concentration (34). As given in this study, the comparative efficiency of two filters was tested regarding particle number and mass concentration. To achieve a representative outcome, different types of particles with different characteristics were considered. From the studies it was clear that the efficiency of a filter depends on the different types of particles and their sources (33). Considering these circumstances, it seemed a good choice to select three different locations based on traffic density and environmental conditions. In chapter 4, the discussion was done based on particle sources from different locations and how they distributed throughout the environment. Multiple studies concluded that particles emitted from vehicles show their peak concentration inside urban tunnels, because insufficient atmospheric saturation happens inside the tunnel. A similar situation could be calculated for the urban highway. But atmospheric saturation reduces the concentration with increased distance from the freeway (34). In contrast to the highway, the rural area shows lower density of smaller particles, as the atmospheric saturation is high and traffic density is low. Consequently, factors affecting particles characteristics, which might have influences in the filter activity are considered during the test preparations. Figure 7.5 and figure 7.6 show the test tracks of this experimental. Figure 7.5 displays

the test track called Pyhrn Autobahn (freeway), which is located next to the city of Graz. In the morning, usually traffic density was high due to a lot of commuting people come to the city for their daily work. The GPS location of the test track is 47° 0' 10.368" N 15° 24' 29.412" E.



Figure 7. 5 The freeway road for test-drives in Graz, Austria.

The Plabutsch Tunnel shown in the figure 7.6 is a section of the Austrian Pyhrn motorway, which leads through the Buchkogel and Plabusch located at the west side of Graz. The GPS location of the tunnel is 47° 3' 56.2968" N 15° 22' 42.0312" E.

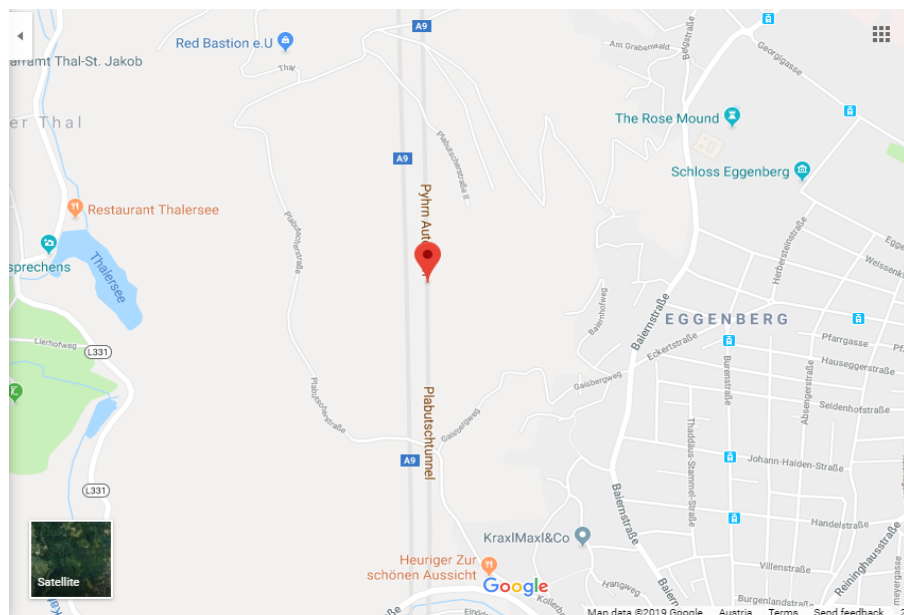


Figure 7. 6: The Plabutsch Tunnel in Graz, Austria (approximately 10.0 km long).

7.4 Test vehicle

Comparatively, the air quality in Asian urban regions is worse than in EU urban regions and in the US (75). However, SUV-shaped vehicles are very popular in the Asian region and in the rest of the world. These lead to choose the BMW X5-35i model (shown in figure 7.7) in this study.

The vehicle itself has a fully electric HVAC control that represents fine and accurate functionalities. The vehicle was in completely new condition, only 163-kilometer mileage at the display. Therefore, the car had a good sealing condition, which is one of the major criteria in this experiment to avoid high leakage rates that would distort expected test results.

A feature that prompted this study was to optimize the vehicle in the air purification system, which is generally not available in the standard configuration. In this vehicle, two pollen filters were used under the windshield, which is the inlet of fresh air from the ambient. This air then streams through the HVAC system, where another micro filter is used (76). This micro filter has been replaced by the HEPA filter in accordance with the test requirements.



Figure 7. 7: Reference vehicle (manufacturer: BMW, model: X5 35i, 2018)

7.5 Filter specifications

The filters installed in the test vehicle can be described as follows: In a first step, two-pollen filters are located in the engine compartment beneath the windscreen presented in figure 7.8. In the second step, one micro filter is installed inside the HVAC box immediately after air recirculation gaps, shown in figure 7.9. All three filters consist of nonwoven synthetic filter medium and are typically pleated in geometry to increase the efficiencies.

The pollen filter is composed by pleated and multilayers polypropylene fibrous. It acts as a mechanically driven sieve with an activated carbon layer. It helps to trap or attract the dust, pollen mold, debris, and unpleasant odorous gas and chemical substances present in the ambient air. (76) The activated carbon layer adheres the odorous chemical and VOCs from the ambient air and ensures a pleasant and comfortable environment inside the cabin. This filter is inefficient to remove the

smaller particles from the ambient airstream due to its fibrous layer arrangements, The usual pollen size available in the environment is $6\ \mu\text{m}$ or less (77), but worst particles are much smaller. Consequently, the second step of air filtration is designed inside the HVAC box to enhance the air purification inside the cabin.

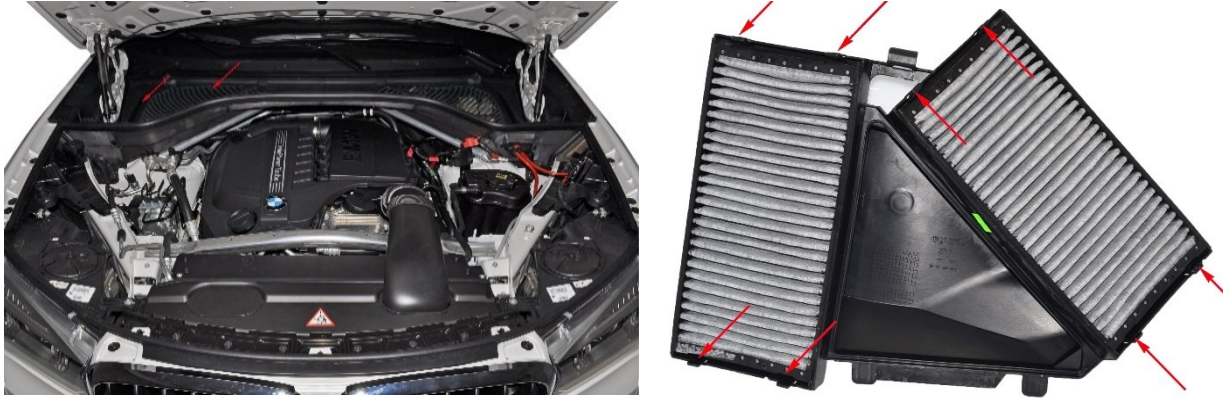


Figure 7. 8: Pollen filter installed under the windshield (manufacturer: Valeo) (78)

The dust holding capacity, pressure drop and solid factor were asked to the supplier for detailed filter specification. However, no reference data was given to specify the filter information. Another alternative way to measure the filter specification is the laboratory test for the required information, for example, fiber diameter, pressure drop, dust-holding capacity. However, MAGNA STEYR FAHRZEUGTECHNIK AG & Co KG (MSF) only integrates several purchased parts, which are delivered within the complete HVAC system by system suppliers. As MSF is no filter producer and does not develop as produce HVAC systems, no facilities were available to measure the filter in own test laboratory. The filter used in the test laboratory is effective against $2.5\ \mu\text{m}$ particles claimed by the supplier side (76)(78). It has two fibrous layers with 40 pleat.

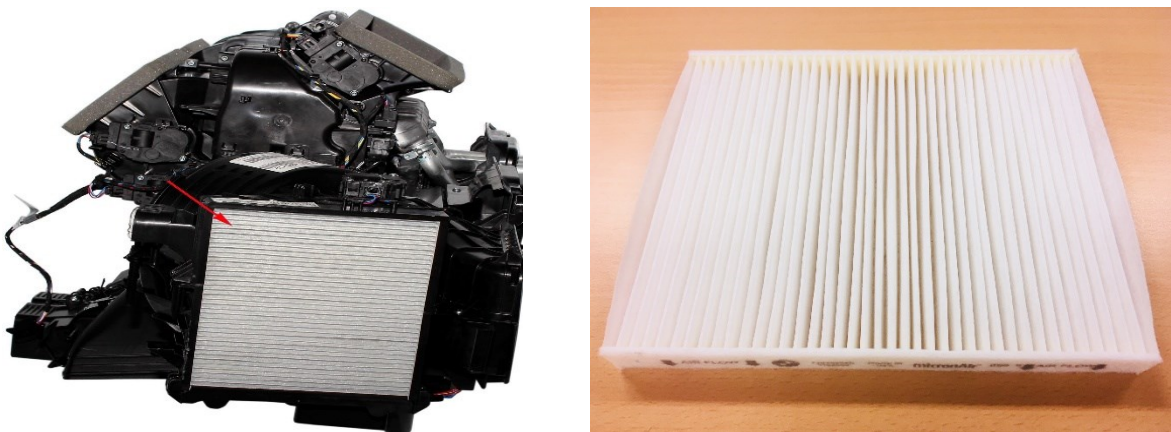


Figure 7. 9: Micro cabin filter installed inside the HVAC box (manufacturer: Micron Air) (78)

For comparison, a HEPA filter was used in this study. This alternative filter replaced the micro filter inside the HVAC box. The filter is produced by a third party supplier (BOSCH) displayed in figure 7.10. The manufacturer claims that the filter is designed and tested according to HEPA standard based on ASTM D2986 and it provides filtration efficiency of 99.7% at $0.3\ \mu\text{m}$ particle diameter. (79)

The filter is consisting of three layers including a support layer, a HEPA layer and static cotton. The layers altogether provide better trapping efficiency than a conventional micro filter. The support layer has a melt blown electrostatic properties that provide better trapping capacities. The support layer is hard and aimed to protect the media on the surface of the filter. HEPA layer arrests the microscopic pollutants and static cotton layer increase the filter capacity and elongate filter life. No further information was found from the manufacturer side. (79)

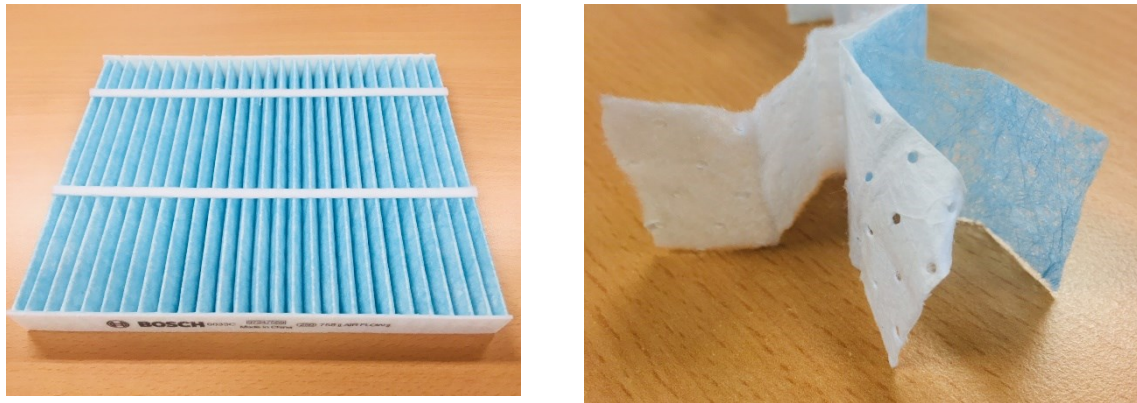


Figure 7. 10: Alternative HEPA cabin filter (manufacturer: Bosch, USA, model: 6003c)

Table 7. 2: Filters specifications

Type	Size (W, H, D)	Pleated	Weight
HEPA Filter	168, 198, 20	22	NA
Micro Filter	168, 198, 20	39	0.038 kg
Pollen Filter	146, 300, 39	27	0.257 kg

7.6 HVAC setting and testing conditions

Testing was conducted in different locations altering climate control inside the cabin. The test conditions were prepared by changing HVAC setting in accordance with outside ambient air and recirculated cabin air. Micro filter and HEPA filter were alternatively used for all test conditions. The HVAC unit of the BMW X5 consists of multiple functionalities. A schematic diagram of HVAC control panel of BMW X5 is shown in figure 7.11. However, not all of them was required during the experiment, but few of them were used. Rear window heating, integrated seat heating, defrost and mist was not taken into consideration. The test conditions were developed based on the factors that have influenced on the filter activity and characteristics (76).

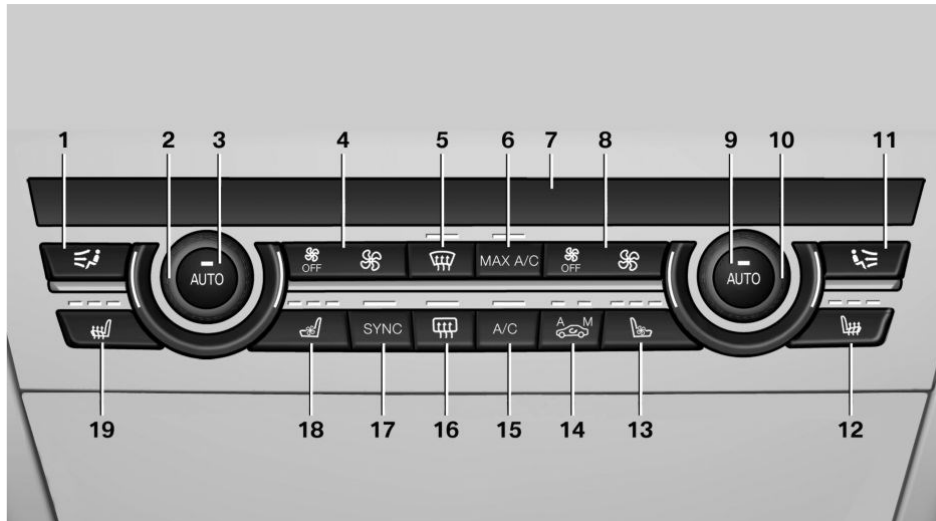




Figure 7.11: HVAC control panel of BMW X5



Table 7.3 includes the functionalities of the HVAC operation box. The cabin environment can be controlled by tuning of these operations. The expected test conditions were generated by adjusting the multiple functions.

Table 7.3: The multifunction control button of HVAC devices and their operations are described below.

1	Air distribution, left	11	Air distribution, right
2	Temperature, left	12	Seat heating, right
3	AUTO program left	13	Active seat ventilation, right
4	Airflow, AUTO intensity, left, residual heat	14	Automatic recirculated-air control/recirculated-air mode
5	Remove ice and condensation	15	Cooling function
6	Maximum cooling	16	Rear window defroster
7	Display	17	SYNC program
8	Airflow, AUTO intensity, right	18	Active seat ventilation, left
9	AUTO program, right	19	Seat heating, left
10	Temperature, right		

The display always shows the set temperature and air distribution programme. The ring button  is toggled to set a desired temperature for the occupant. The HVAC unit achieves this temperature as soon as possible.

The A/C  button is only working with the cooling function of the HVAC unit. The air is cooled and dehumidified depending on the chosen temperature setting. This button is switched on automatically during the AUTO/programme.

The MAX A/C  button has the same function as AC  button, but only works with the lowest temperature (16⁰ c) with maximum airflow through ventilation.

The AUTO mode works automatically and adjusts the ventilation level, air distribution and temperature depending on passenger requirements. Temperature and the intensity of ventilation are set depending on the outside influences. This program is not convenient for the experiment because it automatically controls function by itself.





The air recirculation  button works in two different modes, automatic and manual recirculation mode. However, if the button is turned off, only fresh air from outside can flow continuously into the cabin. When the left LED is switched on, the automatic recirculation mode is activated. This mode switches the air circulation into the cabin from both ambient and recirculated air from the cabin, and only purified filter is activated as described in figure 7.13 (a). A sensor detects the pollutants in the outside air and shuts off the airflows automatically if a noxious concentration level is reached. The manual recirculation  only works with circulated air from inside the cabin as mention in figure 7.13 (b). This self-controlled function was chosen during the test series to avoid the automatic sensor activities.



Figure 7.12: Selection of air circulation mode

There is a logic behind the internal control of the air circulation mode. To maintain the air flows from the inside cabin and outside air, each air duct embodies a flap. In the manual recirculation mode, the flap for outside air ducts completely shuts down and only fresh air continuously flows when all LEDs are switched off, no recirculation occurs. These two modes are taken into consideration for the experiment to separate the inside and outside air. If the LED next to the small index M is on, manual recirculation mode is active.

The forced ventilation  adjusts the intensity of the blower fan level that generates the airflow inside the air cabin as required. The users have the opportunity to choose five different ventilation levels indicated by the number of illuminated LEDs.

The distribution  of air can be selected manually from the upper body region to footwall as well as throughout the complete cabin. The auto function is recommended on the driver side if the windows fogged over. At this point, it utilizes the condensation sensor. All distribution channels will be kept open as the uniform air distribution is recommended.

Three HVAC settings were adjusted concerning cabin environment and outside ambient conditions. A schematic drawing of the air circulation is drawn in figure 7.14 that represents an overview of the preferred HVAC settings. The combination of all HVAC setting is described in table 7.4. As illustrated in figure 17.14 (a), the HVAC setting-1 was defined as the cabin environment selected by entering only the fresh airflow from outside when the other HVAC functions were switched off. That means, the airflow recirculation inside the cabin as well as the blower speed and A/C of the HVAC system was disabled. So the temperature kept ambient compared with outside. The aim of this HVAC-1 was to evaluate the filter activity against the particulate matter present in the ambient air without any influences where the spread of polydispersity of the particulate matter was too high. In contrast, the HVAC-2 and HVAC-3 settings displayed in figure 17.14 (b) and figure 17.14 (c) respectively, were set with environmental influences. Both moods include airflow recirculation inside the compartment only when the inlet of outside fresh air was blocked. The A/C was operated normally. So, all the HVAC functions were normally activated. The only variable between the two moods was changing the temperature and blower speed. The HVAC-2 drawn in 17.14 (b) includes the maximum blower speed and optimum temperature, whereas HVAC-3 mentioned in figure 17.14 (c) includes the minimum blower and minimum temperature inside the compartment. The selection of both conditions was insisted from the literature research, where both temperature and airflow had great impact on filter activity.

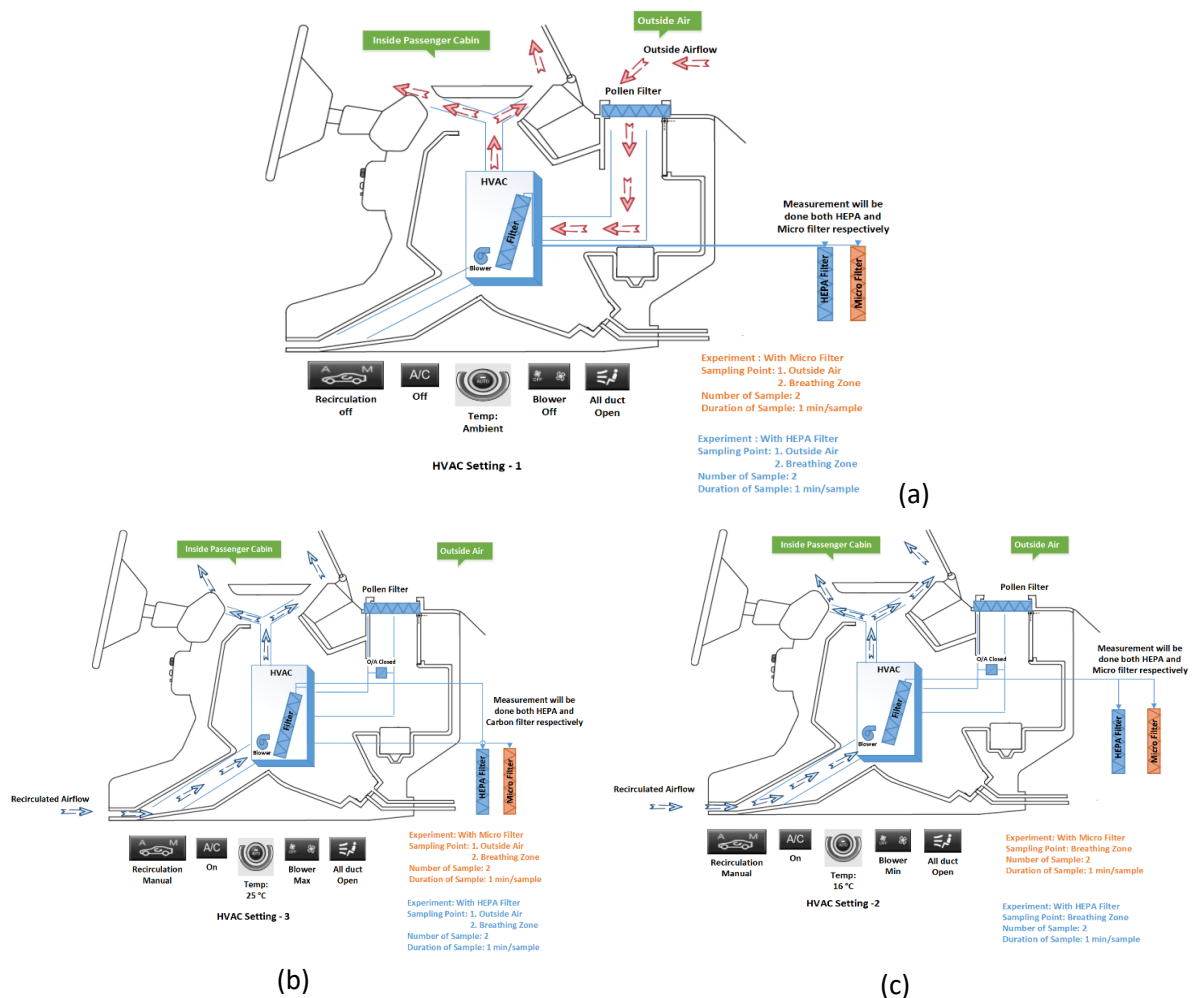







Figure 7. 13: Air Flow (fresh air from outside and recirculation into the cabin) inside the HVAC box according to the different settings.

Table 7. 4: Cabin environment settings for the experiment

	Recirculation 	Air Condition 	Temperature 	Blower speed 	Air Distribution 
HVAC Setting 1	Off	Off	Ambient	Off	All duct open
HVAC Setting 2	Manual	On	16 ⁰ c	Min	All duct open
HVAC Setting 3	Manual	On	25 ⁰ c	Max	All duct open

7.7 Sampling of air

The measurement was done in the vehicle compartment as well as outside ambient air simultaneously for monitoring the particulate matter present in the air. Two sets of instrument with sampling probe were installed for concurrent measurement of inside cabin air and outside ambient air quality. Both instruments were located inside the cabin. One sampling probe was placed in the driver breathing zone and another sampling point was set up where the fresh airflow inlet into the HVAC system. A sampling probe was isokinetically mounted presented in the figure 7.14 (18). All doors and window were closed during the sample collection inside the cabin. The length of the probe was as short as possible to reduce the measurement error.

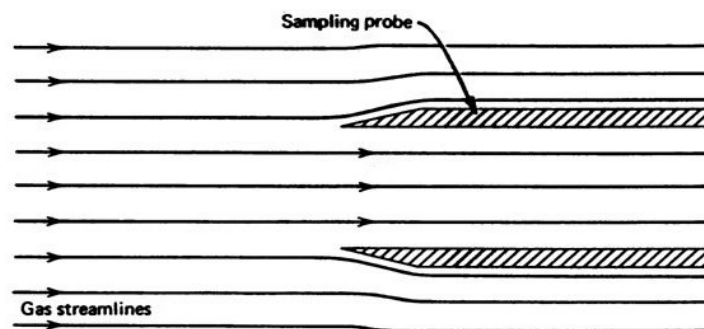


Figure 7. 14: Isokinetic sampling method.

Deposition usually occurs by inertial and diffusion method. During sampling, the free stream velocity and the gas stream velocity inside the probe were considered aligned together that met the isokinetic sampling condition as shown in figure 7.14. If the sampling flow rates were misaligned with the probe, the concentration of particles would be underestimated. Due to this, the probe was placed with the flow direction of the airflow inside the cabin and outside air as well.

7.8 Instruments and test equipment

The instrument and devices used in this study were opted based on the experimental plan and measurement. This master thesis is particularly focused on the particular number concentration, their size distribution, and particle mass-number correlation. A massive effort has been given into the precise acquisition of vehicle data, environmental record and number & concentration of air quality both inside and outside of the vehicle. Target was to get a clear understanding of which parameter creates an impact on and how they influence the air quality. All equipment was installed both inside and outside the vehicle and collected synchronized sampling data. For measuring the particle number

concentration, mass concentration and environmental monitoring an optical particle counter with six different bin size, a dust measurement, and a multifunction ventilation meter were used respectively. The equipments were cast off from the TSI because of their accuracy and installed them for optimum sampling data. All devices were calibrated against reference standards that ensures the truthfulness of the measurements. All measured data were transferred electronically for further evaluation.

7.8.1 Optical particle counters

An optical particle counter from TSI was used having six different channel simultaneous functionalities. The sampling probe was installed at the drivers breathing zone for measuring the in-cabin particle count and connected to OPC's through silicon tube. The software installed in the device counts diffraction and a cumulative number of the particles. The salient feature of the device is given in figure 7.15 (80).


Title	Specifications	Image
Brand	TSI	
Device name	AeroTrak portable particle counter	
Model No.	9310	
Particle Channel Sizes	0.3, 0.5, 1.0, 3.0, 5.0, 10 μm (simultaneous data)	
Concentration Limit	820,000 particles/ft ³ (29,000,000/m ³) with 10% coincidence loss	
Flow Rate	1.0 CFM (28.3 L/min) \pm 5% accuracy	
Standard	Complies with all requirements of ISO 21501-4	

Figure 7. 15: AeroTrak portable particle counter (brand: TSI, model: 9310)

Optical Particle counters use light scattering method to measure the particle size and number concentration. The mechanism of measurement is explained schematically in figure 7.16. A flow of aerosol is flown through a focus light or laser beam as a thin stream so that only one particle can scatter pulse to the detector, which is converted to the electrical signal. The intensity of the scattered light is analysed by the complex function wavelength and geometry of the optical detector and the diameter, shape and refractive index of the particles. The detector detects the intensity of the scatter light illuminated from each particle and interpret them to the proper size channel where the total count is accumulated for each size range (81).

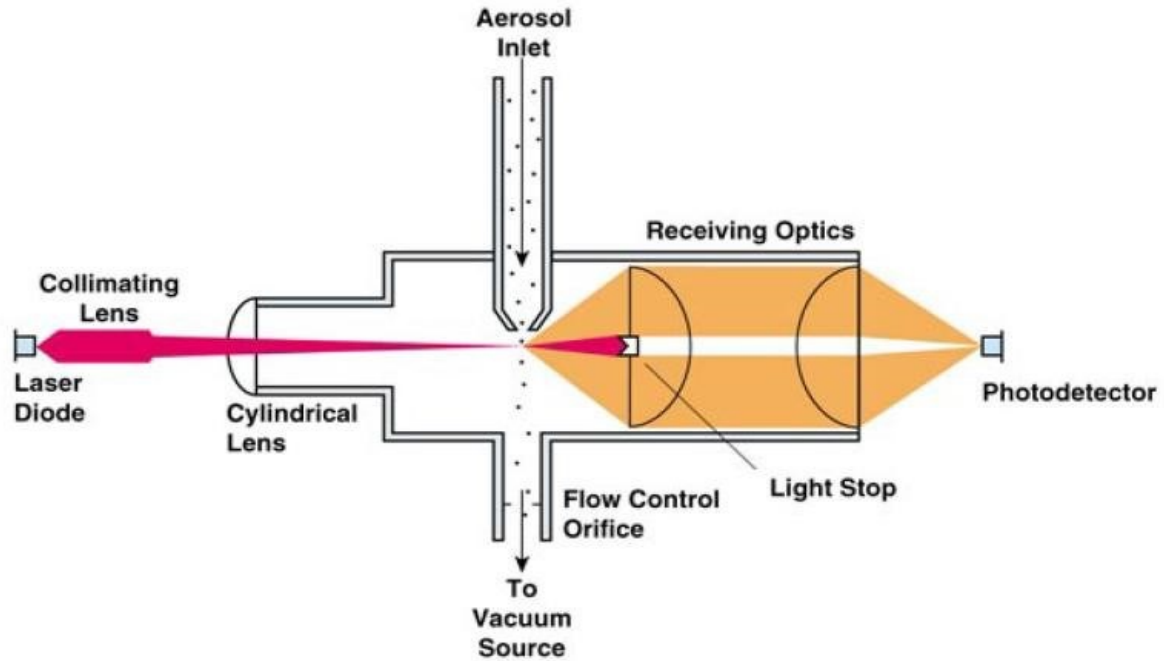


Figure 7. 16: Measurement principle of optical particle counter.

7.8.2 Photometer

For measuring the particle mass concentration, the DUSTTRAK aerosol monitoring device was installed inside the cabin. The device has four different size measuring channel with concentration ranges from 0.001 to 150 mg/m³. The features are mentioned along with an image of the device in figure 7.17. A sampling probe was fixed isokinetically underneath the windshield to measure the outside air where fresh air streams into the passenger cabin. During test drive, mass concentration was monitored continuously. (82)

Title	Specifications	Image
Brand	TSI	
Device name	DUSTTRAK DRX AEROSOL MONITOR	
Model No.	8533	
Particle Channel Sizes	PM1, PM2.5, PM 4, PM10 and PM Total size fractions	
Concentration Limit	0.001 to 150 mg/m ³	
Flow rate	3L/min	
Standard	ISO 12103-1, A1 test dust	

Figure 7. 17: Dusttrak Drx Aerosol Monitor (brand: TSI, model: 8533)

The Photometer is generally used to measure the relative mass concentration of particulate matter calculating the collectively scattered light generated unitedly from the particles. The measurement method of the photometer is discussed schematically in figure 7.18. Samples of aerosol particles are taken continuously through a suction pump drawn in figure 7.18 as a sample inlet. Using either an impactor or cyclone, different sized fractions of particles can be collected from the air stream. The defined sized sample then are transferred to the photo detecting sensing chamber through focus nozzle. The chamber has a laser diode and a set of focusing optics. When the sample particles pass through the chamber, it contacts with the light and are scattered into all directions. A photodetector, which is calibrated by known reference mass concentration, transform the light into the voltage. As a safety precaution to protect the instrument from fouling, filtered and reinjected as sheath air, which surrounds the particle and shields the instrument optics from fouling. (81)

Usually, photometer can measure the particle size ranges from 0.1 μm to 10 μm in diameter and concentration starts from 0.01 to 100 mg/m^3 . The particles, which is not between the above ranges are called ultrafine particles and can't detect by the photometer. A photometer can only detect the cluster of particles not the single ones, even if the particles are relatively large. For calibration of the photometer, Arizona Road dust is used as a reference standard test dust that provides estimation against polydisperse particles, for example, ambient air. (81)

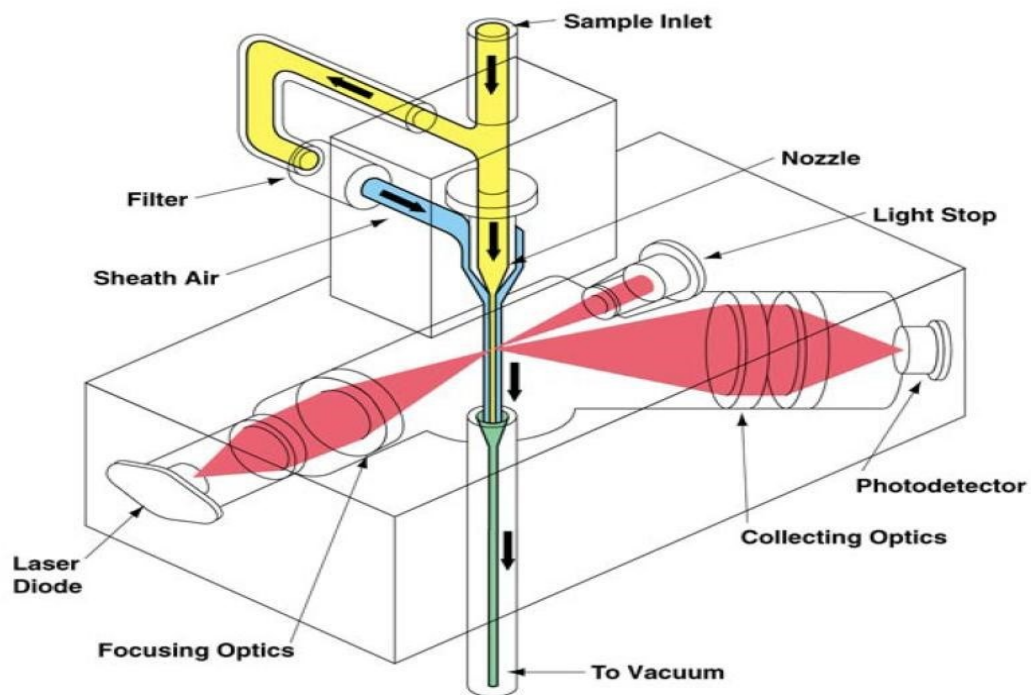


Figure 7. 18: Measurement principle of a photometer

7.8.3 Ventilation meter

The multifunction ventilation meter is designed to measure the wide array of critical parameters to investigate environmental conditions. The typical measuring attributes include air velocity, air flow, differential air pressures, humidity, and the temperature can be measured simultaneously (83). For this study, a multi-function ventilation meter was chosen from TSI (model: 9565) having thermo-anemometer plug & play probe as shown in figure 7.19. The easy handling operation and features were optimized to the experimental plan that provided robust and accurate sampling data. The probe used to monitor both inside cabin and outside ambient environmental factors. The setup of the probe is explained more precisely in section 7.2.



Figure 7. 19: Ventilation meter with thermos-anemometer-probe (model- 9565)

8 RESULTS AND DISCUSSION

The outcomes of this study illustrate particle characteristics and behavior in different locations and using different climate control settings inside the passenger cabin. Both filters performances were significantly variable, depending upon both the location and setting. In this chapter, the activities and evaluations of filters represent a clear overview of their performance and correlation with the theoretical part.

8.1 Total particle count

The overall total particle number concentrations under different conditions is shown in figure 8.1. The X axis indicates the different environmental conditions inside the cabin whereas the Y axis indicates the particle number concentrations. The total number of particles do not reflect the actual air quality of an environment, due to dependence on particle size and source of generation e.g. fine particle from engine combustion, but it gives an overview. The graph shows particle concentration between the HEPA filters and micro filters based on different locations and settings as well as on different ambient locations. Figure 8.1 clearly illustrates that the air quality inside the tunnel was worst compared to all measuring points of inside and outside the cabin. Similar particle concentration inside the tunnel was also found by another study group, which supports this study outcome (84), but there was no discussion about the particle size distribution. The ambient air was measured with an open window during driving inside the tunnel as well as in parking mode (static condition), where the particles were counted next to the freeway in an open environment.

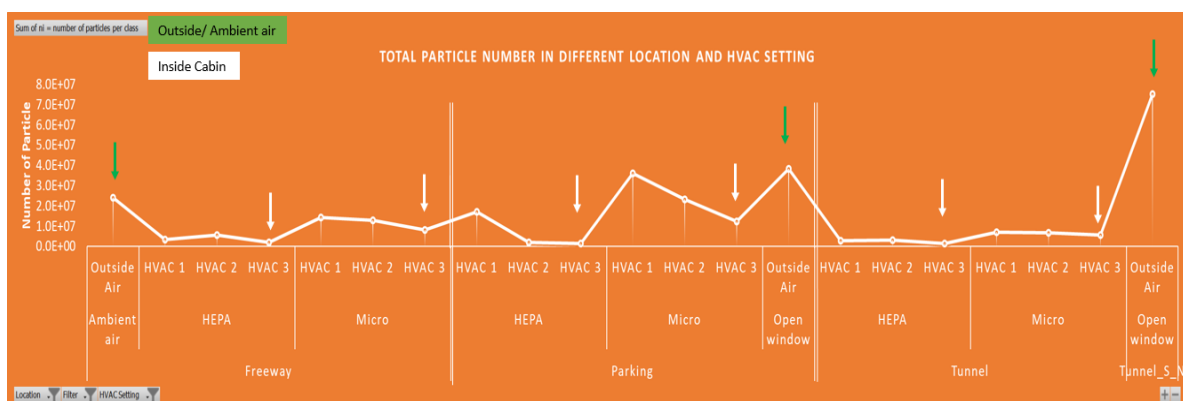


Figure 8. 1: Total number of particles in different locations (outside environment and window open) and climate control by using both filters.

The HEPA filter shows a better performance than micro filters in all HVAC settings and different locations. Both filters show nearly identical activities under HVAC conditions and in different locations accordingly. Comparison between the conventional filter and high efficiency filter was done by another study group and they also found the inadequacy of the current filtration system (5). In this study, the HVAC setting-1 was designed to measure the filter activity excluding any environmental influences inside the cabin, whereas other HVAC settings include varying parameters of air recirculation, temperature and air velocity changes.

From literature research, we know both diffusional and inertial effects are proportional to the airflow pressure (33). In this context, HVAC setting-3 shows the best performance among all three.

8.2 Influences of locations on particle size distribution

Additionally, an increase in temperature reduces the air humidity, which represents the optimal combination inside the cabin. Ambient air quality inside the tunnel shows highest total particle concentration measured among all locations.

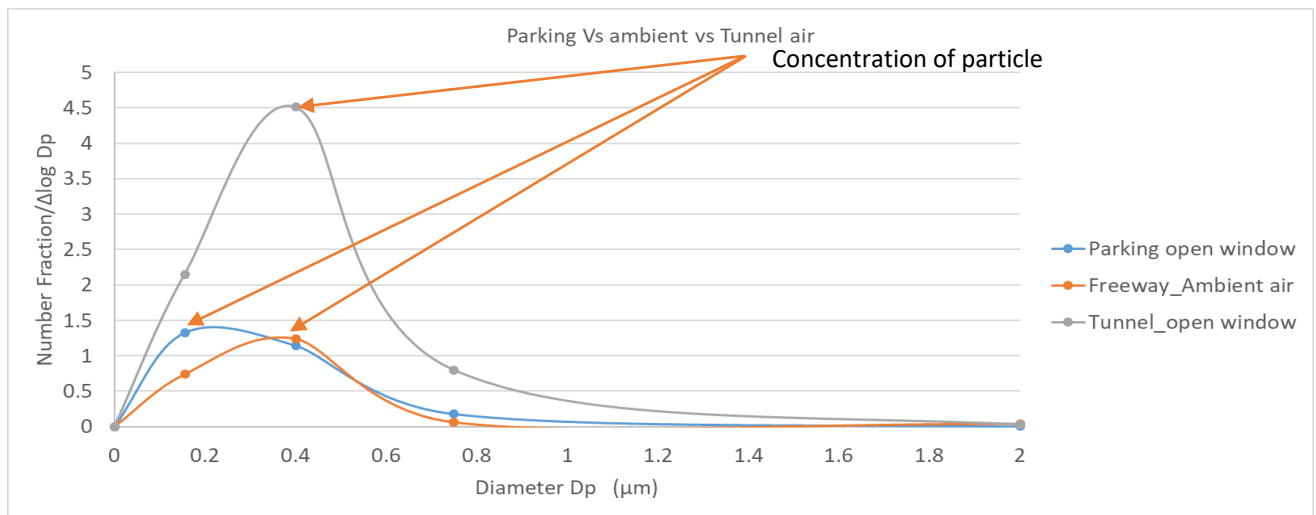


Figure 8. 2. Location influences on particle size distribution.

The particle concentration and its size distribution are strongly influenced by changing locations and environmental conditions. Similar influence was noticed by several study group (3) (85) (84). During the experiment, the particle number concentration in the ambient air was measured inside the drivers breathing zone, using an open window ventilation mode, which allows air to freely flow into the car from the outside, during tunnel drive at 80 km/h and in parking mode inside the parking lot. On the freeway, the ambient air was measured in the open environment beside a freeway street accordingly. Figure 8.2 illustrates that the particle concentration inside the tunnel was nearly three times higher than both on the freeway and at the parking location.

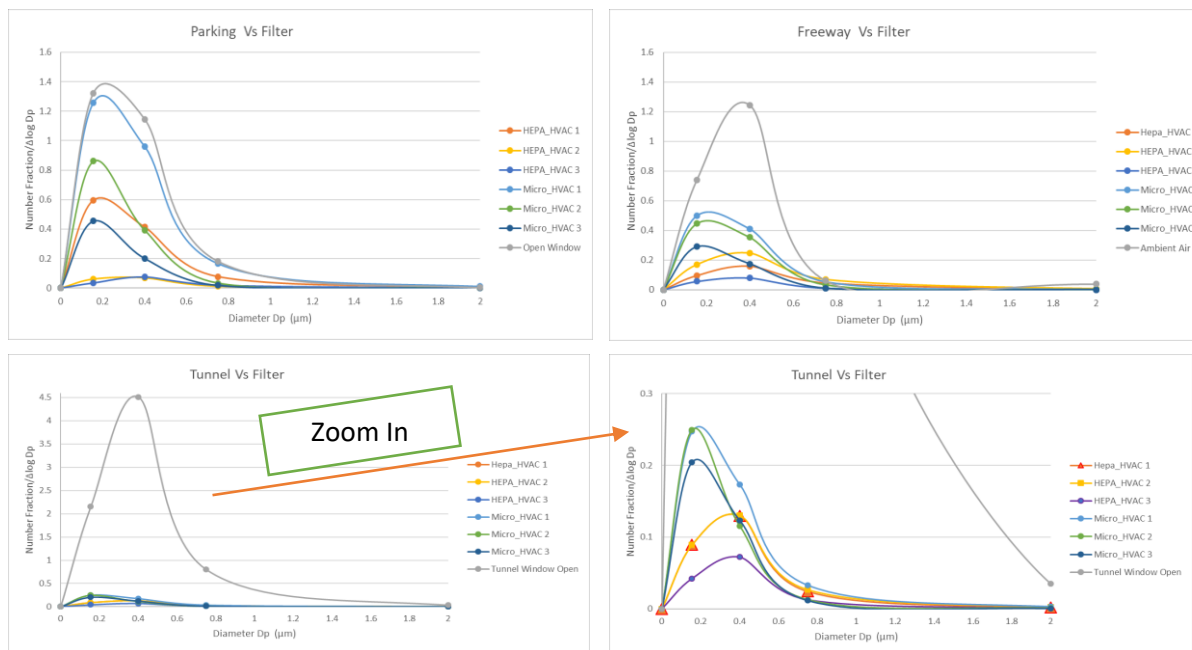


Figure 8. 3. Filter activity against different locations.

Figure 8.3 illustrates both filter activities in different locations. Particle properties and behavior depend upon the particles size, shape, and source of generation. From the comparative study of both filter activities against three different locations, it can be concluded that both filters work better inside the tunnel and HEPA works significantly better than microfilter. As previously discussed and from figure 8.2, it is clear that the concentration of fine particles inside the tunnel is much higher than in any other location, but filters show considerable activity. Normally, filters are tested against specific particle size in the laboratory, which shows better functionality against less spread particle distribution. The HEPA filter is designed for better activity against the smaller particles by including to dominate the diffusion efficiency (79) as well, whereas the microfilter works better with inertial and interception activity. The presence of fine particles (preferably accumulation mode) is much less inside the cabin when using the HEPA filter and the mode of frequency is trending towards the larger particles in location. In contrast, the microfilter works better with coarse particle of more than 2.5 μm by using inertial and interception methods. The driver's cabin is most likely getting contact with the fine particle having 0.3 μm or less due to filter insufficiency.

8.3 Geometric standard deviation in different location

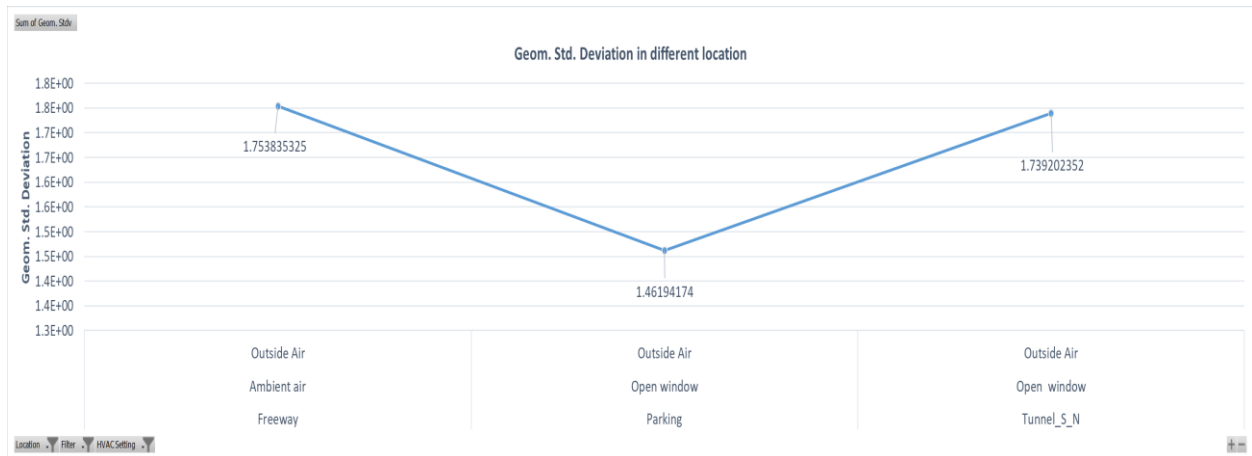


Figure 8. 4. Geometric standard deviation of particle size distribution.

Figure 8.4 illustrates the geometric standard deviation of the particle size distribution. From the discussion in the theoretical part, we have known that geometric standard deviation expresses the magnitude of polydisperse particles. The increased value of σ_g confirmed the higher size distribution of polydisperse particles (33). From the experiment, the geometric standard deviation σ_g was recorded 1.46, 1.75 and 1.74 for parking, freeway and tunnel ambient air respectively. The values were $\sigma_g > 1.25$, which represents the polydispersity of particles in all three locations (65). As the parking place had less traffic density, it was assumed that comparatively less particles variances were present in the ambient air. The standard deviation in the parking location $\sigma_g = 1.46$, was relatively lower than freeway $\sigma_g = 1.75$ and tunnel $\sigma_g = 1.74$ respectively. The reason undoubtedly the high traffic influences in the freeway and tunnel. So, it can be concluded that much traffic impacts increase the dispersity of the particle size distribution.

8.4 Particle size distribution for all HVAC settings

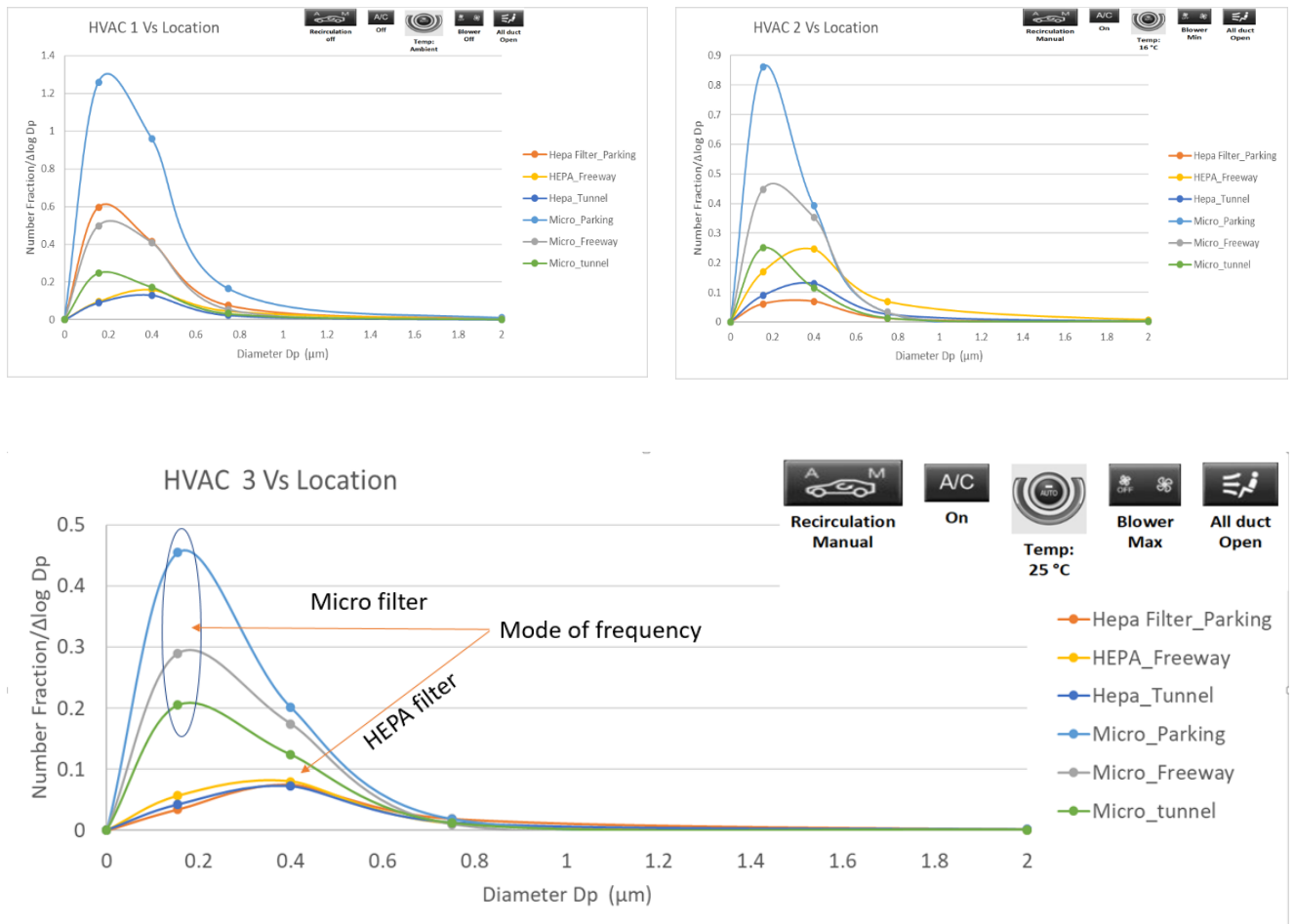


Figure 8.5. Performance of different climate controls in different locations.

To evaluate particle holding capacity, different HVAC settings were changed in different locations. In case of HVAC setting-1 when recirculation was turned off and fresh air flowed freely without any HVAC effect, the mode of particle concentration is always high for three different locations and does not show steady performance, whereas HVAC-3 shows best withholding capacity for both HEPA and micro filters. Another study was done by using two filters that have the analogous outcome with this study (5). It is assumed that filters do not work properly (and particles easily find their way into the cabin), when the HVAC is not active and recirculation is shut off. The influence of recirculation air is also proved by other study outcomes (5) (3). HVAC setting-3 was a combination of maximum air velocity and optimum temperature. Furthermore, including complete recirculation of cabin air, which overall represent the maximum withholding capacity with consistent activity. In this setting, the filter has the opportunity to clean the cabin air only. From the literature research it is known that optimum temperatures and maximum blower speed increase the particle movement inside the cabin and thus filters can remove particles through recirculation of air. Though both filters work better in this condition, HEPA worked much better than micro filter.

8.5 Mass concentration in different locations

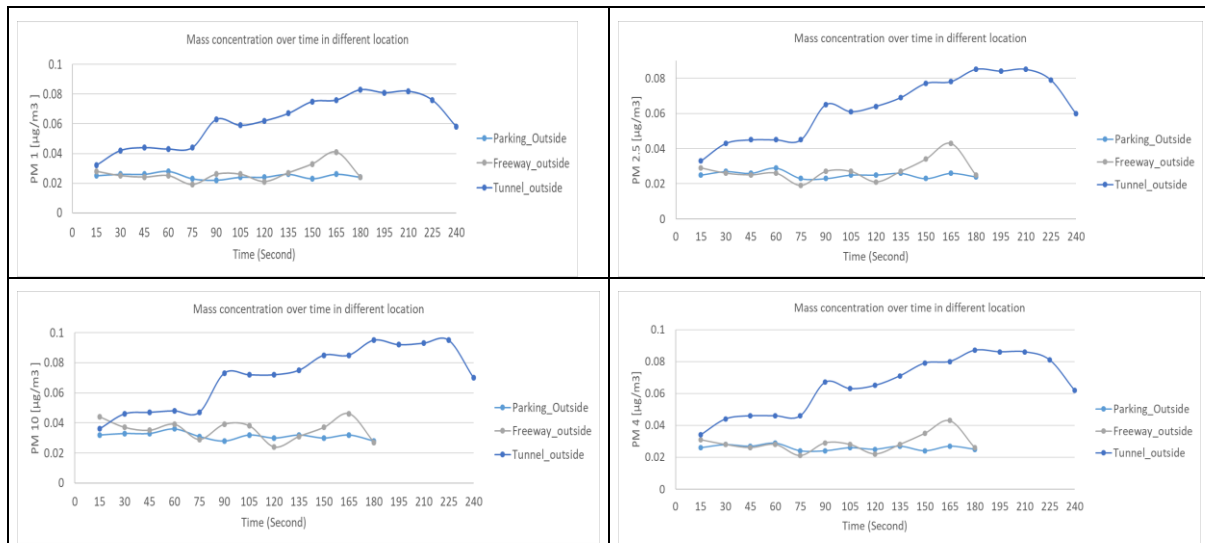


Figure 8. 6. Influence of different locations on mass concentration in the ambient air.

During the test drives in different locations, a Dusttrak aerosol monitor in the ambient air measured the particle mass concentration(82). The most obvious trend in the graphs represents the dissimilar particle mass concentration in the different locations. The particle mass concentration graph remains smooth but not steadily stable in the parking area, whereas the concentration at the freeway fluctuates between $0.02 \mu\text{g}/\text{m}^3$ to $0.04 \mu\text{g}/\text{m}^3$, which highlights considerable variations of particle concentration around the environment. Nearly similar findings were also observed by other research groups regarding particle concentration in freeway (3). In contrast, the tunnel ride measurement shows an enormous particle density inside the tunnel. The traffic was random during the experiment. The rate of particles accumulations is also supported by tunnel study in Northern California, USA (86). During this experiment, the particle size distribution was investigated for different sizes, which was less investigated in other studies. Into the tunnel, the changes of particle concentration with time reflect the massive numbers of fine and coarse particles. The mass concentration was nearly the same for all particle sizes as freeway at the entrance of the tunnel, which later on rose smoothly three times more with fluctuation until the end of the tunnel. From the particle size distribution, it is clear that the highest number of fine particles is present inside the tunnel. Additionally, it is shown that the highest number of coarse particles is also found inside the tunnel. The absence of breeze prevented any atmospheric saturation inside the tunnel.

8.6 Filter efficiency

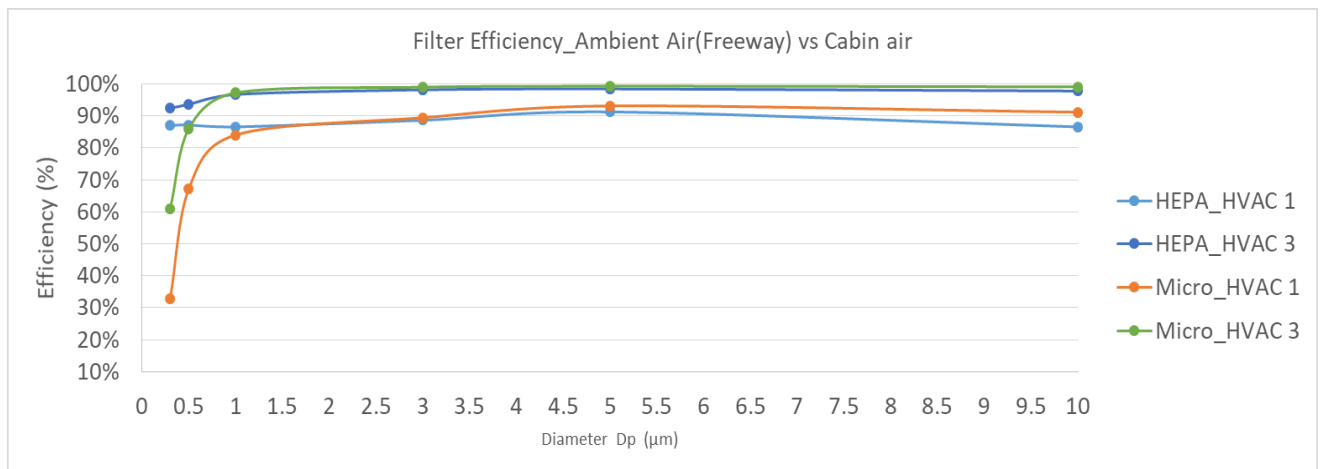


Figure 8. 7. Comparison of filter efficiency.

This type of investigation took less attention before lack of available high efficient cabin. Consequently, experimental data on the above topics is not available that much except few. Figure-8.6 shows the average particle removal efficiency for both filters comparing inside cabin air and outside ambient air under freeway conditions. The ambient sample was measured under static conditions, whereas the concentration inside the cabin was measured during driving at 80km/h on a rural freeway. Across the measured size ranges from 0.3 µm to 10 µm, the inside cabin particle reduction showed its highest efficiency when using the HEPA filter, followed by the micro filter. Figure-8.6 indicates that the effectiveness of cabin particle reduction that can be different across different particle sizes. For instance, HVAC setting-3, where the recirculation was enabled, showed an above 90% efficiency for 0.3 µm size, whereas the micro filter shows a 60% efficiency using the same climate setting. For coarse particles, the micro filter reached an efficiency of more than 95 % whereas HEPA activity was nearly 90%. Relevant experiment was done by developing a fine filter that showed the inadequacy of the conventional filtration system (5).

8.7 Number vs mass concentration

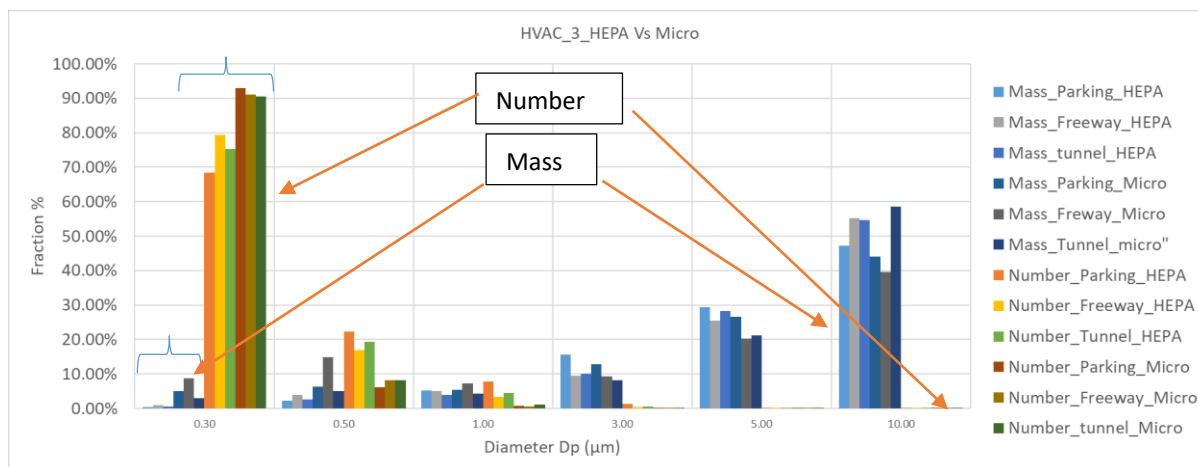


Figure 8. 8. Particle mass against particle number distribution depends on variable particle size.

The correlation between particle number and mass concentration is a quite new research topic because of a lack of clear legislation of particle number concentration according to their size. These topics are still in the discussion phase for the regulatory body, which might be included into an upcoming regulation. Although, few research groups are focusing their investigations behind this area but still they are in the development phase (87). This thesis also shows a correlation between mass and number concentration that has correspondences with some research work (70). Particle mass versus number correlation varies depending on location and source of generation of particulate matter. The same number of particles does not always contain the same mass. In this conversion, particle density was considered constant as according to the previously established aerodynamic diameter $1\text{g}/\text{cm}^3$. As discussed in previous research, particles having smaller diameter contribute most to the total number of particles, but do not exert this effect on particle mass. In figure 8.7, the graph expresses for both filter activities that $0.3\ \mu\text{m}$ diameter particles acquire highest number of quantity with least particle mass concentration. For example, during the use of the microfilter, 90% particle of the total numbers inside the cabin contains approximately 5% of the total particle mass. On the other hand, approximately 1% of the total particle number having $10\ \mu\text{m}$ in diameter occupy 50% of the total particle mass. Regulation and legislation regarding air quality only focus on the particle mass without considering the particle numbers - especially fine particles, which are mainly responsible for COPD (Chronic Obstructive Pulmonary Disease).

8.8 Velocity vs pressure

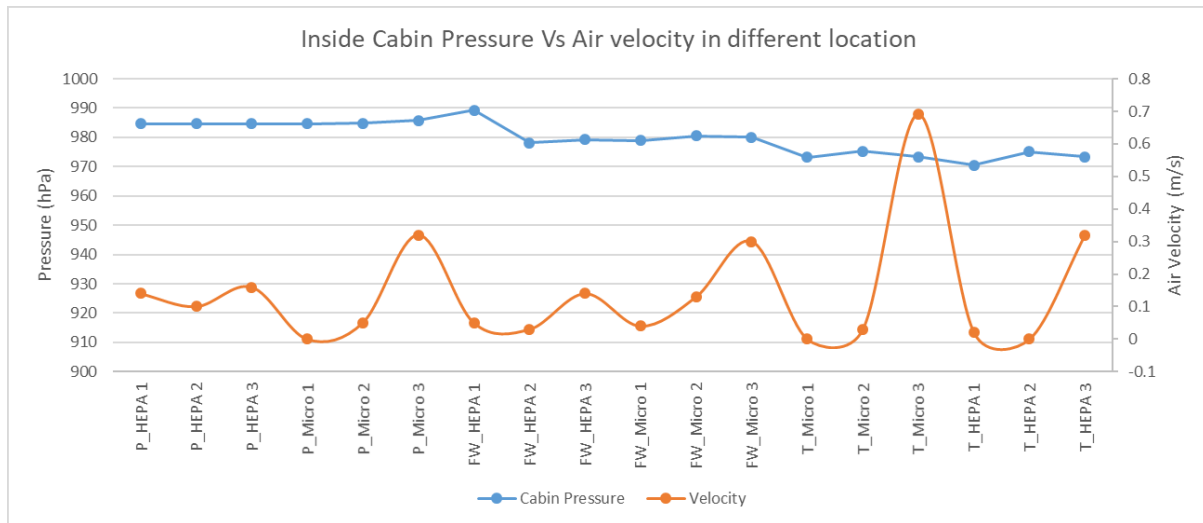


Figure 8. 9. Air pressure inside the cabin for both filters and changing blower speed.

The decision was ambiguous before experiment regarding the pressure drop of the new filter. However, except deformation of some parts of the used HEPA filter, might be due to the blower pressure, the output was nearly identical. Both HEPA and microfilter are made of fibrous filter technology. In this study, the air pressure inside the cabin was measured to compare both HEPA and micro filter to evaluate air pressure inside the compartment against different HVAC settings. By changing blower speed, different air velocity was delivered to the filter. No significant difference was noticed during the experiment. Both HEPA and micro filter deliver nearly similar air pressure inside the passenger compartment. Air velocity was measured by ventilation meter, which records different air velocity during the test drive.

The objective of this Master Thesis was designed to provide (manifold) information regarding vehicle interior air quality, and mainly focus on the simultaneous real-time measurement of fine and ultrafine particulate matter present in both outside ambient air and inside the passenger compartment. The conventional filtration efficiency was investigated and compared with an additional HEPA (High-Efficiency Particulate Air) filter. This research also showed the correlation between particulate mass concentration and their number contribution. To appreciate the actual particle behavior, test samples were collected from three different locations and particle characteristics were analyzed. The study represents the limitation of a conventional filtration system of passenger cars to remove the fine and ultrafine particles from the compartment having diameter less than 1.0 μm . The study showed that the outdoor particle concentration was predominantly influenced by means of traffic conditions. The implementation of DEP (diesel exhaust particle) filters is only an answer for exhaust particles from diesel engine combustion - however, non-exhaust emissions are contributing significantly to overall particles count. As the passenger car itself, as well as the surrounding traffic, is continuously creating particles from exhaust and non-exhaust sources simultaneously, passengers are continuously exposed to these harmful chemical substances during commuting time. Due to an ineffective filtration systems, the passengers can be expected to be directly exposed to fine and ultrafine particulate matter inside the compartment.

The conducted experiments measured the performance of a specific vehicle model by altering filter and modifying air circulation, as well as modifying the environmental boundary conditions. Certainly, different cars may have different air purification system installed, which would possibly lead to aberrations in measurement values. However, this could be expressed by an overall scenario about the typical filtration competence of the passenger compartment. The experiment was carried out within two consecutive days during 3 October and 4 October in 2018, inside a tunnel, on a freeway and in rural areas within the same city of Graz. The results could be affected by changing different cities, season and vehicle as well. The inadequacy of the filter technical information from the supplier and OEM for legislative issue also acted as a disruption to explore the more scientific information of filtering systems. Finally, different seasons may significantly change the particles concentration and characteristic in the ambient air, which could have also influence filtration performance and passenger cabin air quality.

One of the major challenges of this experiment was the measurement of particles inside the cabin as the fine particles are not visible and human themselves also produces a lot of particle every moment. During the experiment, maximum precautions and less movement were followed to maintain the proper experimental environment. The monitoring device for particle counting could only measure the specific particles that were predefined. However, the identification of particle diameter as required information could be more robust for specific particle size analysis. The detailed information of filter media presumably adds another dimension into this master thesis.

Many discussion points inside this topic are still open and further comprehensive investigation is recommended by examining details of filtration techniques. The measurement by changing influencing factors including other types of vehicles, different cities and seasons will also assist to generate an elaborate idea of behaviors of particles and filter activity. Improvement of filters could be done through the improvement of dust holding capacity for specific Particulate Matter. Future development in this area is recommended to focus more on submicron particulate matter and mitigate the problem. A driver and the passengers should have control of their exposure to harmful particles in the passenger compartment during travelling. The regulations and legislations regarding air quality should convey a clear message concerning health concern. Soon, the total number of emitted particles is going to include in vehicle emission regulation (EURO 6). However, lack of tangible information regarding submicron particles number into different guidelines and legislations, these are still captured in the dark state.

10 BIBLIOGRAPHY

1. Galatsis K, Wlodarski W. Car Cabin Air Quality Sensors and Systems. *Encycl sensors*. 2006;X:1–11.
2. Burtscher H, Windisch C-, Mayer A, Loretz S, Keller A, Kasper M, et al. Air quality filtration in vehicle cabins. *J KONES Powertrain Transp*. 2009;16(2).
3. PTAK TJ, FALLON SL. PARTICULATE CONCENTRATION IN AUTOMOBILE PASSENGER COMPARTMENTS. *Part Sci Technol [Internet]*. 1994 Oct 24 [cited 2018 Jul 12];12(4):313–22. Available from: <http://www.tandfonline.com/doi/abs/10.1080/02726359408906658>
4. Lowell &, Ashbaugh LL. Chemical Mass Balance Source Apportionment of PM 10 during the Southern California Air Quality Study. *Aerosol Sci Technol [Internet]*. 1994 [cited 2019 Apr 15];21(1):1–36. Available from: <https://www.tandfonline.com/action/journalInformation?journalCode=uast20>
5. Lee ES, Zhu Y. Application of a high-efficiency cabin air filter for simultaneous mitigation of ultrafine particle and carbon dioxide exposures inside passenger vehicles. *Environ Sci Technol [Internet]*. 2014 [cited 2018 Aug 13];48(4):2328–35. Available from: <https://pubs.acs.org/sharingguidelines>
6. Valavanidis A, Fiotakis K, Vlachogianni T. Airborne particulate matter and human health: Toxicological assessment and importance of size and composition of particles for oxidative damage and carcinogenic mechanisms. *J Environ Sci Heal - Part C Environ Carcinog Ecotoxicol Rev*. 2008;26(4):339–62.
7. Chellam S, Kulkarni P, Fraser MP, Fraser MP. Emissions of Organic Compounds and Trace Metals in Fine Particulate Matter from Motor Vehicles : A Tunnel Study in Houston , Texas Emissions of Organic Compounds and Trace Metals in Fine Particulate Matter from Motor Vehicles : A Tunnel Study in Houston ,. Vol. 2247. 2016.
8. Swain S. *IN Immunology*. *J Info*. 2011;0022.
9. Harrison RM, Yin J. *ScienceDirect - The Science of The Total Environment : Particulate matter in the atmosphere: which particle properties are important for its effects on health?* 2000; Available from: http://www.sciencedirect.com.proxy.lib.uiowa.edu/science?_ob=ArticleURL&_udi=B6V78-4019BVW-9&_user=440026&_coverDate=04/17/2000&_rdoc=1&_fmt=high&_orig=search&_origin=search&_sort=d&_docanchor=&view=c&_acct=C000020939&_version=1&_urlVersion=0&_userid=4400
10. USEPA. Air Quality Index (AQI). *A Guid to Air Qual Your Heal [Internet]*. 2014 [cited 2018 Aug 12];(February):12. Available from: https://www3.epa.gov/airnow/aqi_brochure_02_14.pdf
11. Kanchan, Gorai AK, Goyal P. A review on air quality indexing system. *Asian J Atmos Environ*. 2015;9(2):101–13.
12. Stieb DM, Doiron MS, Blagden P, Burnett RT. Estimating the public health burden attributable to air pollution: An illustration using the development of an alternative air quality index. *J Toxicol Environ Heal - Part A*. 2005;68(13–14):1275–88.
13. USEPA. Technical Assistance Document for the Reporting of Daily Air Quality – the Air Quality Index (AQI). *Environ Prot*. 2013;(May):1–28.

14. European Union. CAQI Air quality index: Comparing Urban Air Quality across Borders [Internet]. 2012 [cited 2018 Jul 29]. Available from: www.citeair.eu
15. federal register Environmental Protection Agency 40 CFR Part 58 Air Quality Index Reporting; Final Rule [Internet]. 1999 [cited 2018 Aug 15]. Available from: <https://www3.epa.gov/airnow/air-quality-index-reporting-final-rule.pdf>
16. Lee SW. Fine particulate matter measurement and international standardization for air quality and emissions from stationary sources. *Fuel* [Internet]. 2010;89(4):874–82. Available from: <http://dx.doi.org/10.1016/j.fuel.2009.03.023>
17. WHO Air quality guidelines for particulate matter, ozone, nitrogen dioxide and sulfur dioxide [Internet]. 2006 [cited 2019 Jan 24]. Available from: https://apps.who.int/iris/bitstream/handle/10665/69477/WHO_SDE_PHE_OEH_06.02_eng.pdf;jsessionid=34539E23788F1480C586C84687A8AA84?sequence=1
18. Hinds WC. *Aerosol technology: Properties, Behavior, and Measurement of Airborne Particles*. [Internet]. Wiley-Interscience Publication. 1999 [cited 2018 Aug 14]. 233–259 p. Available from: <https://books.google.at/books?hl=en&lr=&id=qIkYjPXfWK4C&oi=fnd&pg=PT11&dq=aerosol+technology+hinds&ots=52NzLe8toY&sig=RS28Ia26jtf7d-50lr2SPLGlsj4#v=onepage&q=aerosol+technology+hinds&f=false>
19. Eastwood P. *Particulate Emissions from Vehicles* [Internet]. Chichester, UK: John Wiley & Sons, Ltd; 2007 [cited 2018 Aug 26]. (Wiley-Professional Engineering Publishing Series). Available from: <http://doi.wiley.com/10.1002/9780470986516>
20. Seinfeld JH, Pandis SN. *Atmospheric chemistry and physics : from air pollution to climate change* [Internet]. [cited 2019 Jan 13]. Available from: https://books.google.at/books?hl=en&lr=&id=n_RmCgAAQBAJ&oi=fnd&pg=PR5&dq=John+H.+Seinfeld+and+Spyros+N.+Pandis.+Atmospheric+Chemistry+and+Physics:+From+Air+Pollution+to+Climate+Change.+2.+Edition.+John+Wiley+and+Sons,+Inc.,+2006&ots=gRjDFPtgaR&sig=noc_fO4
21. Lehnert BE. Pulmonary and thoracic macrophage subpopulations and clearance of particles from the lung. *Environ Health Perspect* [Internet]. 1992 Jul [cited 2019 Jan 13];97:17–46. Available from: <https://ehp.niehs.nih.gov/doi/10.1289/ehp.929717>
22. Utell Chair MJ, Branch MC, Henderson R, Rennard SI, Rockette Professor H, Samet Professor JM, et al. Helmut Greim Frank E Speizer BOARD OF DIRECTORS HEALTH RESEARCH COMMITTEE HEALTH REVIEW COMMITTEE OFFICERS & STAFF Cristina I Cann Staff Scientist Aaron J Cohen Principal Scientist Maria G Costantini Principal Scientist Debra A Kaden Senior Scientist [Internet]. 2002 [cited 2019 Jan 13]. Available from: www.healtheffects.org
23. Watson AY, Bates RR, Kennedy D. Potential Carcinogenic Effects of Polynuclear Aromatic Hydrocarbons and Nitroaromatics in Mobile Source Emissions. 1988 [cited 2019 Jan 13]; Available from: <https://www.ncbi.nlm.nih.gov/books/NBK218134/>
24. Watson AY, Bates RR, Kennedy D. Assessment of Carcinogenicity: Generic Issues and Their Application to Diesel Exhaust. 1988 [cited 2019 Jan 13]; Available from: <https://www.ncbi.nlm.nih.gov/books/NBK218143/>
25. Watson AY, Bates RR, Kennedy D. Biological Disposition of Vehicular Airborne Emissions: Particle-Associated Organic Constituents. 1988 [cited 2019 Jan 13]; Available from: <https://www.ncbi.nlm.nih.gov/books/NBK218157/>

26. Lambert B, Bastlova T, österholm A-M, Hou S-M. Analysis of mutation at the hprt locus in human T lymphocytes. *Toxicol Lett* [Internet]. 1995 Dec 1 [cited 2019 Jan 13];82–83:323–33. Available from: <https://www.sciencedirect.com/science/article/pii/0378427495034854>
27. Monks TJ, Hanzlik RP, Cohen GM, Ross D, Graham DG. Quinone chemistry and toxicity. *Toxicol Appl Pharmacol* [Internet]. 1992 Jan 1 [cited 2018 Jul 10];112(1):2–16. Available from: <https://www.sciencedirect.com/science/article/pii/0041008X9290273U>
28. Kidd P. Th1 / Th2 Balance Th1 / Th2 Balance : The Hypothesis , its Limitations , and Implications for Health and Disease. *Altern Med Rev* [Internet]. 2003;8(3):223–42. Available from: https://www.researchgate.net/profile/Parris_Kidd2/publication/10591467_Th1Th2_Balance_The_Hypothesis_its_Limitations_and_Implications_for_Health_and_Disease/links/56f9fe5e08ae7c1fda311e3c/Th1-Th2-Balance-The-Hypothesis-its-Limitations-and-Implications-for
29. Fulvio Amato, Martijn Schaap, Cristina Reche and XQ. Road traffic_A major source of particulate matter in EuropeNo Title. Available from: https://link.springer.com/chapter/10.1007/698_2012_211
30. O'BYRNE PM, POSTMA DS. The Many Faces of Airway Inflammation. *Am J Respir Crit Care Med* [Internet]. 1999 May 14 [cited 2019 Jan 13];159(supplement_2):S1–63. Available from: http://www.atsjournals.org/doi/abs/10.1164/ajrccm.159.supplement_2.mfa-1
31. Salvi S, Holgate ST. Mechanisms of particulate matter toxicity [Internet]. [cited 2019 Jan 13]. Available from: <https://onlinelibrary.wiley.com/doi/pdf/10.1046/j.1365-2222.1999.00576.x>
32. Dockery DW, Pope CA, Xu X, Spengler JD, Ware JH, Fay ME, et al. An Association between Air Pollution and Mortality in Six U.S. Cities. *N Engl J Med* [Internet]. 1993 Dec 9 [cited 2018 Jul 10];329(24):1753–9. Available from: <http://www.nejm.org/doi/abs/10.1056/NEJM199312093292401>
33. Xu Z, Zhou B. Fundamentals of air cleaning technology and its application in cleanrooms. Vol. 9783642394, *Fundamentals of Air Cleaning Technology and Its Application in Cleanrooms*. 2014. 1–871 p.
34. Yakushev, E.V., Newton A. Redox Interfaces In Marine Waters. *Chem Struct Pelagic Redox Interfaces Obs Model Hdb Env Chem*. 2013;22(October):1–12.
35. WHO | Database on source apportionment studies for particulate matter in the air (PM10 and PM2.5). WHO [Internet]. 2015 [cited 2018 Aug 22]; Available from: http://www.who.int/quantifying_ehimpacts/global/source_apport/en/
36. Karagulian F, Belis CA, Dora CFC, Prüss-Ustün AM, Bonjour S, Adair-Rohani H, et al. Contributions-to-cities--ambient-particulate-matter--PM---A_2015_Atmospheric [Internet]. Vol. 120, *Atmospheric Environment*. Pergamon; 2015 [cited 2018 Jul 16]. 475–483 p. Available from: <https://www.sciencedirect.com/science/article/pii/S1352231015303320>
37. Amato F, Pandolfi M, Moreno T, Furger M, Pey J, Alastuey A, et al. Sources and variability of inhalable road dust particles in three European cities. *Atmos Environ* [Internet]. 2011 Dec 1 [cited 2018 Jul 18];45(37):6777–87. Available from: <https://www.sciencedirect.com/science/article/pii/S1352231011005942>
38. Simons A. Road transport: new life cycle inventories for fossil-fuelled passenger cars and non-exhaust emissions in ecoinvent v3. *Int J Life Cycle Assess* [Internet]. 2016 Sep 27 [cited 2018 Jul 21];21(9):1299–313. Available from: <http://link.springer.com/10.1007/s11367-013-0642-9>
39. Kagawa J. Health effects of diesel exhaust emissions--a mixture of air pollutants of worldwide

- concern. *Toxicology* [Internet]. 2002 Dec 27 [cited 2019 Jan 13];181–182:349–53. Available from: <http://www.ncbi.nlm.nih.gov/pubmed/12505335>
40. Thorpe A, Harrison RM. Sources and properties of non-exhaust particulate matter from road traffic: A review. *Sci Total Environ* [Internet]. 2008 Aug 1 [cited 2019 Jan 13];400(1–3):270–82. Available from: <https://www.sciencedirect.com/science/article/pii/S004896970800658X>
 41. Timmers VRJH, Achten PAJ. Non-exhaust PM emissions from electric vehicles. *Atmos Environ* [Internet]. 2016;134:10–7. Available from: <http://dx.doi.org/10.1016/j.atmosenv.2016.03.017>
 42. Miguel AH, Kirchstetter TW, Harley RA, Hering S V. On-road emissions of particulate polycyclic aromatic hydrocarbons and black carbon from gasoline and diesel vehicles. *Environ Sci Technol*. 1998;32(4):450–5.
 43. Bergmann M, Kirchner U, Vogt R, Benter T. On-road and laboratory investigation of low-level PM emissions of a modern diesel particulate filter equipped diesel passenger car. *Atmos Environ* [Internet]. 2009 Apr [cited 2019 Jan 13];43(11):1908–16. Available from: <https://linkinghub.elsevier.com/retrieve/pii/S1352231008011850>
 44. EUR-Lex - 32007R0715 - EN - EUR-Lex [Internet]. [cited 2019 Jan 13]. Available from: <https://eur-lex.europa.eu/legal-content/EN/ALL/?uri=celex%3A32007R0715>
 45. Antonio H. Miguel †, Thomas W. Kirchstetter and, Harley* RA, Hering S V. On-Road Emissions of Particulate Polycyclic Aromatic Hydrocarbons and Black Carbon from Gasoline and Diesel Vehicles. 1998 [cited 2019 Jan 13]; Available from: <https://pubs.acs.org/doi/abs/10.1021/es970566w>
 46. Anders R. Johnsen *,†, Julia R. de Liphay ‡, Fredrik Reichenberg §, Søren J. Sørensen †, Ole Andersen ||, Peter Christensen ||, et al. Biodegradation, Bioaccessibility, and Genotoxicity of Diffuse Polycyclic Aromatic Hydrocarbon (PAH) Pollution at a Motorway Site. 2006 [cited 2019 Jan 13]; Available from: <https://pubs.acs.org/doi/abs/10.1021/es060008u>
 47. Sandy Owega, Badi-Uz-Zaman Khan, Ryan D’Souza, Greg J. Evans *, Mike Fila and, Jervis RE. Receptor Modeling of Toronto PM2.5 Characterized by Aerosol Laser Ablation Mass Spectrometry. 2004 [cited 2019 Jan 13]; Available from: <https://pubs.acs.org/doi/abs/10.1021/es035177i>
 48. Chow JC, Watson JG, Ashbaugh LL, Magliano KL. Similarities and differences in PM10 chemical source profiles for geological dust from the San Joaquin Valley, California. *Atmos Environ* [Internet]. 2003 Mar 1 [cited 2019 Jan 13];37(9–10):1317–40. Available from: <https://www.sciencedirect.com/science/article/pii/S135223100201021X>
 49. and AC, Harrison* RM. Fine (PM2.5) and Coarse (PM2.5-10) Particulate Matter on A Heavily Trafficked London Highway: Sources and Processes. 2005 [cited 2019 Jan 13]; Available from: <https://pubs.acs.org/doi/abs/10.1021/es050462i>
 50. Kaarle J. Kupiainen* †,‡ and, Tervahattu‡ H, Räisänen M, Timo Mäkelä, Minna Aurela and, Hillamo R. Size and Composition of Airborne Particles from Pavement Wear, Tires, and Traction Sanding. 2004 [cited 2019 Jan 13]; Available from: <https://pubs.acs.org/doi/abs/10.1021/es035419e>
 51. Räisänen M, Kupiainen K, Tervahattu H. MINERALOGY, TEXTURE AND MECHANICAL PROPERTIES OF ANTI-SKID AND ASPHALT AGGREGATES CONTRIBUTING TO URBAN DUST [Internet]. [cited 2019 Jan 13]. Available from: [http://www.vegagerdin.is/vefur2.nsf/Files/Raisanen/\\$file/Raisanen.pdf](http://www.vegagerdin.is/vefur2.nsf/Files/Raisanen/$file/Raisanen.pdf)

52. Abu-Allaban M, Gillies JA, Gertler AW, Clayton R, Proffitt D. Tailpipe, resuspended road dust, and brake-wear emission factors from on-road vehicles. *Atmos Environ* [Internet]. 2003 [cited 2019 Jan 13];37:5283–93. Available from: <https://eis.hu.edu.jo/deanshipfiles/pub104283181.pdf>
53. Moriyoshi A, Takano ei, Ono M, Ogasawara aki, Tabata M, Miyamoto N, et al. Analysis of Contribution to SPM by Organic Matters Using High-Performance Liquid· Chromatography (HPLC) [Internet]. [cited 2019 Jan 13]. Available from: https://eprints.lib.hokudai.ac.jp/dspace/bitstream/2115/42824/1/moriyoshi_SAE2002-01-0653.pdf
54. García-Morales M, Partal P, Navarro FJ, Gallegos C. Effect of waste polymer addition on the rheology of modified bitumen. *Fuel* [Internet]. 2006 May [cited 2019 Jan 13];85(7–8):936–43. Available from: <http://linkinghub.elsevier.com/retrieve/pii/S0016236105003789>
55. Ostermeyer G. On the dynamics of the friction coefficient. *Wear* [Internet]. 2003 May 1 [cited 2019 Jan 13];254(9):852–8. Available from: <https://www.sciencedirect.com/science/article/abs/pii/S0043164803002357>
56. Mosleh M, Blau PJ, Dumitrescu D. Characteristics and morphology of wear particles from laboratory testing of disk brake materials. *Wear* [Internet]. 2004 Jun 1 [cited 2019 Jan 13];256(11–12):1128–34. Available from: <https://www.sciencedirect.com/science/article/abs/pii/S0043164803005817>
57. Talib RJ, Muchtar A, Azhari CH. Microstructural characteristics on the surface and subsurface of semimetallic automotive friction materials during braking process. *J Mater Process Technol* [Internet]. 2003 Sep 22 [cited 2019 Jan 13];140(1–3):694–9. Available from: <https://www.sciencedirect.com/science/article/pii/S0924013603007696>
58. Camatini M, Crosta GF, Dolukhanyan T, Sung C, Giuliani G, Corbetta GM, et al. Microcharacterization and identification of tire debris in heterogeneous laboratory and environmental specimens. *Mater Charact* [Internet]. 2001 Apr [cited 2019 Jan 13];46(4):271–83. Available from: <http://linkinghub.elsevier.com/retrieve/pii/S104458030000098X>
59. Pierson WR, Brachaczek WW. Particulate Matter Associated with Vehicles on the Road. II. *Aerosol Sci Technol* [Internet]. 1982 Sep 20 [cited 2019 Jan 13];2(1):1–40. Available from: <http://www.tandfonline.com/doi/abs/10.1080/02786828308958610>
60. Sternbeck J, Sjödin Å, Andréasson K. Metal emissions from road traffic and the influence of resuspension—results from two tunnel studies. *Atmos Environ* [Internet]. 2002 Oct [cited 2019 Jan 13];36(30):4735–44. Available from: <http://linkinghub.elsevier.com/retrieve/pii/S1352231002005617>
61. Heideman Thesis BG. With references-With summary in English and Dutch [Internet]. 2004 [cited 2019 Jan 13]. Available from: https://ris.utwente.nl/ws/portalfiles/portal/6071186/thesis_Heideman.pdf
62. Terry B, Councell, Kea U, Duckenfield, Edward R, Landa * and, Callender E. Tire-Wear Particles as a Source of Zinc to the Environment. 2004 [cited 2019 Jan 13]; Available from: <https://pubs.acs.org/doi/abs/10.1021/es034631f>
63. US EPA O. Particulate Matter (PM) Basics. [cited 2019 Jan 16]; Available from: <https://www.epa.gov/pm-pollution/particulate-matter-pm-basics>
64. Pich J. Aerosol Measurement [Internet]. Vol. 11, *Journal of Aerosol Science*. 1980. 225 p. Available from: <http://linkinghub.elsevier.com/retrieve/pii/0021850280900373>

65. TSI Incorporated. TSI Applicatin note PR-001 - Aerosol statistics, lognormal distributions and $dN / d\log D$ p. 2012;1–6.
66. John W, Wall SM, Ondo JL, Winklmayr W. Modes in the size distributions of atmospheric inorganic aerosol. *Atmos Environ Part A Gen Top* [Internet]. 1990 Jan 1 [cited 2019 Jan 13];24(9):2349–59. Available from: <https://www.sciencedirect.com/science/article/pii/096016869090327J>
67. Venkataraman C, Friedlander SK. Size Distributions of Polycyclic Aromatic Hydrocarbons and Elemental Carbon. 2. Ambient Measurements and Effects of Atmospheric Processes. *Environ Sci Technol* [Internet]. 1994 Apr [cited 2019 Jan 13];28(4):563–72. Available from: <http://pubs.acs.org/doi/abs/10.1021/es00053a006>
68. Noll KE, Pontius A, Frey R, Gould M. Comparison of atmospheric coarse particles at an urban and non-urban site. *Atmos Environ* [Internet]. 1985 Jan 1 [cited 2019 Jan 13];19(11):1931–43. Available from: <https://www.sciencedirect.com/science/article/pii/0004698185900198>
69. Friedlander SK, K. S. Smoke, dust and haze: Fundamentals of aerosol behavior. New York, Wiley-Interscience, 1977 333 p [Internet]. 1977 [cited 2019 Jan 13]; Available from: <http://adsabs.harvard.edu/abs/1977wi...book.....FÜ>
70. Merkisz J, Pielecha J. Nanoparticle Emissions from Combustion Engines Springer Tracts on Transportation and Traffic STTT.
71. Zhu Y, Hinds WC, Kim S, Shen S, Sioutas C. Study of ultrafine particles near a major highway with heavy-duty diesel traffic. *Atmos Environ* [Internet]. 2002 Sep 1 [cited 2019 Jan 13];36(27):4323–35. Available from: <https://www.sciencedirect.com/science/article/pii/S1352231002003540>
72. Atlas copco [Internet]. Available from: <https://www.atlascopco.com/en-au/compressors/service/parts/LineFilters>
73. Ghiwe S, Srinivasan K V, Chaudhari K. ANALYSIS ON EFFECT OF TEMPERATURE ON MOISTURE SEPARATION IN AIR COMPRESSOR. *Int J Sci Eng Appl Sci* [Internet]. 2015 [cited 2019 Jan 20];(1). Available from: www.ijseas.com
74. Payatakes AC. Model of transient aerosol particle deposition in fibrous media with dendritic pattern. *AIChE J* [Internet]. 1977 Mar 1 [cited 2019 Jan 23];23(2):192–202. Available from: <http://doi.wiley.com/10.1002/aic.690230208>
75. Baldasano J., Valera E, Jiménez P. Air quality data from large cities. *Sci Total Environ*. 2003;307(1):141–65.
76. Owner’s Manual for Vehicle The Ultimate Driving Machine. Available from: www.bmw.com/bmw_drivers_guide
77. Burtscher H, Mayer A, Loretz S, Keller A, Kasper M, Czerwinski J. Improvement of air quality in vehicle cabins by nanoparticle filtration. *J KONES* [Internet]. 2010;Vol. 17, N(4):79–88. Available from: <http://yadda.icm.edu.pl/baztech/element/bwmeta1.element.baztech-article-BUJ7-0017-0051>
78. Home - A2Mac1 - Automotive Benchmarking [Internet]. [cited 2019 Jan 14]. Available from: <https://portal.a2mac1.com/?redirect=%3Ffromredirect>
79. HEPA Cabin Filters | Bosch Auto Parts [Internet]. [cited 2019 Jan 14]. Available from: <https://www.boschautoparts.com/en/auto/filters/hepa-cabin-filters>

80. AeroTrak Portable Particle Counter 9310 - [Internet]. [cited 2019 Jan 14]. Available from: <https://www.tsi.com/products/cleanroom-particle-counters/portable-particle-counters/aerotrak-portable-particle-counter-9310/>
81. Particle Detectors GETTING DATA YOU NEED WITH PARTICLE MEASUREMENTS [Internet]. [cited 2019 Jan 14]. Available from: <https://www.kenelec.com.au/ken/wp-content/uploads/2018/04/TSI-PD-001-Getting-Data-You-Need-With-Particle-Measurements-AppNote.pdf>
82. DustTrak DRX Aerosol Monitor 8533 - [Internet]. [cited 2019 Jan 14]. Available from: <https://www.tsi.com/products/aerosol-and-dust-monitors/dust-monitors/dusttrak-drx-aerosol-monitor-8533/>
83. VelociCalc Multi-Function Ventilation Meter 9565 - [Internet]. [cited 2019 Jan 14]. Available from: <https://tsi.com/velocicalc-multi-function-ventilation-meter-9565/>
84. Knibbs LD, de Dear RJ, Morawska L, Mengersen KL. On-road ultrafine particle concentration in the M5 East road tunnel, Sydney, Australia. *Atmos Environ* [Internet]. 2009 Jul 1 [cited 2018 Jul 1];43(22–23):3510–9. Available from: <https://www.sciencedirect.com/science/article/pii/S1352231009003628>
85. Weiss M, Bonnel P, Kühlwein J, Provenza A, Lambrecht U, Alessandrini S, et al. Will Euro 6 reduce the NOx emissions of new diesel cars? – Insights from on-road tests with Portable Emissions Measurement Systems (PEMS). *Atmos Environ* [Internet]. 2012 Dec 1 [cited 2018 Aug 27];62:657–65. Available from: <https://www.sciencedirect.com/science/article/pii/S1352231012008412>
86. Measurements of Particle Number and Mass Concentrations and Size Distributions in a Tunnel Environment. 2005 [cited 2019 Jan 15]; Available from: <https://pubs.acs.org/sharingguidelines>
87. Seminar A, Fritz O. GDI engine development according EU 6 [Internet]. [cited 2019 Jan 15]. Available from: <https://www.avl.com/documents/10138/0/04-GDI+engine+development+acc+to+EU+6-Fritz.pdf/4a1621f6-c7f4-454c-a511-444a788e6938>